AN EVALUATION OF THE BREED/BURN FAST REACTOR CONCEPT

by

Bahman Atefi

B.S., Cornell University
(1975)

M.S., Massachusetts Institute of Technology
(1977)

Nuclear E., Massachusetts Institute of Technology
(1977)

SUBMITTED IN PARTIAL FULFILLMENT
OF THE REQUIREMENTS FOR THE
DEGREE OF DOCTOR OF
SCIENCE

at the

MASSACHUSETTS INSTITUTE OF TECHNOLOGY

December 1979
(i.e February, 1980)

Signature of Author _____
Department of Nuclear Engineering, December 10, 1979

Certified by _____
Thesis Supervisor

Certified by _____
Thesis Supervisor

Accepted by _____
Chairman, Departmental Committee
on Graduate Students

AN EVALUATION OF THE BREED/BURN FAST REACTOR CONCEPT

by

Bahman Atefi

Submitted to the Department of Nuclear Engineering on December 10, 1979, in partial fulfillment of the requirements for the degree of Doctor of Philosophy.

ABSTRACT

A core design concept and fuel management strategy, designated "breed/burn", has been evaluated for heterogeneous fast breeder reactors. In this concept internal blanket assemblies after fissile material is bred in over several in-core cycles, are shuffled into a moderated radial blanket and/or central island. The most promising materials combination identified used thorium in the internal blankets (due to the superior performance of epithermal Th-U233 systems) and zirconium hydride (ZrH_{16}) as the moderator (because of the compact assembly and core designs it permitted).

The advantage of moving the U233-enriched thorium internal blankets to the zirconium-hydride-moderated radial blanket included production of 20-30% of the total system power by the radial blanket, which resulted in a 10-15% reduction in the peak core linear heat generation rate (LHGR). This in turn can be translated into either a 10-15% increase in the total power production from the core or a 15-20% reduction in the core fuel assembly fabrication requirements for the same amount of energy delivered. Other advantages of this core include a 40% reduction in the total reprocessing requirements, and a 25% reduction in the transportation and reprocessing of the plutonium-bearing assemblies compared to a more conventional heterogeneous core on the U-Pu cycle with no blanket shuffling or moderation.

The reduced plutonium handling and the ability to denature U-233 with U-238 offer a potential improvement in proliferation resistance.

The alternative shuffling strategy of moving the enriched internal blankets to the middle of the core, and creation of a near-critical moderated central island resulted in a 27% reduction in the total core fissile plutonium requirement, a 50% reduction in the total reprocessing requirements, and a 60% reduction in the transportation and reprocessing of

plutonium-bearing assemblies.

It was found that the unit price of plutonium has a large effect on the levelized fuel cycle cost. At a plutonium price of 27 $/gr (the indifference value of plutonium in LWRs) the core with the central island had a 20% lower fuel cycle cost compared to the reference heterogeneous core. This reduction in fuel cycle cost increased to 40% when plutonium was assigned zero value.

It is concluded that the breed/burn fuel management concept is a useful addition to the FBR core designer's repertoire of variations which can be worked into the same basic core frame.

Thesis Supervisor: Michael J. Driscoll
Title: Associate Professor of Nuclear Engineering

Thesis Supervisor: David D. Lanning
Title: Professor of Nuclear Engineering

To my Mother

ACKNOWLEDGMENTS

The author wishes to express his sincere appreciation for the time and guidance contributed by his principal advisor, Professor M. J. Driscoll, throughout the author's graduate work at M.I.T. In addition, Prof. D. D. Lanning who served as co-supervisor provided valuable assistance.

Financial support for this work was provided by the U.S. Department of Energy in the form of a research assistantship on Contract EY-76-S-02-2250, and is grate-acknowledged.

Many long and interesting discussions with Mr. Dale Lancaster have been extremely helpful. His assistance in using a variety of computer codes is also appreciated. Mr. Wee Tee Loh collaborated in the neutron and gamma heating analyses as part of his own thesis research on the FMSR concept.

Computer calculations in this work were performed at the Laboratory of Nuclear Science and at the M.I.T. Information Processing Center. The help of Ms. Rachel Morton in computational matters is acknowledged.

I wish to thank Ms. Annette Holman for her help in organizing and typing the final manuscript.

TABLE OF CONTENTS

LIST OF FIGURES

LIST OF TABLES

CHAPTER ONE

INTRODUCTION

1.1 Foreword

The rapid depletion of the world's non-renewable resources, with the resulting prospect of future shortages, has prompted a vigorous effort to devise more efficient means of using the remaining resources. Most of the electricity in today's world is generated using oil, coal or uranium as the fuel. Major alternative sources such as fusion and solar electricity are not expected to contribute significantly before well into the next century, if ever (B1). By all estimates, at the current rate of consumption the economically viable oil reserves will be essentially depleted by the middle of the twenty-first century (K1). The cost of generating electricity from oil has already become prohibitively expensive, and very few new oil-fired plants are expected to be built.

Coal, although abundant in the United States, has some basic drawbacks due to its health hazards in all phases from mining to transportation to combustion to waste (ash and scrubber) disposal. The adverse health effects due to the emission of the sulfur dioxide and other compounds can be reduced considerably using scrubbers, and coal is expected to generate a large part of the United States' future electricity needs.

Nuclear energy has made a modest contribution to the total United States' electrical generating capacity to date, currently generating on the order of 12% of the total electric production in this country. However, considering the status of the different means of generating electricity, nuclear power appears to be an essential ingredient in the future U.S. and world energy mix.

Currently, most of the electricity from nuclear power in the world is generated using light water reactors on a once-through cycle. But light water reactors use uranium at a rate which limits their economically useful life span. This will result in a rapid depletion of the moderate-cost uranium, and even plutonium and uranium recycle is not expected to change the situation radically (A1).

The problem of finite moderate-cost uranium resources can essentially be eliminated if breeder reactors are used. Currently, however, Fast Breeder Reactors (FBRs) are perceived by some to have disadvantages arising from their projected high capital costs and greater proliferation potential. Thus there are considerable incentives to examine design and fuel management options which will be compatible with schemes to increase FBR proliferation resistance, and which can further decrease fuel cycle costs to help offset their higher capital costs.

It is the purpose of the present work to evaluate one such concept, the so-called breed/burn fuel cycle, in which internal fast breeder reactor blankets are irradiated in the core to breed-in a substantial fissile content and then

shuffled to a moderated radial blanket and burned to materials-limited burnup values. By this means the amount and quality of the weapons-grade bred material in the ex-reactor phase of the fuel cycle can be considerably reduced.

The emphasis in this work is on conventional technology as far as the fuel and the structural materials and the operating limits such as temperature, fluence and burnup are concerned.

1.2 Background

Although most of the past effort on FBR core design, fuel management and fuel cycle economics is relevant to the present effort, we will restrict our attention here to the specific topics of direct applicability to the present work. These topics include:

a. internal blanket design considerations related to improved safety and neutronic performance.

b. thorium blankets and their relation to crossed-progeny fuel cycles and higher levels of safeguards against nuclear proliferation.

c. moderated blankets, their advantages and disadvantages.

d. The Fast Mixed Spectrum Reactor (FMSR), a recent innovation having some similarity to the older fast-thermal coupled reactor, and the breed/burn concept, but with the main emphasis on proliferation resistance.

1.3 Heterogeneous Fast Breeder Reactors with Internal Blankets

The interest in the development of heterogeneous designs, i.e., cores with internal blankets is twofold: 1. enhanced safety; 2. better neutronic performance.

The safety related concern is basically related to the magnitude of the sodium void coefficient in large LMFBRs. If the sodium in the core of an LMFBR is voided during the course of an accident, the spectrum hardens in the core due to reduced moderation by sodium. Near the center of the fissile fueled zones the higher value of the fissile η in the harder spectrum offsets the increase in leakage, and a reactivity addition results.

In large homogeneous reactors the low-leakage zones can be large enough to permit generation of substantial void reactivity if coherent voiding by a properly shaped and distributed sodium vapor bubble can be achieved. Commercial size (1000 MWe) homogeneous core designs have positive void potentials of as much as 2% Δk (i.e. approximately \$5.0 if $\beta = 0.004$) at the beginning of life (BOL) and 2.5% Δk (\$6.0) under end-of-equilibrium cycle (EOEC) conditions (B2).

In the unlikely event of an unprotected loss of flow accident, the high positive reactivity surge that might result due to coherent sodium voiding could threaten the integrity of the core.

Recent safety studies have suggested that a sodium void worth of less than 1% Δk (approximately 2-3 dollars) can protect against highly energetic consequences (P1).

The sodium void coefficient can be reduced by either enhancing the leakage to less reactive parts of the core (e.g. use of pancake cores, parfait cores or radially heterogeneous designs) or reducing the effect of the spectrum hardening (moderated cores).

The enhancement of the safety by lowering the sodium void coefficient using any of the above designs is coupled with a higher fissile inventory requirement. This is shown in Table 1.1 where the specific inventory (Kg fissile/KWe) and several other parameters of a reference homogeneous core is compared with several other concepts designed to reduce the sodium void coefficient (B3). As can be seen, the small-pin tightly-coupled heterogeneous core has the best neutronic performance among the concepts studied.

Focusing on the heterogeneous designs with internal radial blankets, there has been some controversy over the neutronic improvements that might be gained by adopting heterogeneous cores instead of the conventional homogeneous cores.

An early French study (M1) indicated that there were substantial improvements in the neutronic performance of heterogeneous cores. These included an improvement in doubling time by a factor of 2, a 50% reduction in reactivity

Table 1.1

Neutronic Performance of Several Low Sodium Worth Cores, Reference (P1)

Concept	Sodium Void Worth (dollars) Total Core Height	Specific Inventory (Kg/KWe)	Breeding Ratio	Compound System Doubling Time
Cylindrical Homogeneous (reference)	5.00	3.75	1.35	13
Pancake Core H/D=0.1	1.75	4.35	1.18	30
Tightly Coupled Heterogeneous (large fuel pin)	1.5*	5.95	1.46	17
Tightly Coupled Heterogeneous (small fuel pin)	1.7*	4.25	1.36	16
Less Tightly Coupled (Heterogeneous)	1.5*	5.25	1.55	14
Modular Island Heterogeneous	0.25	5.60	1.34	21
Be-O Moderated	2.2	4.30	1.07	90

*Fuel Assemblies Voided

swing over a burnup cycle (hence reducing control requirements by a factor of 2) and power flattening without use of several enrichment zones. This study was analyzed by others (C1, C2), and while the improvements were confirmed, it was shown that they were not due to the heterogeneity of the core per se, but rather stemmed from the fact that the original homogeneous design was not optimized with respect to the fuel volume fraction. This can be best understood by looking at the definition of the compound system doubling time (CSDT) (B4):

$$CSDT = 0.693 \times \frac{M_{in} + M_{ex}}{(G-L_p-L_d)\ C} \qquad (1.1)$$

where:

M_{in} is the in-reactor fissile inventory and is equal to the beginning of the equilibrium cycle core and blanket fissile inventory (M_{BOEC})

M_{ex} is the external cycle fissile inventory, given by: $M_{BOEC} \times RF \times \frac{T_{ex}}{T_{cycle}}$, where RF is the fraction of the core refueled at each refueling shutdown, T_{ex} is the ex-reactor interval between fuel discharge and recycle back into the reactor (typically one year) and T_{cycle} is the cycle length, i.e., the in-reactor reactor residence time

G is the fissile gain/cycle

L_p is the fuel cycle losses due to fabrication and reprocessing and is equal to $M_{EOEC} \times RF \times f$, where M_{EOEC} is the end-of-equilibrium cycle fissile inventory and f is the fraction which is lost in the external cycle, (typically around 1%)

L_d is the Pu241 decay loss for the external cycle and is equal to $M_{EOEC} \times RF \times [1-\exp(-\lambda T_{ex})]$ where λ is the deacy constant of Pu241

C is the number of refueling cycles per year

Note that $G >> (L_p + L_d)$

The breeding ratio (BR) is defined as:

$$BR = \frac{\text{fissile fuel produced during one operating cycle}}{\text{fissile fuel destroyed during one operating cycle}} \qquad (1.2)$$

The fissile gain G is related to the breeding ratio by the relation

$$G = (BR-1) \times (\text{fissile fuel destroyed during one operating cycle}) \qquad (1.3)$$

Thus the compound system doubling time is directly proportional to fissile inventory and is inversely proportional to the breeding gain. Both the breeding gain and the fissile inventory are monotonically increasing functions of the fuel volume fraction, but the breeding gain value saturates at high fuel volume fractions. Because of this, the CSDT decreases

initially as the fuel volume fraction is increased, goes through a minimum, and then increases as the breeding ratio value saturates at high fuel volume fractions. This behavior is shown in Fig. (1.1) for one particular study (C2). This figure shows the breeding ratio and the compound system doubling time (CSDT) as a function of the fuel volume fraction. Based on this discussion, if a particular homogeneous core, such as the one used in the French study (M1), is designed to have a fuel volume fraction below the optimum, adding internal blankets will push the system toward the optimum region with lower CSDT. It should be noted that there are many other design constraints that influence the optimum fuel volume fraction, but the region indicated by the CSDT minimum is the region of best neutronic performance. Current studies have indicated that the optimum fuel volume fraction for large UO_2/PuO_2 cores lies in the range of 40 to 44% (T1, C3).

Overall, besides the sodium void coefficient discussed earlier, there are several other advantages and disadvantages is going to heterogeneous designs with internal radial blankets as compared to equivalent homogeneous designs (B2).

The advantages include: a) lower flux levels by 30 to 40%, and in particular, a lower damage flux (i.e. flux over 0.1 M_{ev}) by about 30% in heterogeneous cores. This is mainly

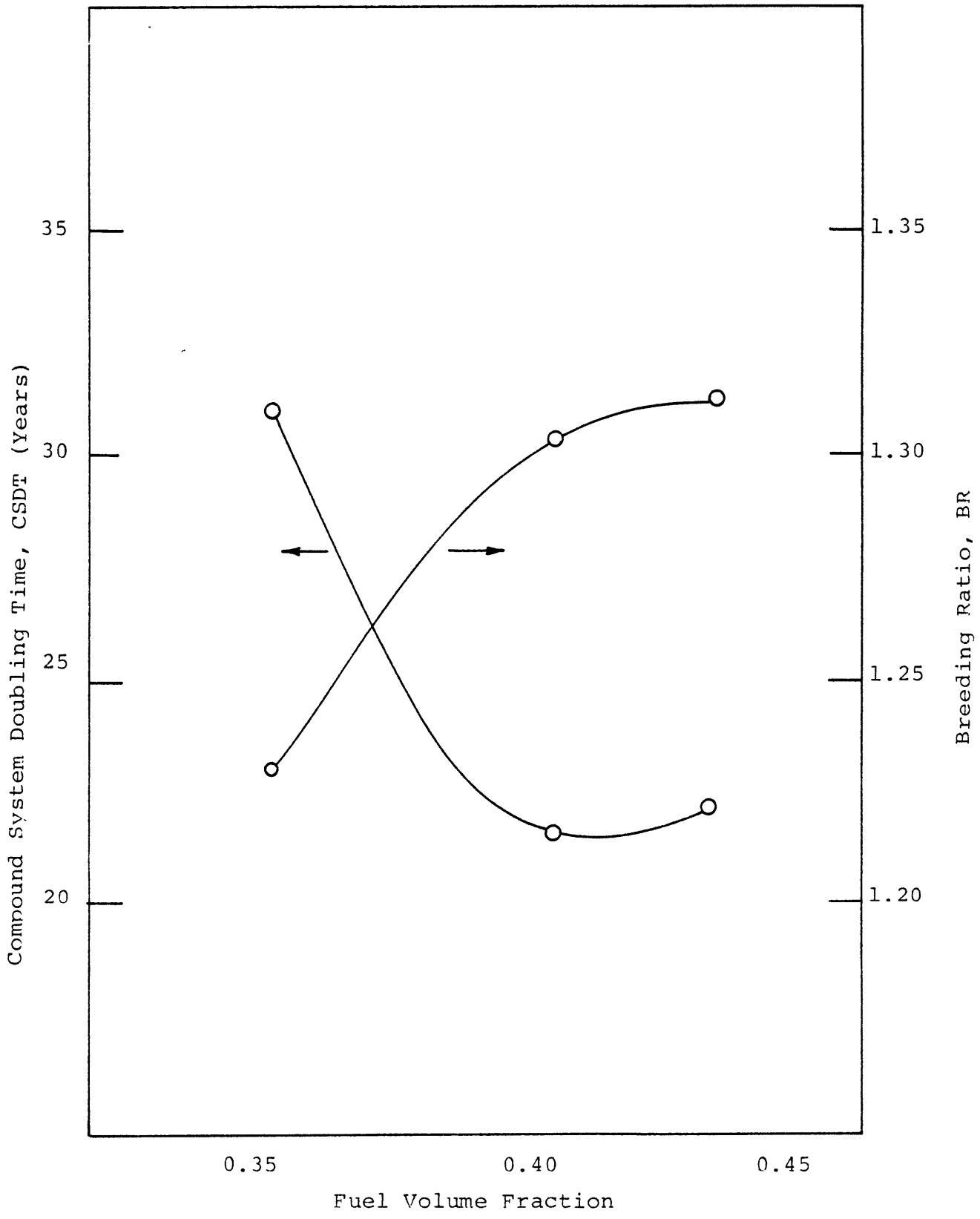

Fig. 1.1 Breeding Ratio and Compound System Doubling Time as a Function of Fuel Volume Fraction

due to the higher fissile enrichment of the heterogeneous cores. This lower flux leads to lower duct dilation due to creep and swelling; lower reactivity burnup swings in heterogeneous cores; and higher breeding gains in heterogeneous cores.

The disadvantages include: a) higher fissile inventory by about 30 to 40% in heterogeneous cores. This higher fissile inventory is partially offset by the higher breeding gain in heterogeneous designs, resulting in similar or slightly worse doubling times for the heterogeneous cores compared to the equivalent homogeneous designs, b) lower Doppler coefficient, c) lower peak and average burnup in heterogeneous designs for the same residence time as homogeneous designs.

1.4 Utilization of Thorium in Fast Breeder Reactors

Studies on the possibilities of thorium utilization in Fast Breeder Reactors had been performed from the earliest days of Fast Reactor design.

As a part of the Fast Reactor Blanket Project at M.I.T., Wood (W1) studied the use of thorium in the radial and axial blankets of homogeneous LMFBR cores. Compared to conventional uranium-blanketed cores it was shown that although the performance of the thorium-blanketed LMFBR is slightly inferior to a uranium blanketed system as regards to the overall breeding ratio, the fuel cycle cost can be considerably lower due to the production of U233, which has a high value in a system based on thermal and epithermal reactors.

The interest in the use of thorium in fast breeder reactors has been renewed recently due to the current concern over nuclear nonproliferation. This interest revolves around the concept of cross-progeny fuel cycles involving fast reactors, thermal reactors and advanced converters (C4, S1, L1, L2). In this concept the plutonium fueled reactors such as LMFBRs are built and operated in secure centers. Other reactors outside of these centers are fueled with either low enriched uranium or denatured uranium (U238 mixed with either 12% U233 or 20% U235).

As for the neutronic performance of thorium in fast breeder reactors, recent studies have looked at different ways thorium can be used in the core, axial or radial blankets (H1, M2).

The results show that replacing U238 in the radial blanket with thorium has a very slight effect on reactor performance, with a very small decrease in overall breeding ratio. The weak dependence of reactor core physics parameters on fertile blanket composition was also confirmed by Shin (S2). Replacing U238 with Th232 in the core, however, reduces the breeding ratio by 0.13 to 0.16. If the plutonium is replaced by U233 in the core (i.e., going to an all U233-Th cycle) the breeding ratio is reduced by another increment of 0.13 to 0.16, leaving the core with a very small breeding ratio ($\sim$1.054).

Thus the overall performance of thorium in fast breeder reactors is inferior to U238; but with the increasing concern over nuclear proliferation, the use of the thorium cycle in fast reactors may still be seriously considered.

1.5 Moderated Blankets

The first major study on the use of moderated blanket assemblies in fast reactors was carried out more than twenty years ago by Avery (A2). The objective in that particular design was to increase the neutron lifetime of the LMFBR to a value comparable to that of thermal reactors.

Perks (P2) looked at inner radial moderator assemblies using graphite, graphite-steel and sodium as the moderator. The results showed a small reduction in critical mass and an increase in the internal breeding ratio but a reduction in the radial blanket breeding ratio. The economic analysis showed that the reduction in core critical mass is not high enough to offset the reduction in overall breeding of the reactor and so the concept did not seem to be economically attractive.

Several other studies have also looked at moderated radial blankets (H2, M3, E1, S2). The moderators in these studies included graphite, ZrH_2 and BeO.

In all cases it was concluded that the inclusion of the moderator in the radial blanket results in a reduction in the overall breeding ratio. This is basically due to the fact that some fertile material is displaced by the moderator, plus the additional disadvantage of neutron capture by the moderator,

which results in a decrease in the number of neutrons available for capture in fertile material.

1.6 Fast Mixed Spectrum Reactor (FMSR)

The Fast-Mixed Spectrum Reactor (FMSR) is a new concept in the design and fuel management of fast breeder reactor cores, currently being studied at Brookhaven National Laboratory (F1).

The unique characteristic of this concept is that the reactor operates on a once-through fuel cycle.

The feed fuel material is natural or depleted uranium, which after about 17 years of residence in the blanket and several regions of the core, is discharged with an average enrichment of 7% fissile plutonium. While this discharged fuel can be used for other fast or thermal reactors, there is no reprocessing needed to operate the FMSR.

Therefore, this design offers the highest level of proliferation resistance (characteristic of no reprocessing requirements) among all of today's fast breeder reactor designs and fuel cycles. Currently, both sodium and gas-cooled versions of this concept are being studied.

Figure 1.2 shows a representative R-Z plan of the core, blanket and moderator zones of the FMSR. Zones 1 and 2 represent the outer and inner moderated blanket zones. Zones 3 through 6 represent the fast core and zones 7 through 12 represent the axial blanket.

The reactor can be started upon an average uranium enrichment of 7%, and a maximum of 11%. Several fuel management strategies have been, and currently are, being studied for

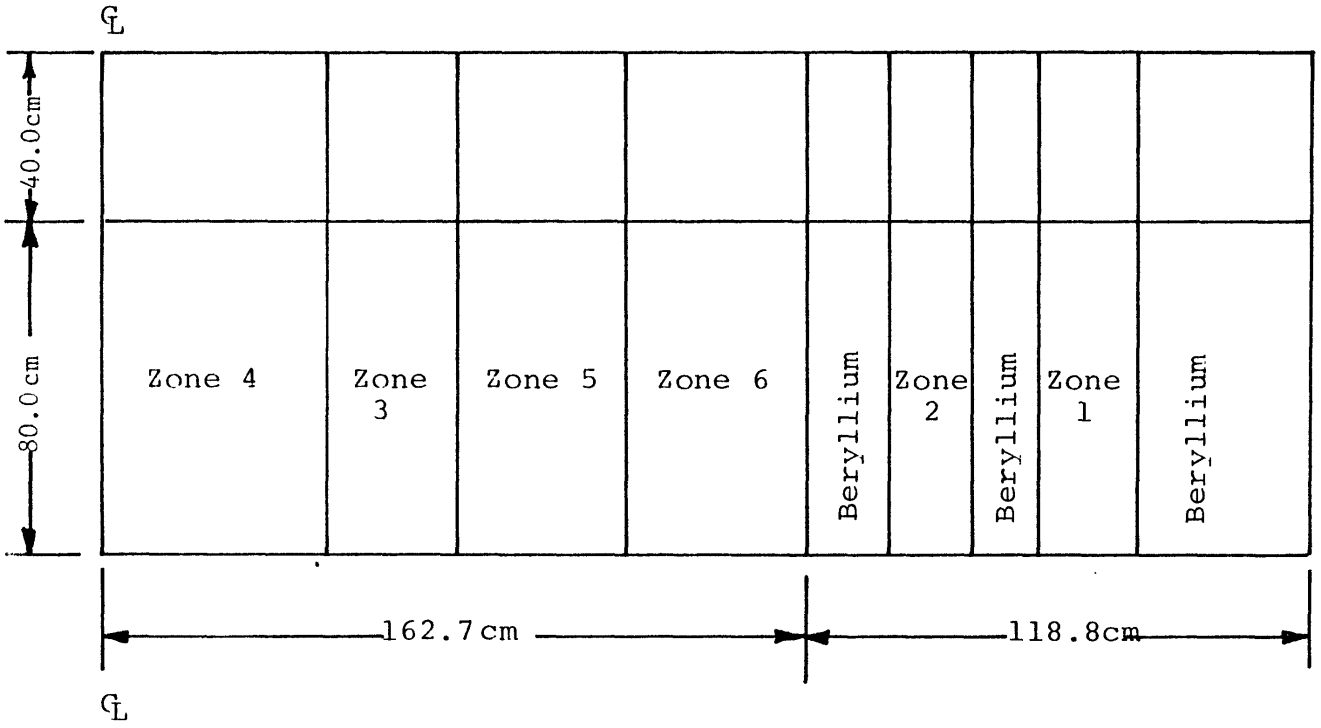

Fig. 1.2 R-Z Model of the Fast-Mixed Spectrum Reactor (FMSR)

this reactor. In one version, which has shown a very good neutronic performance, it takes 34 cycles of 185 days or about 17 years to reach to the steady state cycle. Once on the equilibrium cycle, the natural or depleted uranium is fed into Zone 1 (Fig. (1.2)). From there the fuel resides in the blanket for several cycles, building up plutonium and is then shuffled toward the fast core in succeeding cycles.

The fuel is next shuffled from the blanket into Zone 3 in the fast core; at this point, the fuel contains an average of 2.7% fissile plutonium.

The fuel, after several cycles of residence in Zone 3, is moved to Zone 4, and then outward to Zones 5 and 6, following which it is discharged.

The plutonium in the core builds up from an average enrichment of 2.7% fissile plutonium (as fed from the radial blanket) to the saturation level of 7%, which is essentially the enrichment of the discharged fuel. Total residence time of the fuel in the radial blanket and core is about 17 years.

The proposed fuel for this reactor is uranium metal clad with type 316 stainless steel. The burnup of the heavy metal is about 13-15%. Also, the cladding, and duct walls would be exposed to very high fluences, of the order of 8×10^{23} neutrons/cm^2 ($E > 0.1$ Mev), which is higher than the currently qualified limits for stainless steel 316.

Thus the problem of high fuel residence time, which results in these very high fluences, is one of the principal

areas under current study. Active work in this area includes evaluation of core designs and fuel management strategies which would lower the fuel residence time or flux level in the fast core, and consideration of materials technology developments which would improve the prospects for achieving FMSR design goals.

1.7 Purpose of the Present Work

The objective of the present work is the evaluation of a particular core design and fuel management strategy which synthesizes several current ideas as to how the fuel cycle economics and non-proliferation characteristics of conventional LMFBRs can be enhanced. The concept is based on a fuel management scheme in which the internal blankets, after several cycles of residence in the core (and hence fissile buildup), are moved into a moderated radial blanket. In this way the enriched internal blankets, when moved into the radial blanket, will generate a substantial fraction of the total core power. In larger LMFBR's radial blanket assemblies stay in the reactor for up to six years depending on the fuel management scheme employed (i.e., batch, in-out, out-in, or zone scatter).

The average beginning-of-cycle fraction of the total core power delivered by the radial blanket in a normal LMFBR is about 2.0%, which increases to about 5.5% by the end of the equilibrium blanket-cycle (B5). In the proposed fuel management strategy this power fraction is expected to increase

by an order of magnitude, with the additional advantage of improved power flattening: in particular the radial blanket power will vary less in both space and time.

These advantages can be translated into the capability of generating either higher power from the same core, or the same amount of power using a smaller fissile-fueled core. To enhance the power production from the radial blankets, the blanket spectrum is softened using zirconium hydride as the moderator. Moderation of the radial blanket will shift the spectrum toward the epithermal region, where the fission cross sections of both fissile plutonium and U233 are higher than in the fast region, resulting in enhanced power production.

There are two basic differences between the current and past studies as regards the use of moderator in the radial blanket assemblies. The first difference is related to the fact that the moderation is not used as the means to enhance the breeding of fissile material; rather it is used to increase the power production and the reactivity of the radial blanket assemblies which are already pre-enriched. The second difference lies in the choice of the moderator. In most of the previous studies graphite, beryllium or beryllium oxide were proposed as the moderator. In this study zirconium hydride is used as the moderator. Zirconium hydride has a much higher moderating power than C, Be or BeO (S3). This will permit a much more compact radial blanket design. Other potential advantages include: lower net leakage of core neutrons into

the radial blanket (hence lower steady state core enrichment), and lower overall reprocessing throughput. As was mentioned earlier the emphasis in this work is on conventional LMFBR technology and the breed/burn concept will be developed with a view toward retrofit capability into the current generation of fast reactor designs..

While GCFR applications will not be considered explicitly at this time, the potential for use in this class of fast breeder reactors will be kept in mind in the overall assessment.

1.8 Outline of the Present Work

The emphasis in the analysis of the proposed breed/burn fuel cycle will be on use of conventional state-of-the-art LMFBR technology. Thus a heterogeneous core typical of present-day designs is chosen as the reference core (B5) and all characteristics will be compared to those of this base case, similarly computed.

In Chapter 2 the arrangement and properties of this reference core are discussed. This is followed by a discussion of moderated blankets, including the relevant properties of the moderator and moderated blanket assembly design. The details of the cross section preparation are discussed next, including a description of the basic cross section library and the methods and models used for group-collapsing of the cross sections to be used in burnup calculations. The next section deals with the methods employed in the burnup analysis, and includes a description of the core model and isotope

chains used in this analysis. The validity of the assumptions underlying these calculations is also discussed. The economics model is described next, covering the basic assumptions inherent in the model and their validity. The final section includes a summary assessment of the preceding discussions of methods and models.

Chapter Three deals with the depletion calculations. In this chapter the neutronic performance of the reference core is first studied, and compared with the results reported in the reference study (B5) to confirm the procedures and methods employed in the burnup analysis. The neutronic properties of the (U-Pu)O_2 cores with thorium blankets, and employing the in/out, moderated shuffling strategy, is considered next. In this study an optimum configuration for the internal and moderated radial blankets is found first. This is followed by a depletion analysis of several breed/burn cores having different degrees of moderation, burnup cycle length and core and blanket designs. Several related topics such as the criticality of U-Pu and Th-U233 blanket assemblies as a function of moderation, and the possibilities of using moderator in the internal blankets as a means to control the excess reactivity is also discussed. The results of the depletion calculations are summarized in the last section.

In Chapter Four the results of the depletion analysis performed in Chapter Three are used to calculate the levelized fuel cycle cost. A reference economic environment which

includes all the relevant unit costs and financial parameters is first defined. Uncertainties associated with these values and their effect on the fuel cycle cost are discussed. The relationships used for the calculation of the levelized fuel cycle cost are discussed next, followed by calculation of the fuel cycle cost for the reference core and the breed/burn core. A summary of the results and conclusions are presented at the end of the chapter.

The neutron and gamma heating of the core and blankets are discussed in Chapter Five. In this chapter the relative importance of the neutron and gamma heating and the contribution of the gamma and neutron heating to the total heating rate and linear heat generation rate are discussed. To insure that moderator pins can be used in the radial blanket environment, the maximum moderator pin temperature due to neutron and gamma heating is calculated and compared to the maximum allowable temperatures of the moderator.

In the final chapter a summary of the work performed in this study, and the final recommendations are presented.

CHAPTER TWO

REACTOR MODELS AND METHODS OF CALCULATIONS

2.1 Introduction

The primary objective of the current work is the evaluation of blanket fuel management strategies through which the economic and nonproliferation characteristics of LMFBR's can be enhanced.

To study the proposed ideas, a reference LMFBR core was chosen and two sets of cross sections were generated: one for $(U\text{-}Pu)O_2$ cores with depleted uranium internal and radial blankets, and another for $(U\text{-}Pu)O_2$ cores with thorium internal and radial blankets. In this context, the contents of this chapter includes discussion of:

1. The reference core configuration and composition.
2. Cross section preparation and group collapse.
3. Burnup analysis, including core modeling and fuel management methods.
4. The economics model used to assess the options examined.

In this chapter only the procedures relating to the various calculations are discussed. The actual calculations and results are discussed in Chapter Three.

2.2 Reference Reactor

The reference core has been chosen based on a study done at Argonne National Laboratory (B5). In this study several homogeneous and heterogeneous cores were examined. The heterogeneous cores differed in the number and the arrangement of the internal blankets. Among the tightly coupled heterogeneous cores the results were quite similar with respect to neutronic, safety and economic performance. One of these configurations was taken as the reference core for the present work. Figure 2.1 shows the planar view of a 60° section of the core and radial blanket. The core consists of 780 fuel assemblies, two enrichment zones with outer to inner core enrichment ratio of 1.15. There are 415 internal blanket assemblies distributed over several rings, three rows of radial blankets consisting of 414 assemblies, and three rows of radial shield.

General data about the reactor is given in Table 2.1. Data related to the fuel and blanket assemblies are given in Tables 2.2 and 2.3, respectively. The internal and radial blanket assemblies are exactly the same. The fuel material is $(U\text{-}Pu)O_2$, and the internal and radial blanket material is depleted uranium in the reference core. In this study a $(U\text{-}Pu)O_2$ core with thorium internal and radial blankets was also analyzed. In both cases the internal and radial blanket fuel smear-density as a percentage of the theoretical density is kept the same. The duct wall and cladding material is 20% cold worked stainless steel 316.

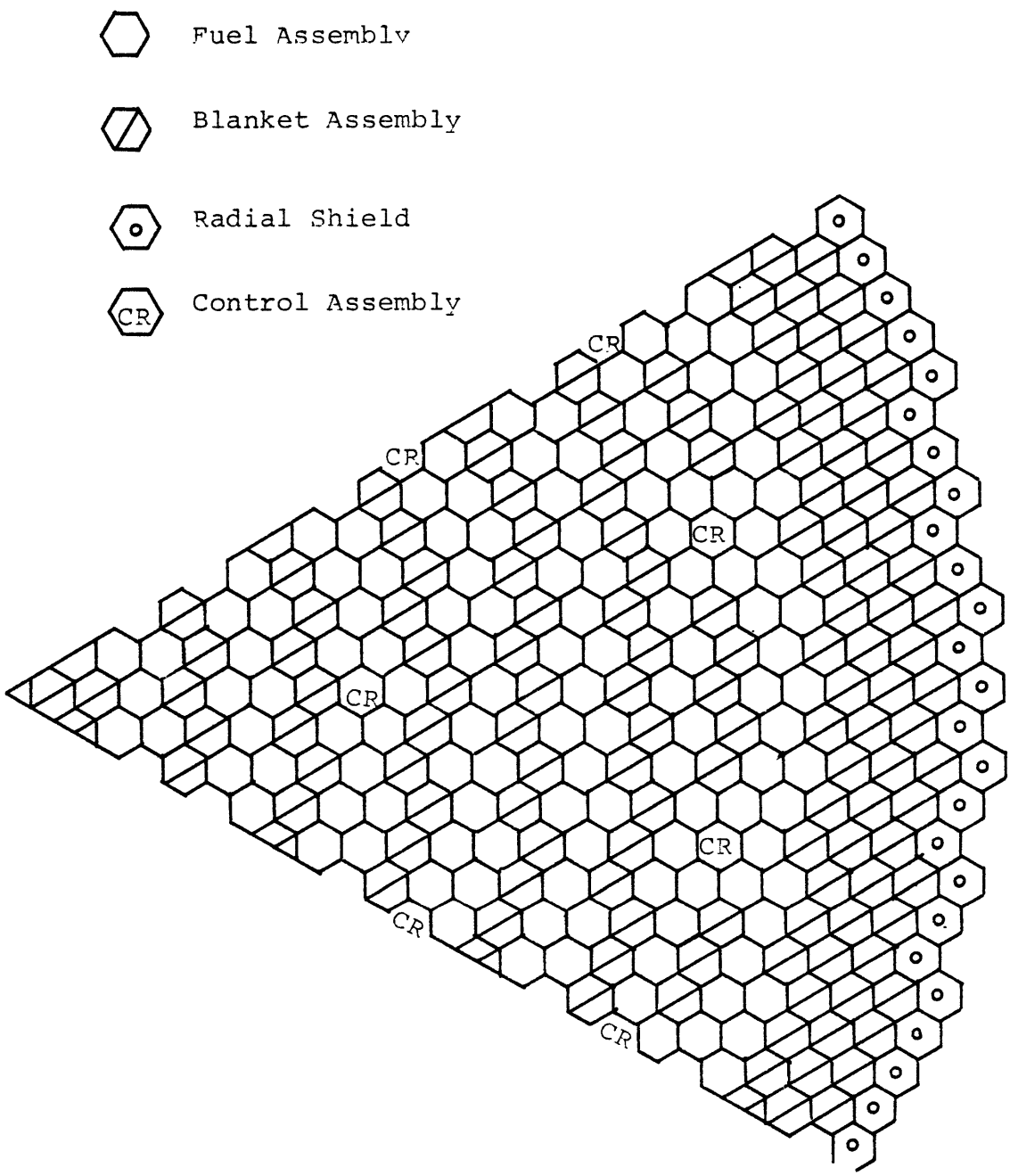

Fig. 2.1 Planar View of the Reference Core

Table 2.1

General Reactor Characteristics

Reactor Power, MWt	4124
Plant Electrical Power, MWe	1200
Reactor Vessel ΔT,°F	249
Reactor Vessel Outlet Temperature, °F	895
Maximum Coolant Velocity, ft/sec	21.0
Bundle ΔP, Psi	46.5
Full Power Capacity Factor, %	70
Clad/Duct Material	316SS, 20% CW

Table 2.2

Fuel Assembly Parameters

No. of Assemblies	780
Assembly Pitch, in	4.682
Duct Outside Flat-to-Flat, in	4.575
Duct Wall Thickness, in	0.12
Pins Per Assembly	217
Pin Pitch/Diameter	1.24
Active Core Height, in	36
Axial Blanket Height, in	14
Pin OD, in	0.23
Clad Thickness, in	0.015
Oxide Smear Density, % TD	85.5
Peak Pellet Linear Power, (3σ, 15% overpower) KW/ft	14.4
Axial Blanket Pellet Density, % TD	95.9
Volume Fractions	
Fuel	0.3591
Structure	0.2436
Coolant	0.3973

Table 2.3

Blanket Assembly Parameters

No. of Assemblies	
Internal	415
Radial	414
Assembly Pitch	4.682
Duct Outside Flat-to-Flat, in	4.575
Duct Wall Thickness	0.12
Pins Per Assembly	127
Pin Pitch/Diameter	1.102
Pin OD, in	0.506
Cladding Thickness, in	0.015
Fuel Height, in	64
Oxide Smear Density, %TD	93.7
Peak Linear Pin Power, (3σ, 15% overpower), KW/ft	20
Volume Fractions	
Fuel	0.5278
Structure	0.2634
Coolant	0.2088

The homogenized fuel plus internal blanket volume fraction is 0.4177 for the core under study, which is in the optimum fuel volume fraction range of 40 to 44% mentioned in Chapter 1.

2.3 Moderated Blanket Assemblies

As was mentioned in Chapter One, to enhance the power production of the radial blanket, the spectrum in the radial blanket is softened using zirconium hydride as the moderator. This spectrum softening increases the power production in the radial blankets, which are self-enriched with the plutonium or U233 produced in the internal blanket assemblies, while they were in the core. As will be shown in the next chapter, the strategy of moving enriched internal blankets to the radial blanket also increases the reactivity of the radial blanket and reduces the neutron leakage from the core to the radial blanket. This results in a modest reduction of the core enrichment for the $(U\text{-}Pu)O_2$ core with a depleted uranium blanket. For the case with thorium internal and radial blankets, the moderated Th-U233 system has a much higher reactivity due to the higher value of η for U233 in epithermal spectra. However, as will be shown later, this advantage only helps to cancel the fissile inventory penalties that are encountered in using thorium instead of uranium in the internal blanket assemblies.

In this section the properties of the moderator, i.e., zirconium hydride, and a proposed assembly design for the moderated blanket assemblies will be discussed. Studies on

the optimum level of moderation and the physics of moderated blankets will be discussed in Chapter Three.

2.3.1 Properties of Zirconium Hydride

The moderator used in the radial blanket assemblies is zirconium hydride ($Zr\ H_{1.6}$) (S3). The major advantage of zirconium hydride over other solid moderators, such as beryllium or graphite is the high moderating power ($\xi\Sigma_s$) of zirconium hydride due to its high hydrogen content (approximately the same as that of H_2O). The high moderating power of zirconium hydride enables the design of the radial blanket to be much more compact compared to similar designs with other solid moderators, with the additional capability for changing the level of moderation without much change in the number of the moderator pins.

There has been considerable experience with zirconium hydride both in pure form, i.e., zirconium hydride rods cladded with stainless steel and also in fuel elements as a mixture of uranium and zirconium hydride.

In the pure form, zirconium hydride has been successfully used as the moderator in an experimental thermal reactor fueled with $(U\text{-}Pu)O_2$ and cooled with sodium (H3). Their experience showed excellent compatibility of zirconium hydride with stainless steel cladding and sodium and a very stable behavior under irradiation, with no significant hydrogen loss or diffusion. The SNAP reactors (L3) and TRIGA reactors (S4, S5) use zirconium hydride mixed with the fuel to form a combination fuel-moderator element. There have also been studies on the

use of zirconium hydride for shielding applications (V1, A3). Zirconium hydride is essentially a simple eutectoid with four separate phases: Alpha (HCP), Beta (BCC), Delta (FCC) and Epsilon (FCT). At the hydrogen to zirconium ratio of 1.6 (delta phase) the hydrogen dissociation pressure is 1 atmosphere at about 750°C. Due to the absence of a second phase there are no volume changes or cracking as temperature is raised beyond the phase transformation temperature of 540° C. Hydrogen losses and redistribution are also very low at this composition. Based on these properties a zirconium hydride composition of Zr $H_{1.6}$ has been used in most reactor applications.

The range of composition of zirconium hydride extends up to Zr H_2, and its density depends on the hydrogen to zirconium ratio. Table 2.4 shows zirconium hydride's density as a function of H/Zr (G1). With respect to the irradiation effects on zirconium hydride, in addition to the results from SNAP and TRIGA reactors on fuel-zirconium hydride mixtures, there have been several experiments on pure delta and epsilon phase zirconium hydride. In one set of experiments the samples were irradiated at temperatures up to 580°C and fluence up to 1.15×10^{25} n/m^2 (E > 1 Mev). The results were quite satisfactory with no swelling shown in the delta phase zirconium hydride. In another set of experiments zirconium hydride specimens of Zr $H_{1.5}$ and Zr $H_{1.7}$ composition were irradiated in EBR II. The samples were irradiated at 400°C and fluences of 5 to 7×10^{26} n/m^2 (E > 0.1 Mev). The post-irradiation examinations

Table 2.4

Zirconium Hydride Density as a Function of H/Zr
(Measurements at Room Temperature)

H/Zr	Density (gm/cm^3)
0	6.49
1.54	5.66
1.81	5.62
1.87	5.61
1.90	5.59
1.94	5.46

showed no significant damage to the specimens.

Zirconium hydride has been fabricated at General Atomics since 1957. The 1975 cost estimate provided by General Atomics was about $65/Kg (S3).

2.3.2 Moderated Blanket Assembly Design

The design of the internal and radial blanket assemblies for the accommodation of the moderator depends on the level of moderation required, i.e., the volume fraction of zirconium hydride needed in the blanket assemblies. For a given total reactor power, as the volume fraction of the moderator in the blanket assemblies increases, the power density of the blanket assemblies also increases. The optimum volume fraction of the moderator is determined by the highest power density attained without exceeding fuel pin power peaking problems. The analysis leading to the determination of this optimum volume fraction will be presented in Chapter Three. In this section a possible design for the moderated blanket assemblies is presented. Figure 2.2 shows a typical blanket assembly with 127 pins. In this figure the volume corresponding to 28 of the pins or 22.0% of the total fuel volume is taken up by large pins that could be filled with the moderator. It should be noted that the volume of coolant necessary to cool the moderator pins is lower than that for the fuel pins, hence large moderator pins can be employed. In Chapter Five, a discussion of the neutron and gamma heating of the moderator pins will be presented.

A similar type of design has been proposed by engineers

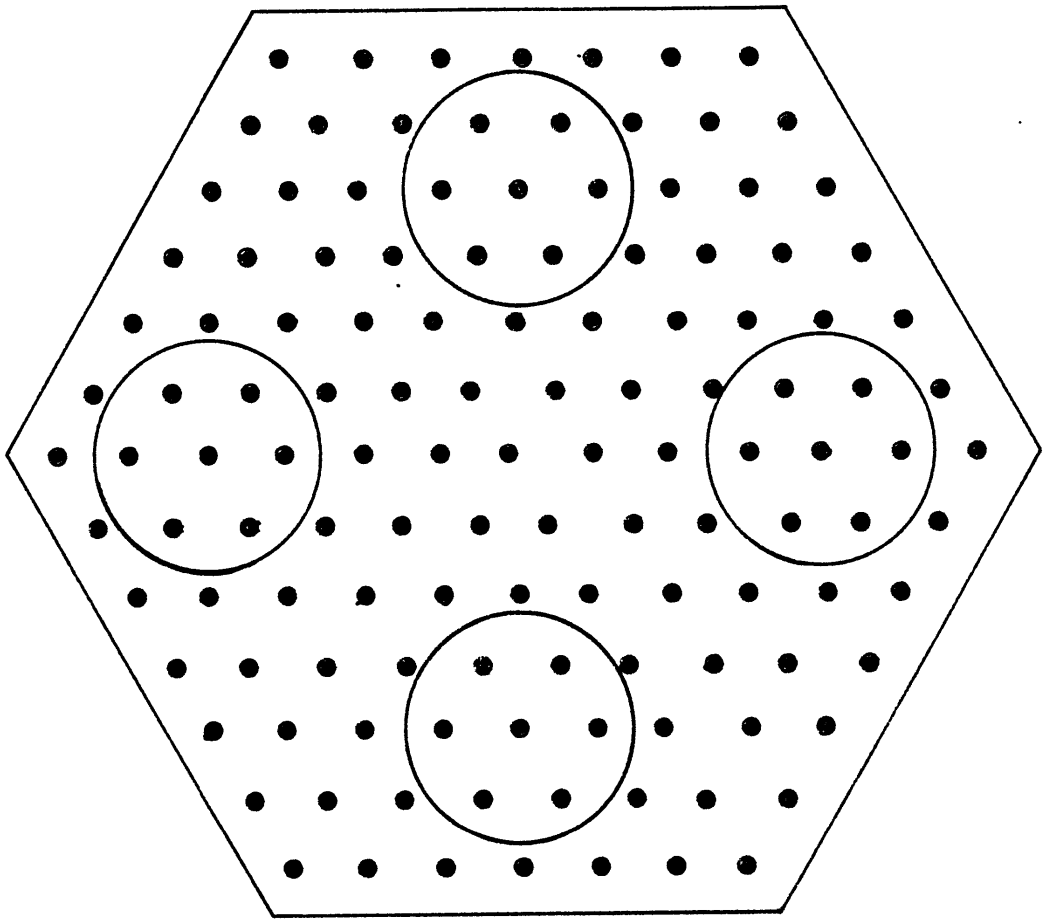

Fig. 2.2 Conceptual Design of a Blanket Assembly Containing Moderator Rods

at Westinghouse Hanford for composite fuel-internal blanket assemblies (C5). Figure 2.3 shows the proposed design, which contains 168 fuel pins and 7 blanket pins. The idea behind this design is to construct a core based on this type of composite fuel-internal blanket assemblies instead of separate fuel and internal blanket assemblies used in conventional heterogeneous designs.

The sketch in Fig. 2.2 showing one possible design for the moderated blanket assemblies is merely intended to suggest a design that can be used for this purpose. The actual design of a blanket assembly must be carried out based on a detailed thermal-hydraulic-mechanical analysis beyond the scope of the present work.

2.4 Cross-Section Preparation

The 50 group LIB-IV microscopic cross sections were used as the basic cross section set (K3). This set was corrected for resonance self-shielding and temperature dependence using the code SPHINX (D1). For the burnup calculations the shielded 50 group cross sections were collapsed to 10 groups based on a one dimensional diffusion calculation by SPHINX on the actual geometry of the core. Table 2.5 gives the structure of the 10 group cross section set used. This structure is similar to a 9 group cross section set used by Oak Ridge National Laboratory with the addition of one extra group in the thermal region (T2). The structure of this cross section set is also shown in Table 2.5. Figure 2.4 shows the one dimensional radial model used for

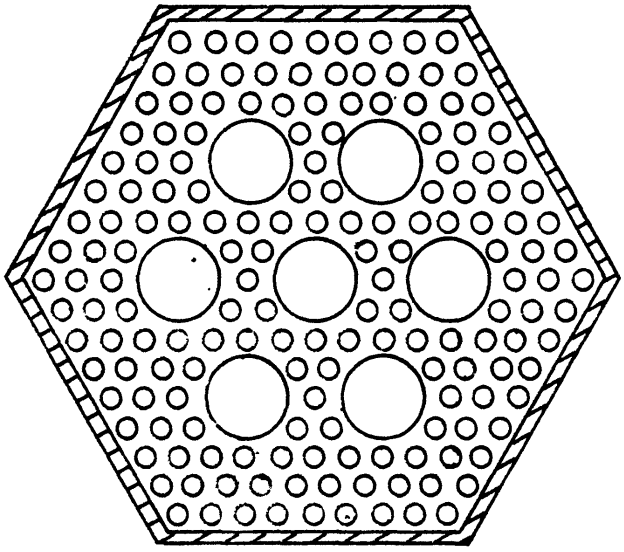

Fig. 2.3 Composite Fuel-Blanket Assembly Design (C5)

Table 2.5

Structure of the 9 Group ORNL Cross Section Set (T2) and the 10 Group Cross Section Set Used Here:

	Upper Energy (ev)	
Group	ORNL (9G)	MIT (10G)
1	1.7733 E7*	1.99711 E7
2	6.0653 E6	6.06531 E6
3	1.1080 E6	1.35335 E6
4	4.9787 E5	4.97871 E5
5	4.0868 E4	4.08677 E4
6	3.3546 E3	3.35463 E3
7	2.6126 E3	2.61259 E3
8	1.0130 E2	1.01301 E2
9	1.0 E1	8.31529 E0
10		6.8256 E-1

*Read as 1.7733×10^7

Zone

1. Internal Blanket (inner core)
2. Fuel (inner core)
3. Internal Blanket (outer core)
4. Fuel (outer core)
5. Radial Blanket Row 1
6. Radial Blanket Rows 2 and 3
7. Radial Shield

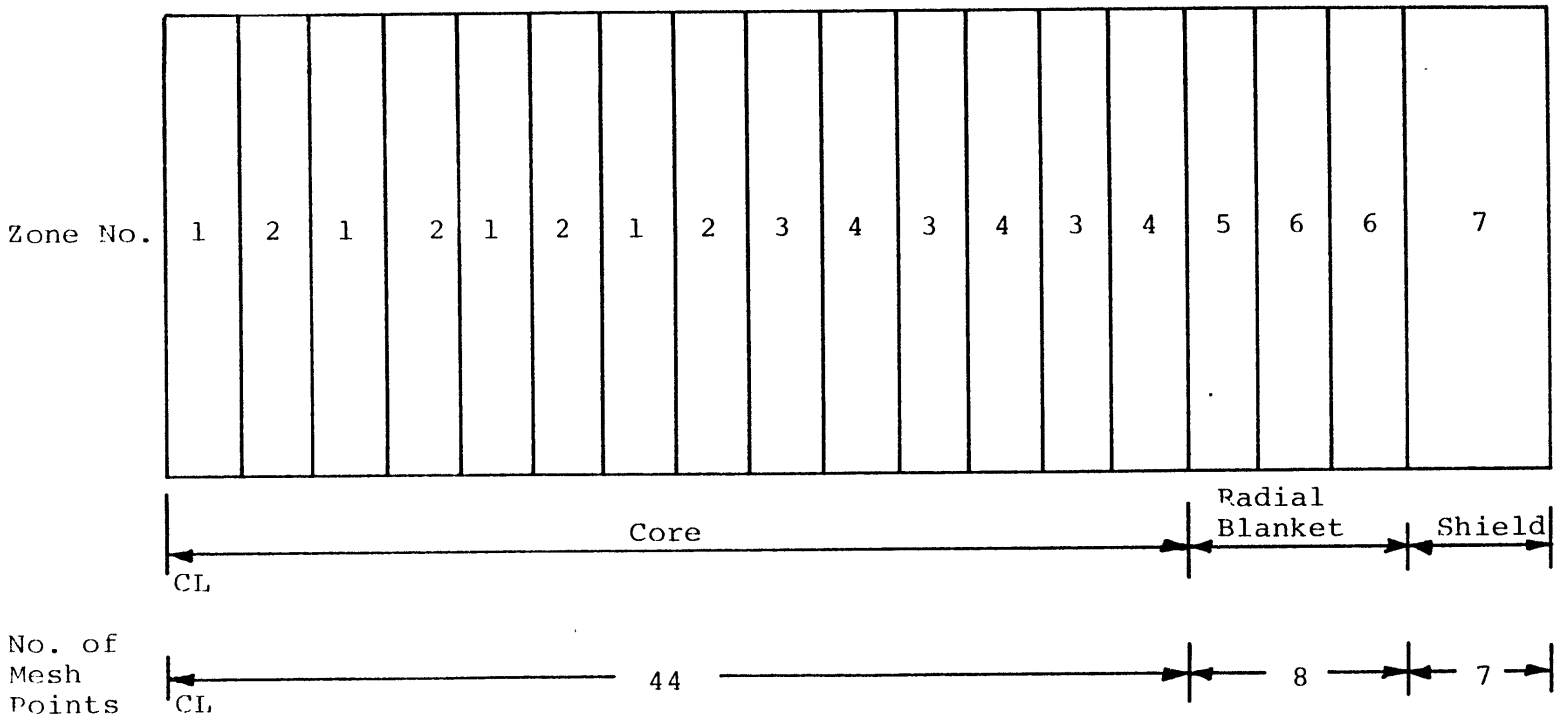

Fig. 2.4 One Dimensional Model Used for Cross Section Collapsing

group collapsing in SPHINX. The core is divided into two regions, where fuel and internal blanket cross sections are collapsed in the inner and outer regions. The axial blanket extensions of the blanket assemblies are collapsed in the Zone 3 spectrum. The axial blanket extensions of the fuel assemblies are collapsed in the Zone 4 spectrum. The control rods and sodium channel cross sections are collapsed in the Zone 2 spectrum. This calculation was performed for the $(U\text{-}Pu)O_2$ core with both depleted uranium and thorium internal and radial blankets, i.e., two sets of cross sections were generated: one for each of the two systems under study.

For the fission products a new set of 50 group cross sections were generated based on the results reported by the Japanese Nuclear Data Committee (JNDC) (K3). The reason for using a different fission product cross section set than the one included in LIB-IV is due to the uncertainty about the fission product values in this library. There are three options for the fission product cross section in the LIB-IV set: these include, saturating, slowly saturating, and non-saturating categories. Currently there is some confusion about the applicability of each set for fast reactor calculations. As an example, Brookhaven National Laboratory has studied this problem for their fast reactor calculations and has chosen the non-saturating set increased by a factor of 2.7, i.e., the fission product cross sections in LIB-IV are multiplied by 2.7 and the resulting set is used as the fission product cross

section set (F1). Also, the LIB-IV fission product cross section set does not have any downscattering matrix.

The JNDC evaluated in detail 28 of the most important fission product nuclides, which constitute about 80% of the total capture by fission products. This was supplemented with 165 nuclides evaluated by Cook (C6). The concentrations of these 193 nuclides were determined for fast reactor burnups of 1, 30, 60, 180, 360 and 720 days. These concentrations were then used to produce lumped fission products in 70 groups and 47 downscattering terms. The variations in the one group fission product cross section set collapsed in a 1000 MWe fast reactor spectrum was less than 2% in the period from 180 to 720 days. Consequently, the values at 360 days were used in our calculations.

Benchmark calculations based on the integral measurements have shown a better agremeent between the results calculated with the Japanese fission product cross section set and experimental results than with the ENDFB/4 fission product cross section set (K3).

The 70 group lumped JNDC set was collapsed to the LIB-IV 50 group energy structure using fission and 1/E spectra (L4). Table 2.6 shows the ratio of the JNDC's 50 group fission product capture cross sections to the LIB-IV cross section set multiplied by 2.7, i.e., the set used by BNL.

The Japanese fission product cross section library does not include values for U233 fission products. To generate U233

Table 2.6

Fission Product Capture Cross Section Ratio of JNDC to LIB IV x 2.7

Group	σ_c^{JNDC}/σ_cLIB IV	Group	σ_c^{JNDC}/σ_c LIB IV
1	0.07937	26	1.15834
2	0.18915	27	1.18386
3	0.53271	28	1.23698
4	0.96746	29	1.20836
5	1.17042	30	1.22464
6	1.20366	31	1.26440
7	1.24069	32	1.29982
8	1.27833	33	1.59619
9	1.29605	34	1.52277
10	1.29803	35	1.07200
11	1.23524	36	0.72979
12	1.16735	37	1.40743
13	1.14966	38	1.40306
14	1.14659	39	2.78448
15	1.14898	40	0.96248
16	1.15344	41	3.03949
17	1.15711	42	1.58189
18	1.15979	43	9.35697
19	1.16517	44	10.68521
20	1.18013	45	1.90879
21	1.18096	46	72.22638
22	1.17810	47	18.38698
23	1.17150	48	31.07376
24	1.16405	49	61.69649
25	1.16184	50	7.24559

fission product cross sections from the existing U235 and U238 values the following procedure was used. It has been shown (P3, P4, P5) that both the prompt and delayed neutron yields from either neutron rich fission fragments or delayed neutron precursors follow the relationship:

$$Y = Y_o \exp [-b\ (3Z-A)] \tag{2.1}$$

where Y is the number of prompt or delayed neutrons per fission, Y_o and b are constants, Z is the atomic number and A is the mass number of the fissioning nuclide.

Based on the fact that delayed neutrons are emitted by fission fragments, the yield of the other fission product isotopes from different isotopes of an element such as uranium should also follow the same relationship. To examine this postulate a set of isotopes with high fission yields from different isotopes of uranium were chosen for examination, as listed in Table 2.7 (N1).

Since

$$Y = Y_o \exp [-b\ (3Z-A)] \approx Y_o [1-b(3Z-A)] \tag{2.2}$$

and Z is the same for all uranium isotopes, the linear relationship should also be valid for the yields vs. the mass number A. Figures 2.5 through 2.7 show the plot of yield as a function of atomic mass for several of the isotopes given in Table 2.7. The straight lines are least mean square fit to the data and they all fall within the error band of the yields for the different isotopes. It is also interesting to note

Table 2.7

The Yield of Several Fission Product Isotopes Produced in the Fission of Uranium Isotopes (N1)

Isotope	Yield (%) U233	U235	U238
$^{90}Kr_{36}$	4.491±16.1%	4.464+9.0%	3.319±7.0%
$^{91}Rb_{37}$	5.892±12.0%	5.262±5.0%	4.01 ±7.0%
$^{90}Sr_{38}$	6.8 ±10.1%	5.46 ±5.0%	3.51 ±5.0%
$^{91}Y_{39}$	6.81 ±10.1%	5.522±5.0%	3.64 ±15.0%
$^{95}Zr_{90}$	6.589±10.1%	6.38 ±3.9%	5.579± 8.0%
$^{131}I_{53}$	3.54 ±10.1%	3.501±10.1%	3.36 ± 6.1%
$^{138}Cs_{55}$	6.767±10.1%	6.485±8.0%	6.25 ± 4.0%
$^{141}Ce_{58}$	6.09 ±15.1%	5.67 ±4.9%	5.044± 5.0%
$^{99}Mo_{42}$	4.89 ±10.1%	6.125±5.0%	6.328± 5.0%
$^{101}Mo_{42}$	2.678±15.1%	5.284±4.0%	6.377± 16.0%
$^{147}Nd_{60}$	1.67 ±10.1%	2.18 ±3.9%	2.631± 5.0%
$^{132}Te_{52}$	4.285±11.0%	4.805±5.0%	4.927± 4.1%

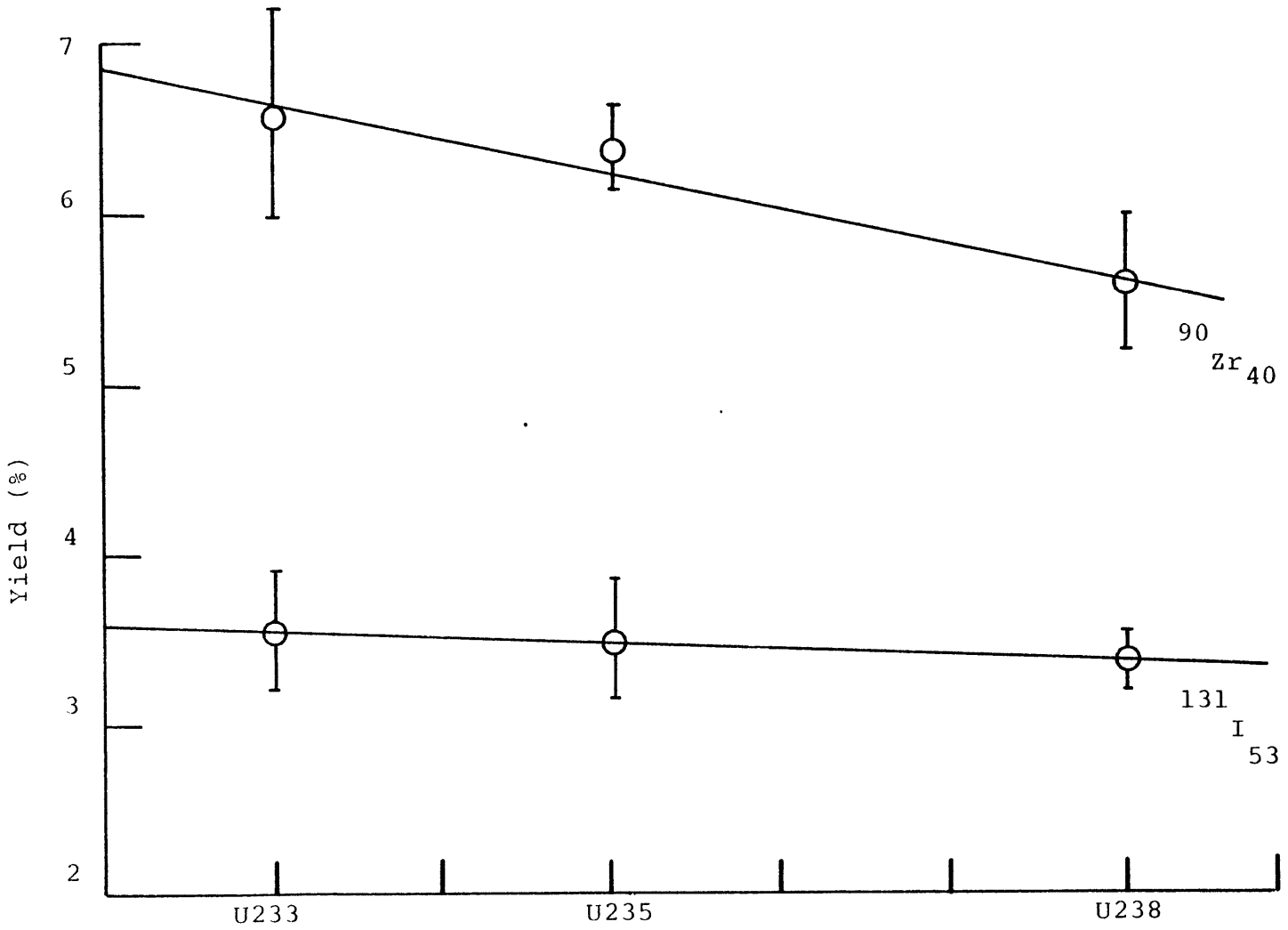

Fig. 2.5 Yield as a Function of Mass of Nucleus Fissioned for $^{90}Zr_{40}$ and $^{131}I_{53}$

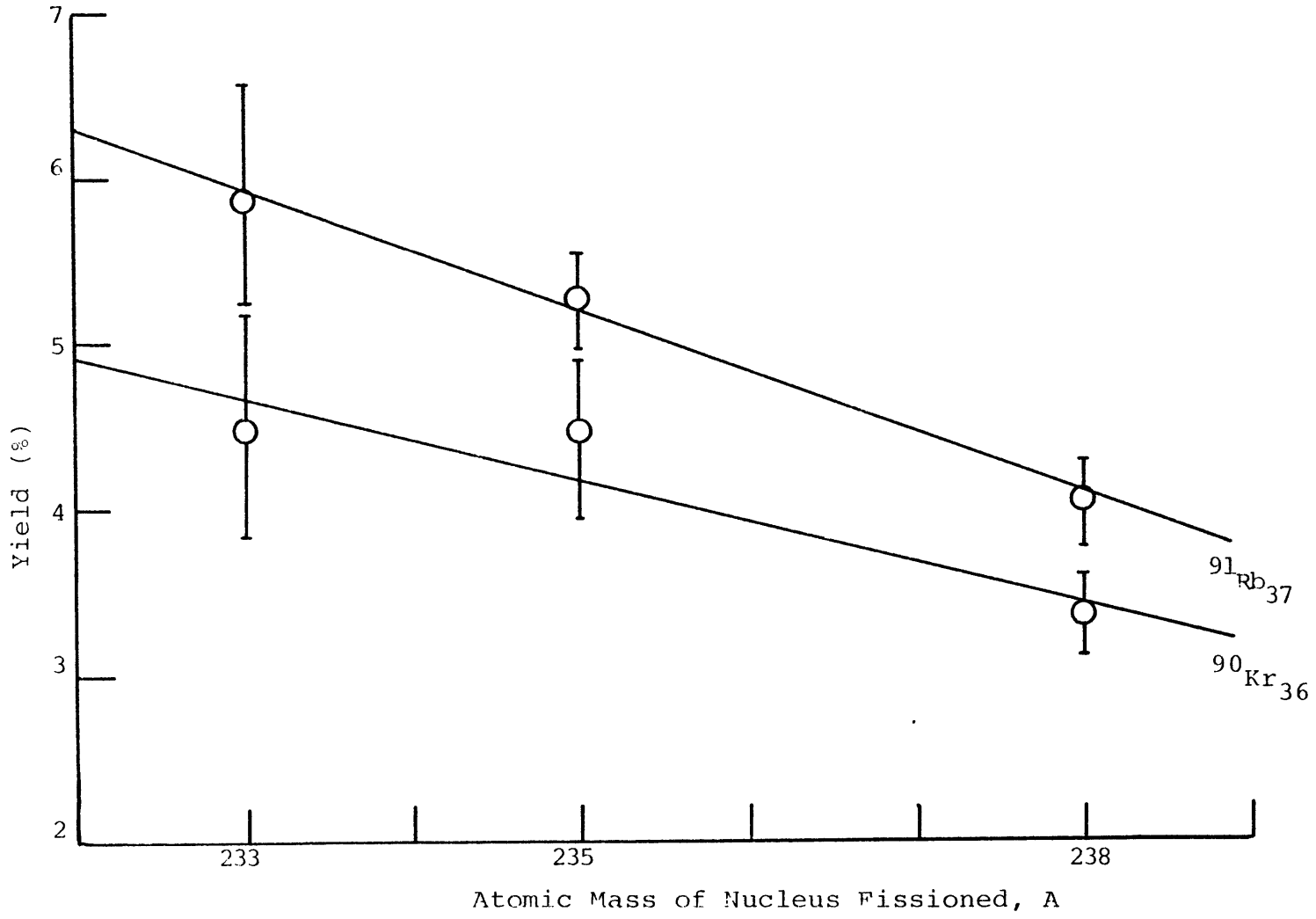

Fig. 2.6 Yield as a Function of Mass of Nucleus Fissioned for $^{91}Rb_{37}$ and $^{90}Kr_{36}$

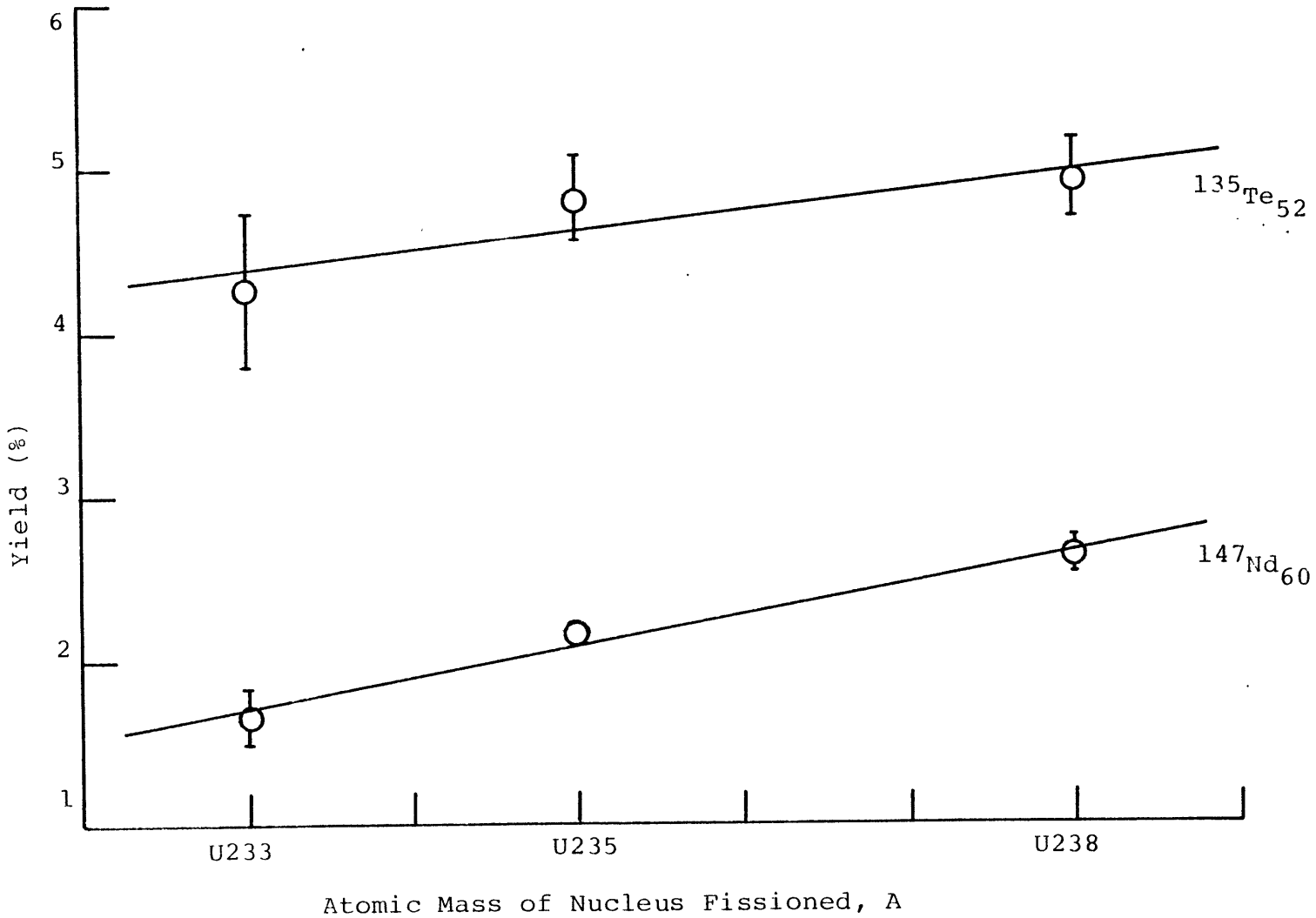

Fig. 2.7 Yield as a Function of Mass of Nucleus Fissioned for $^{135}Te_{52}$ and $^{147}Nd_{60}$

that this linear relationship has either a positive or negative slope, but since the summation of a set of linear equations is also linear, the total fission product yield is also a linear function of mass.

The lumped fission product cross section for interaction X (for example capture) can be found from the relation

$$\overline{\sigma_x} = \frac{\sum_i \sigma_{xi}\, y_i\, f_i}{\sum_i y_i\, f_i} \qquad (2.3)$$

where:

σ_{xi} is the microscopic cross section for interaction x of fission product isotope i.

y_i is the yield for isotope i.

f_i is a factor depending on the decay status of the fission fragment i and is a function of its half life.

Note that $\sum_i y_i = 2$.

Equation (2.3) demonstrates that if the yields of different fission product isotopes for the various isotopes of an element such as uranium follow a linear relationship as a function of mass number A, then the lumped fission product cross sections (for a given energy group or an entire spectrum) should also be a linear function of A. Table 2.8 gives a set of one group lumped fission product capture cross sections for thorium,

Table 2.8

One Group Fission Product Capture Cross Sections

Collapsed over a GCFR Spectrum

Isotope	$\sigma_c^{F.P.}$ (barns)
$^{90}Th_{232}$	0.141
$^{92}U_{233}$	0.115
$^{92}U_{235}$	0.135
$^{94}U_{238}$	0.171
$^{94}Pu_{239}$	0.178
$^{94}Pu_{241}$	0.182

uranium and plutonium isotopes collapsed in a typical GCFR spectrum (L4). The values for uranium isotopes are plotted in Fig. (2.8). It can be seen that the linear hypothesis holds quite well for this set of data.

Using the existing Japanese 70 group lumped fission product cross sections for U235 and U238, a set of 70 group lumped fission product cross sections was generated for U233 using linear extrapolation. The 70 group U233 fission product set was next collapsed to 50 groups compatible with the LIB-IV structure using fission, 1/E and Maxwellian weighting spectra in the appropriate energy ranges. Both the Pu239 and U233 50 group fission product sets were next collapsed to 10 groups using the spectra of the zones shown in Fig. 2.4,determined using the SPHINX program. The lumped one group cature cross section of U233 and of Pu239 collapsed using a 50 group fuel region flux are given in Table 2.9. Note that the ratio of the one group U233 fission product capture cross section to that of Pu239 from the above calculations is very similar to the results reported for GCFR calculations.

The group collapsing from 50 groups to 10 groups has a very small effect on reactor integral parameters such as k_{eff} and breeding ratio. This can be seen in Table 2.10 which shows the results of 50 and 10 group calculations at the beginning and end of cycle for a particular fast reactor core under study at Brookhaven National Laboratory and M.I.T. (F1, L5). Both calculations were performed on an R-Z geometry of

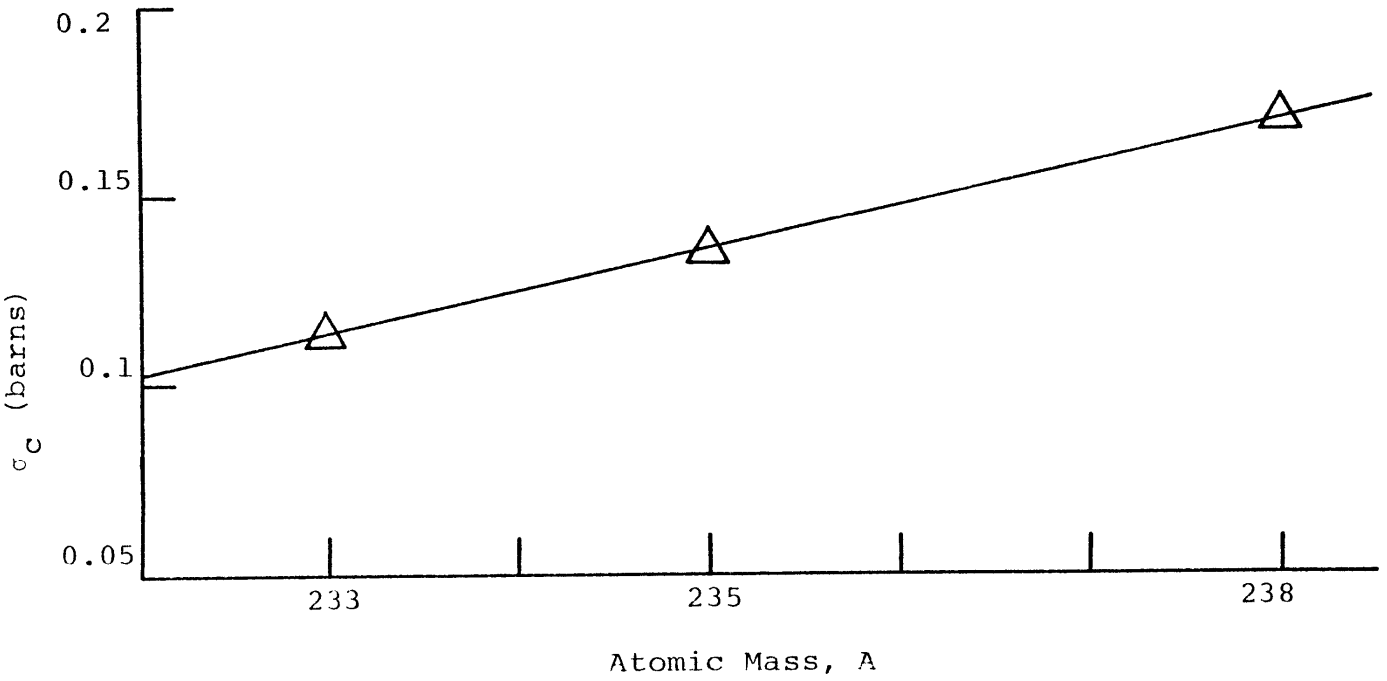

Fig. 2.8 One Group Capture Cross Section for Uranium Fission Products as a Function of Atomic Mass

Table 2.9

One Group Fission Product Capture Cross Section of U233 and Pu239 Collapsed over an LMFBR Spectrum

Isotope	$\sigma_c^{F.P.}$ (barns)
U233	0.3073
Pu239	0.5041
U233/Pu239	0.6096
(U233/Pu239)*	0.6460

*From Table 2.8

Table 2.10

k_{eff} and Breeding Ratio Comparison Between

50 and 10 Group Calculations

	50 Group* Calculation	10 Group** Calculations
K_{eff}		
BOEC	0.982	0.986
EOEC	1.000	1.004
Breeding Ratio		
BOEC	1.67	1.67
EOEC	1.61	1.60

*Calculated at BNL (F1)

**Calculated at MIT (L5)

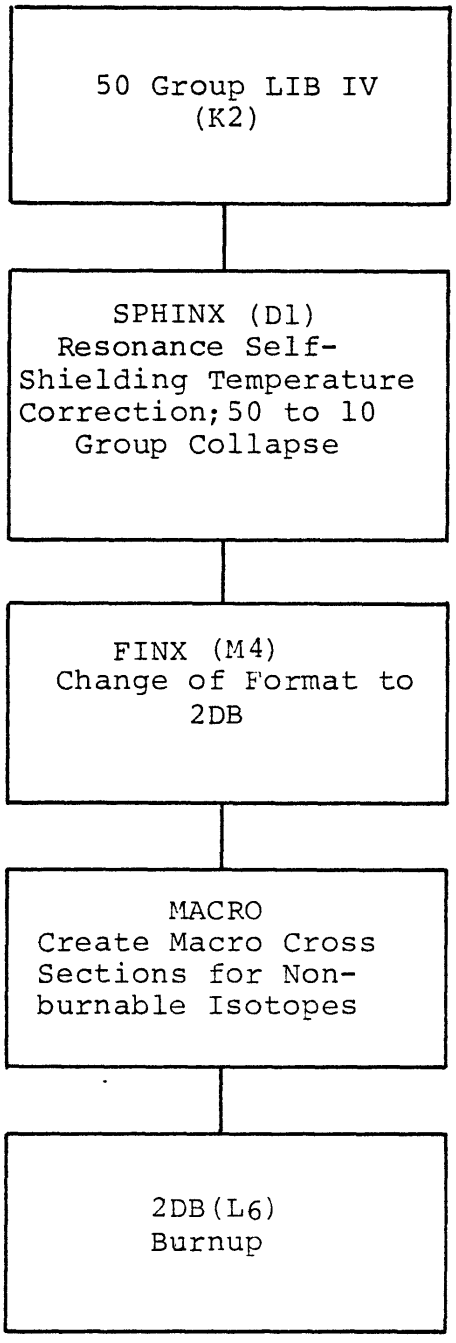

Fig. 2.9 Sequence of Calculations Followed in the Present Work

the core using the code 2DB (L6). In one case the 50 group LIB-IV cross section set was used and in the other case a 10 group cross section set collapsed from the 50 group LIB-IV set using SPHINX and the actual geometry of the core was used. As can be seen the results of the 10 group calculations are quite satisfactory. While the example shown is for a harder than usual core spectrum, the adequacy of ten group calculations for Fast Breeder Reactor fuel cycle studies is widely accepted (B5, H1, M2). The sequence of calculations used in the cross section preparations and their subsequent use are shown in Fig. (2.9).

2.5 Burnup Analysis

2.5.1 Introduction

All burnup calculations were performed using the zone-wise-collapsed 10 group cross sections and the two dimensional burnup code 2DB (L6). The R-Z geometry used in the 2DB calculations is shown in Fig. 2.10. Table 2.11 gives the zones corresponding to each region of the core and blanket shown in Fig. 2.9. The radial boundary for each zone was found by calculating an equivalent radius for each group of core, internal and radial blanket assemblies. The control rod assemblies were homogenized in with the fuel zones. Obviously mixing control material with the fuel does not really provide a true picture, and actual control rod worth can only be found by making a hexagonal, i.e., planar calculation. Even in that case only two situations: control rods completely inserted and

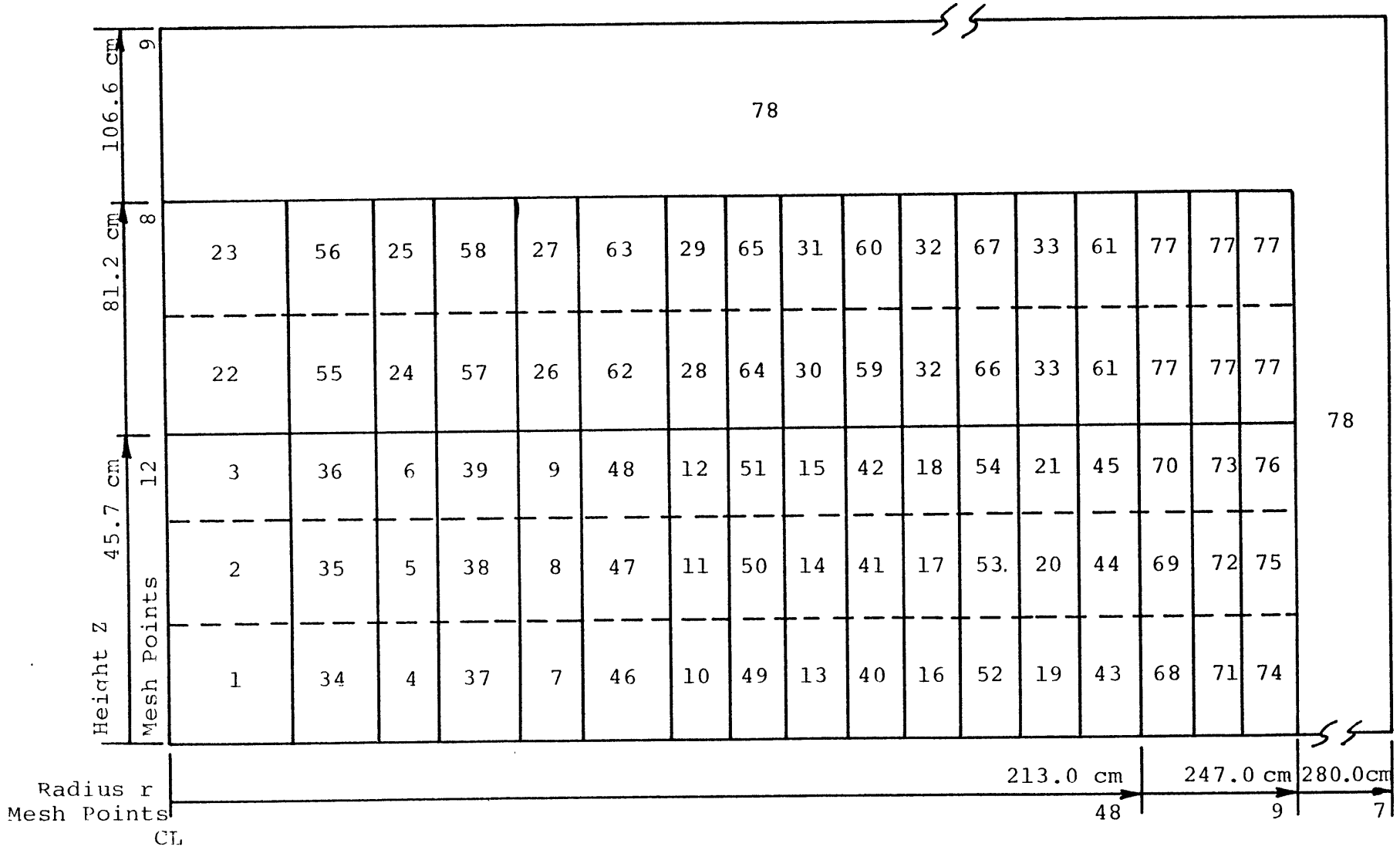

Fig. 2.10 R-Z Model of the Upper Right Quadrant of the Reactor Used in 2DB Calculation

Table 2.11

List of the Burnup Zones Corresponding to Different Regions of the Core Used in 2DB Calculations (See Fig. (2.9) for Burnup Zones)

Burnup Zone	Reactor Region
1 → 21	Internal Blanket
21 → 33	Axial Blanket Extensions of the Internal Blanket Assemblies
34 → 45	Fuel
46 → 48	Fuel*
49 → 51	Fuel*
52 → 54	Fuel*
55 → 61	Axial Blanket Extensions of the Fuel Assemblies
62 → 67	Axial Blanket Extensions of the Fuel Assemblies*
68 → 76	Radial Blanket
77	Axial Blanket Extensions of the Radial Blanket
78	Radial and Axial Shield

*Including sodium occupying withdrawn control rod positions.

completely removed can be simulated correctly. As will be described in the next section no control rods are included in the burnup calculations in this work; the control rod channels are filled with sodium. Exclusion of the control rods from burnup calculations does not introduce any significant error and simplifies the calculations considerably.

2.5.2 Depletion Methods

In the burnup calculations, the major objective is to keep the reactor critical at all times, i.e., $k_{eff} = 1$ throughout the cycle. To do this the movement of the control rods over the burnup cycle must be simulated, a requirement which cannot be performed by 2DB. However in breeder reactors, the reactivity loss over a cycle is not very large due to the good breeding properties of the reactor. Thus, in many studies done on fast breeder reactors, partial rod insertions are not simulated. Exclusion of the control rods in the burnup calculations results in a slightly higher breeding ratio compared to the more realistic case in which partially inserted rods are included.

It should be noted that in the design of the core enough control rod positions must be provided to guarantee the safe shutdown of the reactor. This requirement is satisfied by using two independent sets of control rod assemblies, namely the primary and secondary control systems. The requirement on the primary control rods is that they should be able to shut down the reactor at any time to the refueling temperature with

one bank completely stuck. The secondary control rods are required to be able to shut down the reactor at any time from any operating condition to the standby temperature condition assuming any one control bank is failed (P6). In the reference core design enough control rod positions have been provided to satisfy the above requirements.

Based on the above considerations, in the burnup calculations performed in this work no control rod insertions are included. The control rod positions are replaced by sodium channels consisting of sodium and structural material. Therefore, instead of requiring the k_{eff} to be equal to 1.0 throughout the cycle, it is required that at the beginning of equilibrium cycle (BOEC) there must be enough excess reactivity so that the k_{eff} at the end of equilibrium cycle (EOEC) is equal to 1.0. In this way the reactor is guaranteed to stay critical throughout the burnup cycle.

The BOEC core enrichment which would satisfy this requirement can be found by a trial and error method, i.e., assume a BOEC core enrichment, perform the core burnup over the desired cycle and find the EOEC k_{eff}. By trying different BOEC core enrichments the correct enrichment which would result in an exactly critical system at the EOEC can be found. Alternatively if the reactivity loss over the equilibrium cycle is known from some previous results, a search for the BOEC enrichment that would provide the required excess reactivity can be performed. Then to check the results, the core can be depleted over the

desired cycle length to make sure that k_{eff} is equal to one at the EOEC.

The fuel management strategy for the core and blankets consists of a batch core refueling after two years of residence during reactor operation at 70% capacity factor, i.e., total core refueling after 512 full power days of burnup. (The use of staggered half-core yearly refueling might be preferable in practice but this option was not examined here: the effect will not be important on the blanket studies of interest here.) In 2DB this burnup is done in two steps of 256 full power days each, so that the flux is recalculated at the middle of the cycle. The internal blanket residence time is also two cycles. These assemblies are then moved to the radial blanket. The details of internal and radial blanket movement and burnup are described in Chapter Three. To reach an equilibrium cycle an initial clean core, i.e., a $(U\text{-}Pu)O_2$ core with thorium or depleted uranium internal and radial blankets is depleted for two years, i.e. 512 full power days. At the end of the cycle the internal and radial blankets are moved into radial blanket positions and the core and the internal blanket assemblies are replaced with fresh fuel and depleted uranium or thorium respectively. This core is next depleted for another two years. The radial blanket residence time is a design variable, and several different systems will be considered in Chapter Three. As an example, for the case where radial blanket assemblies also have a two year residence period, the

second two year burnup (the cycle following the internal-to-radial blanket shuffling) is taken as the equilibrium cycle.

2.5.3. Materials Included in the Burnup Chains

The burnup chain for the U-Pu cycle is shown in Fig. 2.11. The only approximation in this chain is the assumption that Pu239 is directly produced from U238, i.e., the intermediate steps of U239 production and its decay to NP239 is ignored. The halflives of U239 and Np39 are 23.5 minutes and 2.35 days respectively, so that ignoring their production will result in a very small overproduction of Pu239. The uranium in the fuel and blanket is depleted uranium with 0.2% U235. In the burnup calculations fission product production due to U235 fission is also included.

The burnup chain for the Th-U233 cycle is shown in Fig. 2.12. There are two approximation in this chain:

1. Th233 production is ignored. This will have negligible effect on the results since the half-life of Th233 is 22.1 minutes.
2. Capture in U233 is assumed to result in Th232 production. In reality capture in U233 results in U234 production where U234 is also a fertile material, which with the capture of another neutron leads to production of U235. In the present calculation, since the U234 and U235 chain was not provided for, the above assumption was used. To see if this minor approximation has any significant effect on the results, the

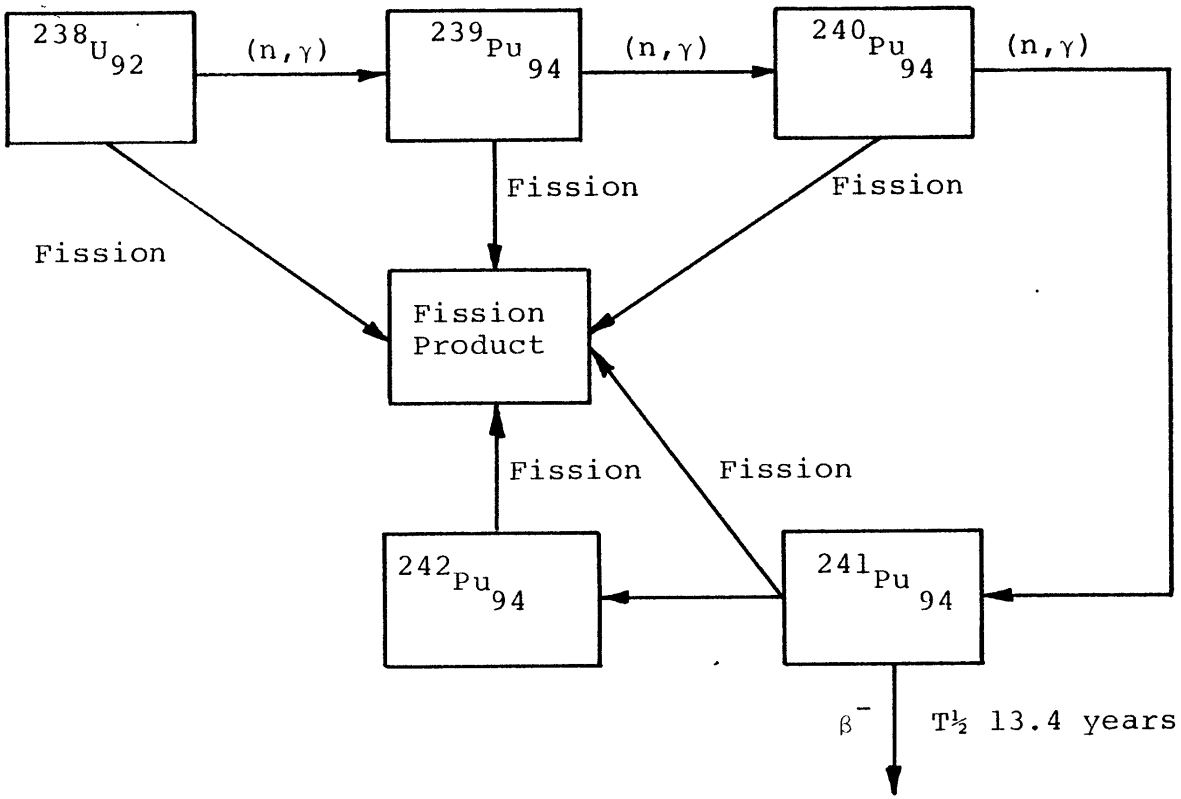

Fig. 2.11 Burnup Chain for the U-Pu Cycle Used in 2DB

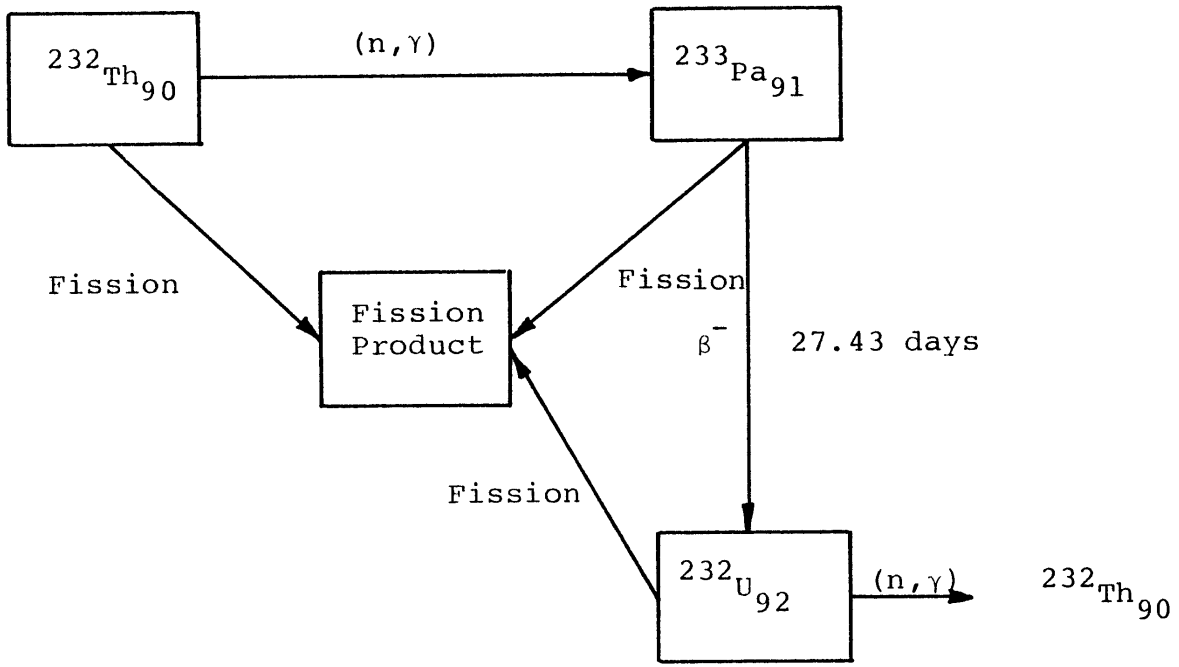

Fig. 2.12 Burnup Chain for the Th-U233 Cycle Used in 2DB

core was depleted for a two year cycle under the extreme-case assumption that U233 capture will instead result in the production of the lumped fission product rather than fertile U234. The multiplication factor at the beginning and end of the equilibrium cycle were affected by less than 0.0003, confirming that the results are not sensitive to the exact nature of the U233 capture product.

2.6 Economic Model

The economic analysis in this work is performed in accordance with the basic cash flow method, as described by Brewer (B6) and as applied to the LWR fuel cycle in the simple model developed by Abbaspour (A4).

There are two important assumptions inherent in the derivation of the simple model for the fuel cycle cost calculations. The first assumption is that all the batches of the fuel or blanket are steady state batches, i.e., the startup and end-of-plant life batches are not separately considered. The second assumpion in Abbaspour's simple model is that for a given batch of fuel or blanket, the revenues from the sale of electricity and the depreciation charges are represented by a single payment at the middle of the cycle. To assess the validity of the assumptions used in the simple model, Abbaspour (A4) checked this model against the more sophisticated model incorporated in the economics code MITCOST (C7), and found good agreement: results agreed within ~ 2% over a wide range of

parameter variations.

As shown by Abbaspour, the fuel cycle cost, e_f (mills/KWhe) can be expressed in the form:

$$e_f = \frac{1}{E} \sum_i M_i C_i F_i G_i \qquad (2.4)$$

where index i refers to different transactions for a given batch and

- E is the total amount of electricity generated by the batch while residing in the core (MWhe)
- M_i is the mass flow for step i (Kg)
- C_i is the unit cost of the transaction in step i ($/kg)
- F_i is a "financial" factor
- G_i is the "escalation" factor

In Chapter Four the equations for the calculation of F_i and G_i will be presented. An improvement over the simple model will be introduced by use of a continuous cash flow for the revenues from the sale of electricity and payments of depreciation. Using Eq. (2.4), and the above improvement, the economic performance of the cores analyzed in Chapter Three will be examined.

2.7 Summary

In this chapter all calculational methods and models used in this work were discussed.

The cross sections for all calculations were generated based on the 50 group LIB-IV cross section set (K2). The

cross sections were corrected for temperature and resonance self-shielding, and collapsed zonewise to 10 groups using the one-dimensional diffusion code SPHINX (D1). The fission product cross sections of plutonium were generated using a 70 group Japanese cross section set (K3). Since the Japanese fission product library does not include U233 fission product cross sections,a method was developed and used to generate U233 fission product cross sections from U235 and U238 fission product cross sections.

All subsequent burnup calculations were performed using the above 10 group cross section sets and the two dimensional burnup code 2DB (L4).

Finally, the economics model, which is based on the work of Brewer (B6) and Abbaspour (A4), was briefly described.

In the next chapter, the neutronic models and methods described in this chapter will be employed to perform detailed neutronic analyses of the cores under study.

CHAPTER THREE

BURNUP CALCULATIONS

3.1 Introduction

The objective of the work reported in this chapter was to use the calculational methods described in Chapter Two to perform detailed burnup analyses on the different cores under study. This chapter is divided into three major parts; these include:

1. Burnup analysis of the reference core
2. Burnup analysis of the (Pu-U)O_2 core with thorium oxide internal, axial and radial blankets
3. Burnup analysis of the (Pu-U)O_2 core with depleted uranium (oxide) internal, axial and radial blankets

In each subsection, the initial physics analysis leading to the steady state core is described first. This is followed by a discussion of the neutronic properties of the steady state core. Several other related topics such as the critical enrichment of the blanket assemblies as a function of moderation and the potential for redesigning the core layout to create a critical internal blanket island (and its effect on the overall neutronic performance of the core) will be discussed. Finally, a comparison of the neutronic performance of the cores discussed in this chapter will be presented.

3.2 Burnup Analysis of the Reference Core

3.2.1 Introduction

As was mentioned in Chapter Two, the reference core is a 1200 MWe heterogeneous LMFBR, studied by Argonne National Laboratory (B5).

All the calculations for the burnup analysis of cases studied in this chapter, such as calculation of zonewise number densities, reactor modeling and cross section generation were performed using the basic information provided by the reference study (B5), but independent of their methods and procedures. Thus, for the sake of consistency, rather than using the results provided by the reference study, a complete burnup analysis was performed on the reference core using the data and methods used throughout this work. In this section the results of this analysis will be presented. As will be seen, our results are in excellent agreement with those reported by the ANL, confirming that the methods and calculational procedures employed in this study represent a state-of-the-art effort.

3.2.2 Initial Physics Study

The fuel management scheme proposed by the reference study for the core and blanket consists of an annual refueling of half of the core and internal blanket assemblies and replacement of 1/6 of the radial blanket. So, in effect, the core, internal blanket and their axial extensions remain in the core for two cycles, whereas the blanket assemblies remain in the reactor for six cycles. Each cycle consists of 256 full

power days (FPD) which corresponds to a capacity factor of 0.7.

The initial $(U\text{-}Pu)O_2$ core is loaded using light water-reactor discharged plutonium. The composition of this plutonium is given in Table 3.1. The internal, axial, and radial blankets are loaded with depleted uranium containing 0.2% U235.

To reach the equilibrium cycle, core and blanket regions were burned for one cycle (256 FPD), then half of the core and internal blanket assemblies were replaced by fresh fuel and the reactor was burned for another cycle. The second cycle was taken as the steady-state cycle for the core and internal blanket regions. As for the radial blanket, to get the composition of the steady state radial blanket (i.e., the 1/6 that is replaced every six cycles), the radial blanket was irradiated for an additional four cycles with the core and internal blanket kept unchanged.

Table 3.2 gives the beginning of cycle (BOC) start up inner and outer core number densities. The core average enrichment is 22% fissile plutonium with an outer to inner enrichment ratio of 1.15. These values are the same as the numbers reported by the reference study. The number densities of the material in the axial blanket extensions of the fuel assemblies are given in Table 3.3. Note the sodium and structural material number densities of these axial blanket extensions are the same as the values for fuel assemblies given in Table 3.2. The number densities of the materials

Table 3.1

Light Water Reactor Discharge Plutonium
Composition Used for Initial Loading of the Core

Isotope	Weight Fraction
Pu238	0.00997
Pu239	0.67272
Pu240	0.19209
Pu241	0.10127
Pu242	0.02395

Table 3.2

Beginning of Cycle Inner and Outer Core
Number Densities

Element or Isotope	Number Density (atoms/barn-cm) Inner Core	Outer Core
Oxygen	0.1515 E-1*	0.1515 E-1
Sodium	0.1009 E-1	0.1009 E-1
Chromium	0.3582 E-2	0.3582 E-2
Iron	0.1432 E-1	0.1432 E-1
Nickel	0.2528 E-2	0.2528 E-2
U235	0.1110 E-4	0.1049 E-4
U238	0.5539 E-2	0.5236 E-2
Pu239	0.1363 E-2	0.1567 E-2
Pu240	0.4096 E-2	0.4711 E-2
Pu241	0.2053 E-3	0.2361 E-3
Pu242	0.4855 E-4	0.5585 E-4
Fission Product (FP)	0.0	0.0

*Read as 0.1515×10^{-1}

Table 3.3

Beginning of Cycle Number Densities of the Axial Blanket Extensions of the Fuel Assemblies

Element or Isotope	Number Density (atoms/barn-cm)
Oxygen	0.1702 E-1*
U235	0.1702 E-4
U238	0.8694 E-2
Pu239	0.0
Pu240	0.0
Pu241	0.0
Pu242	0.0
Fission Product (FP)	0.0

*Read as 0.1702×10^{-1}

included in the blanket assemblies at the beginning of cycle are given in Table 3.4. The number densities of the non-fuel regions, i.e., control rod, sodium channel (control assemblies without the rods inserted) and shield assemblies are given in Tables 3.5 through 3.7.

3.2.3 Neutronic Performance of the Steady State Reference Core

There are several parameters that could be used to evaluate the neutronic performance of a core. The most widely used parameters and properties include: breeding ratio (BR), compound system doubling time (CSDT), flux and power density shape and peak linear heat generation rate (LHGR). In the present analysis we are mostly interested in the flux and power density profile and power peaking characteristics of the core. More specifically, we are interested in the fraction of the power produced by the radial blanket and the peak LHGR in the core. This concern is basically due to the fact that one of the main objectives in using the proposed shuffling scheme for the blanket assemblies is to produce a large fraction of the power from the radial blanket. In this way, the sizable power produced from the radial blanket, together with the possible power flattening advantages, can reduce the peak LHGR in the fuel assemblies. The lower peak LHGR in the core would in turn allow the production of a still higher total power without creation of any local peaking problems. This point will be discussed in more detail later. Thus, although the other parameters such as breeding ratio and compound system

Table 3.4

Beginning of Cycle Number Densities of the Blanket Assemblies

Element or Isotope	Number Density (atoms/barn-cm)
Oxygen	0.2444 E-1*
Sodium	0.5303 E-2
Chromium	0.3873 E-2
Iron	0.1549 E-1
Nickel	0.2734 E-2
U235	0.2444 E-4
U238	0.1219 E-1
Pu239	0.0
Pu240	0.0
Pu241	0.0
Pu242	0.0
Fission Product (FP)	0.0

*Read as 0.2444×10^{-1}

Table 3.5

Number Densities of the Materials Included in the Control Rod Assemblies

Element or Isotope	Number Density (atoms/barn-cm)
B10	0.6375 E-2*
B11	0.2585 E-1
C12	0.8423 E-2
Sodium	0.6871 E-2
Chromium	0.5386 E-2
Manganese	0.5097 E-2
Iron	0.1855 E-1
Nickel	0.3679 E-2
Molybdenum	0.4169 E-3

*Read as 0.6375×10^{-2}

Table 3.6

Number Densities of Materials Included in the Sodium Channels of the Control Assemblies

Element or Isotope	Number Density (atoms/barn-cm)
Sodium	0.2041 E-1*
Chromium	0.1510 E-2
Manganese	0.1429 E-3
Iron	0.5201 E-2
Nickel	0.1032 E-2
Molybdenum	0.1169 E-3

*Read as 0.2041×10^{-1}

Table 3.7

Number Densities of the Materials Included in the Radial and Axial Shields

Element or Isotope	Number Density (atoms/barn-cm)
Sodium	0.2479 E-2*
Chromium	0.1423 E-1
Manganese	0.1347 E-2
Iron	0.4903 E-1
Nickel	0.9725 E-2
Molybdenum	0.1102 E-2

*Read as 0.2479×10^{-2}

doubling time are very important in describing the neutronic performance of a core, they are not especially relevant to the present study.

Figures 3.1 and 3.2 show the midplane, beginning and end of equilibrium cycle flux and power densities in the reference core. As can be seen, by using two enrichment zones the power density can be made to remain more or less flat throughout the cycle.

Table 3.8 shows the beginning of equilibrium cycle (BOEC) peak fast fluxes in the core.

The beginning and end of equilibrium cycle power fractions produced by the core, internal, axial and radial blanket are given in Table 3.9. Peak linear heat generation rates (LHGR) in different regions of the reactor are given in Table 3.10. The values shown in this table, in particular the core peak LHGR, together with the fraction of the power produced by the radial blanket given in Table 3.9, are important factors in the analysis of the cores studied in this chapter, and will be used in subsequent comparisons. The peak LHGRs referred to above were calculated by combining the results of the two dimensional hexagonal (planar) analysis of the core and the two dimensional R-Z analysis of the core. To do this a static 2-D hexagonal search is performed on the axial buckling of the system that produces the same beginning of equilibrium cycle k_{eff} as the two-dimensional R-Z calculations. The core, internal and radial blanket peak power locations are determined

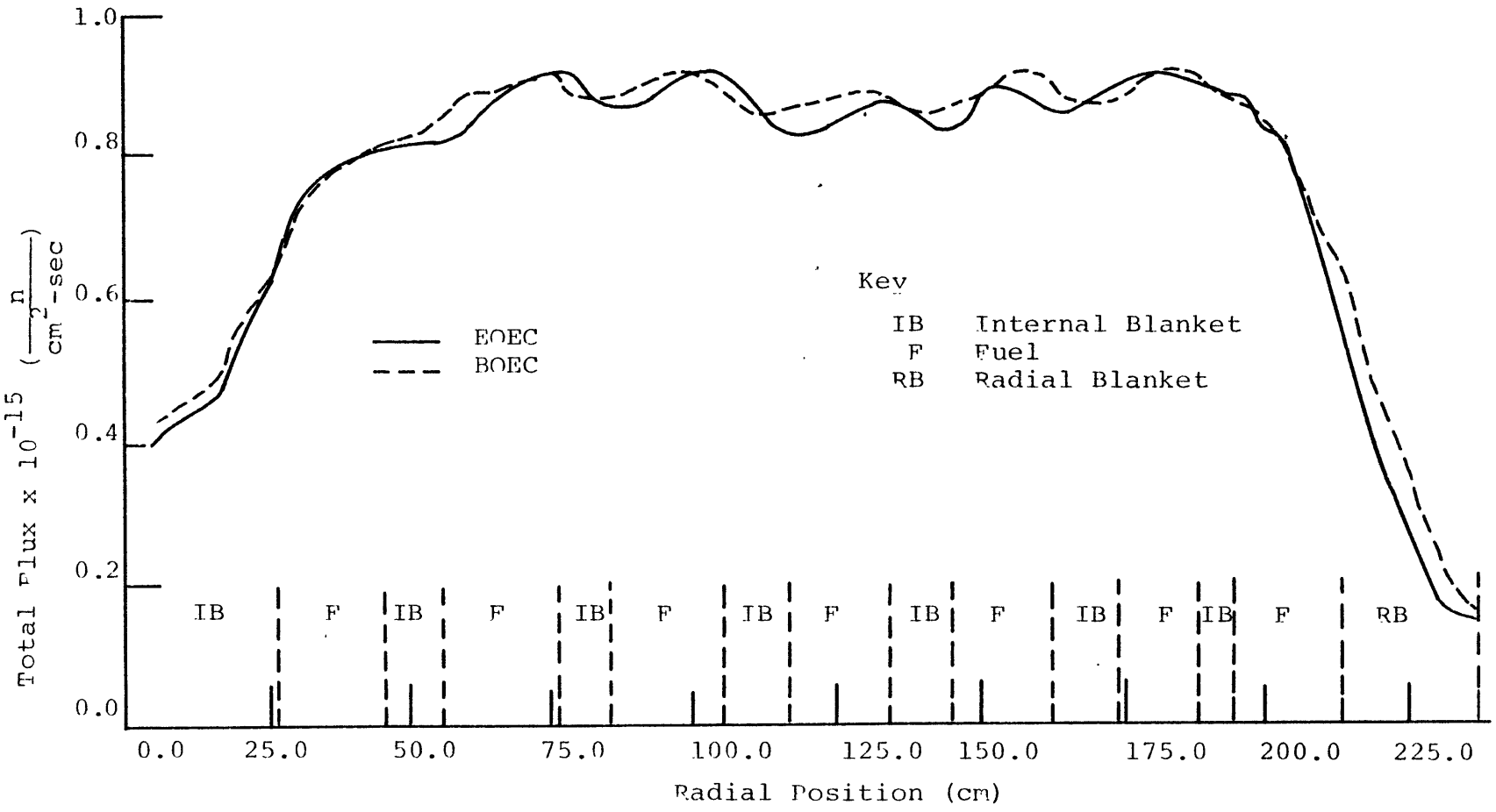

Fig. 3.1 Midplane Total Flux in the Reference Core

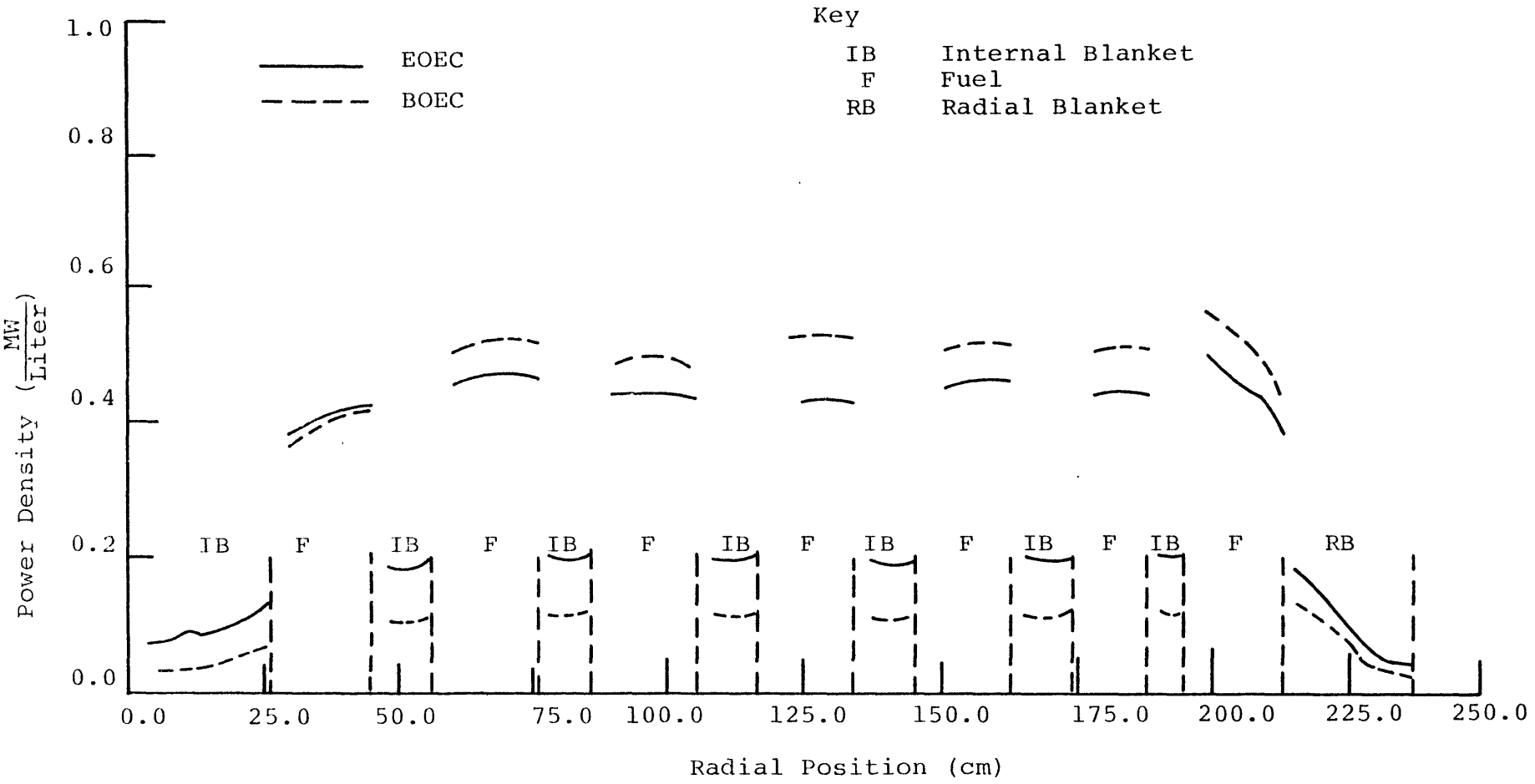

Fig. 3.2 Midplane Power Distribution in the Reference Core

Table 3.8

Beginning of Equilibrium Cycle Peak Fast Fluxes in the Reference Core

Peak fast flux above 0.49 Mev, n/cm^2 - sec	0.79×10^{15}
Fraction of the total flux above 0.49 Mev	0.17
Peak fast flux above 0.04 Mev, n/cm^2 - sec	2.11×10^{15}
Fraction of the total flux above 0.04 Mev	0.47

Table 3.9

Power Produced by Different Regions of the Reference Core

Region	Contribution to Total Power (%) BOEC	EOEC
Core	84.57	75.48
Internal Blanket	9.43	14.59
Axial Blanket	2.42	3.75
Radial Blanket	3.58	6.18

Table 3.10

Beginning of Equilibrium Cycle Peak Linear Heat Generation Rates in Different Regions of the Reference Core

Reactor Region	Peak LHGR (KW/ft)
Fuel	11.23
Internal Blanket	4.56
Radial Blanket	5.42

and the corresponding LHGRs are calculated based on the hexagonal analysis. These values are next multiplied by the axial peak to average ratio found from the R-Z calculations to get a synthesized 3-D peak linear heat generation rate. As can be seen, all the peak LHGRs are lower than the limits given in Tables 2.2 and 2.3, with the internal and axial blanket peaks well below these limits.

Average discharge burnups of assemblies from the different regions of the reactor are given in Table 3.11. Note that the blanket burnups are considerably below the materials-limited burnup values.

Finally Table 3.12 compares the results of several beginning of cycle parameters calculated at MIT and at ANL for the reference core. As can be seen, agreement is quite good.

3.3 Burnup Analysis of the (U-Pu)O_2 Core with Thorium Internal, Axial and Radial Blankets

3.3.1 Introduction

In this section the neutronic and burnup properties of the (U-Pu)O_2 core with thorium internal and radial blankets, which is subjected to the in/out and moderated shuffling strategy, will be discussed.

As has been noted earlier, the basic fuel management strategy proposed in this work is to shuffle the internal blanket assemblies after several cycles of residence in the core (and fissile isotope buildup) to the radial blanket, where, by using moderation, a reactive radial blanket system

Table 3.11

Average Discharge Burnup of the Different Regions of the Reference Core

Reactor Region	Average Burnup* (MWD/MT)
Core	68040
Internal Blanket	11856
Axial Blanket	1692
Radial Blanket	10852

*Megawatt days thermal per metric ton of total initial heavy metal.

Table 3.12

Comparison of Reference Core BOEC Parameters Calculated by MIT and ANL

Parameter	MIT	ANL
Average fissile enrichment* (% fissile plutonium)	22.0	21.93
Breeding ratio	1.26	1.30
Peak core linear heat generation rate	11.1	11.23

*Average over the core volume.

capable of producing a sizable fraction of total power can be created. In studying this system, there are several parameters mostly related to the design of the blanket assembly, that must be investigated to identify the system with the best performance. Choices include: the amount of moderation in the blanket, whether moderator is incorporated from the outset or added after an assembly is shuffled to the radial blanket, and the cycle length for the core and internal blanket assemblies.

To investigate the effect of these parameters, several core and blanket burnup analyses were performed, which will be discussed in the next section. Having found the optimum design of the internal and radial blankets, the neutronic and burnup performance of the core and blankets was analyzed. Several different shuffling strategies related to the radial blanket residence time and number of blanket rows (three rows against six rows) were then examined.

Finally an overall assessment of the performance of these systems is presented.

3.3.2 Initial Physics Analysis

The first point about the core under study that must be analyzed is the design of the blanket assemblies. In Chapter Two a simple design for the moderated blanket assembly was proposed (Fig. 2.2). Irrespective of the level of moderation, there are two ways the radial blanket can be moderated. The first method consists of fixed moderator pins as a part of the blanket assemblies which reside in the core as internal blanket

assemblies and are then moved to the radial blanket. In the second method, the internal blanket assemblies do not include any moderator pins, and the moderator locations (which could be similar to Pressurized Water Reactor (PWR) control rod guide tubes) are either filled with sodium or voided tubes. After moving the internal blanket assemblies to the radial blanket, the moderator can be added to the radial blanket assemblies in a manner similar to the PWR control rod system, i.e., the moderator rods would be inserted into the empty moderator guide tubes when the assembly is in the radial blanket region.

Obviously, the first method is much simpler, although the second method is also practical, since it is similar to the methods used in PWR control rod assembly design and operation.

To see the effect of the above alternatives on the k_{eff} of the system, three BOEC core and blanket systems were studied. The core in all three cases consists of the $(U\text{-}Pu)O_2$ assemblies used throughout this work. The internal blanket assemblies consisted of blanket rods with 40% of the rods filled with either zirconium hydride or sodium or left empty. Before the results of these calculations are presented an important convention must be noted. Throughout this chapter there will be discussions on different levels of moderation of the blanket assemblies. In all cases where the blanket assembly is described as containing a certain percentage of zirconium hydride this means that percentage of the blanket fuel rods is replaced by zirconium hydride rods. For example,

in the case of 40% zirconium hydride, 40% of the blanket rods, (50 out of 127 blanket rods) are replaced by moderator rods. Since no thermal-hydraulic analysis on the blanket assemblies was performed in this work, this procedure was the simplest way to perform the neutronic analysis. In reality once the optimum moderation level is found from the physics analysis, a detailed thermal-hydraulic analysis of the blanket assembly would lead to the correct internal arrangement of the blanket assembly. In fact, since the volume of the coolant necessary to cool the moderator rods is expected to be lower than that for the blanket rods, using needlessly small moderator pins might result in a lower than optimum performance by the blanket assemblies. On the other hand excessively large moderator inserts would probably lead to local power peaking problems. Thus the present analyses should not be construed as defining the ultimately preferable internal configuration of an assembly.

Going back to the original question of the effect of internal blanket moderation on the k_{eff} of the system, Table 3.13 shows the results for the three cases mentioned before. As can be seen, moderation of the internal blanket reduces the k_{eff} of the reactor substantially. The difference in k_{eff} of the cores with the sodium filled or voided blanket assemblies is not large, but the system with the voided pins results in the highest k_{eff}, mainly due to the harder spectrum achieved. Figure 3.3 shows the BOC total flux in the core and blanket assemblies for the moderated and for the sodium-filled internal

Table 3.13

Beginning of Cycle k_{eff} as a Function of Internal Blanket Design

Internal Blanket Design Option	System k_{eff}
40% $ZrH_{1.6}$	0.9001
40% Sodium	1.0375
40% Void	1.0428

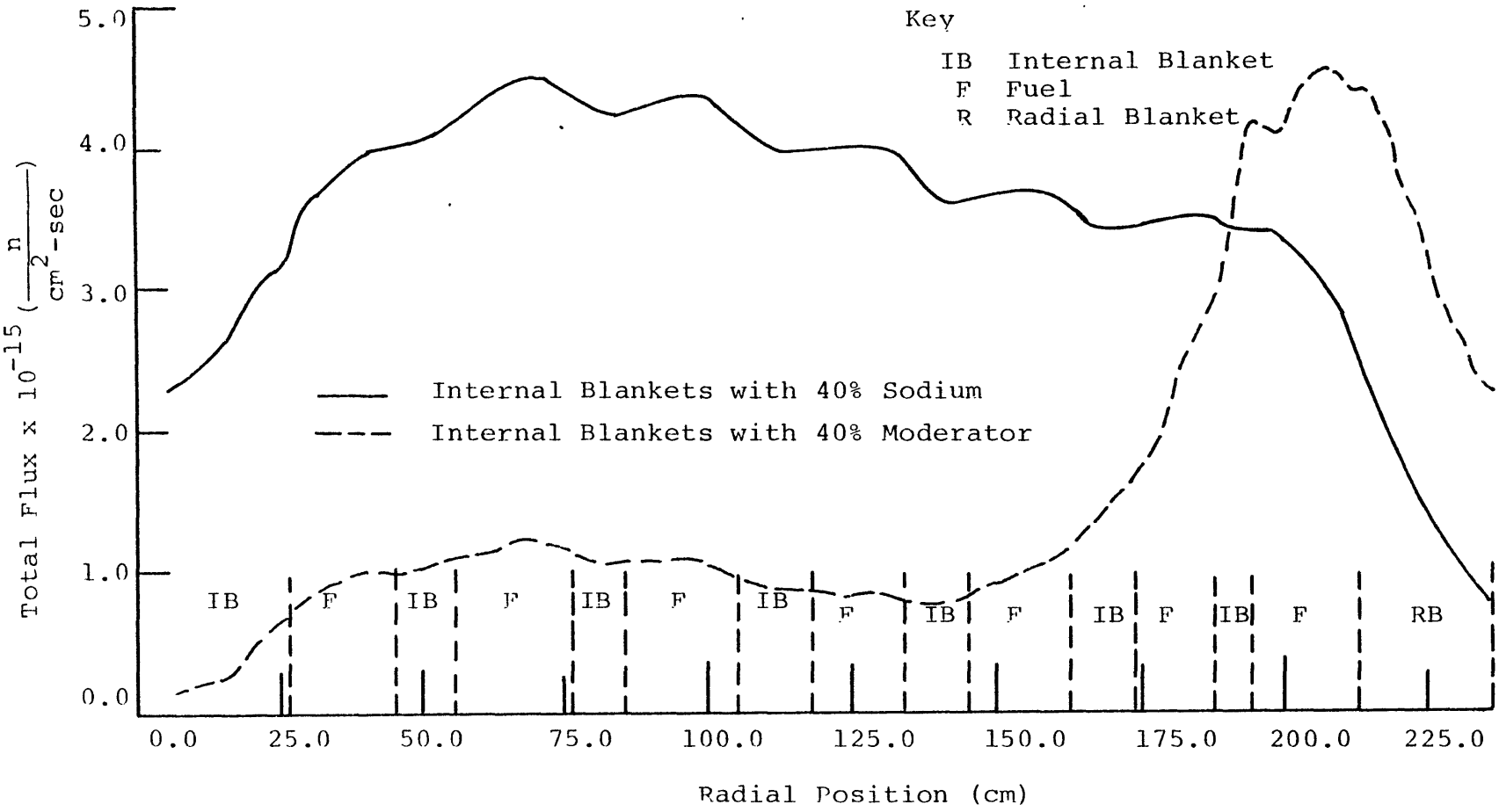

Fig. 3.3 Beginning-of-Equilibrium-Cycle Midplane Total Flux in the $(U\text{-}Pu)O_2$ Core with Thorium Internal Blanket Assemblies which Include Either 40% Sodium or 40% Moderator

blanket systems. It can be seen that moderation of the internal blanket assemblies has resulted in a substantial shift in the total flux in the core and internal blanket assemblies. As a consequence, the power densities in the inner core are reduced, and power is pushed toward the outer core and radial blanket, as shown in Fig. 3.4. This results in a considerable power peaking problem in the outer region of the core and radial blanket. This is not necessarily irremediable, since one could presumably re-arrange the pattern of internal blanket assemblies to re-flatten the power. However the reactivity penalty would persist, and is sufficient reason to reject this option.

Based on these results, in all cases studied in the remainder of this chapter the blanket assembly moderator pin positions will be left voided in the core, and are assumed to be filled with the moderator once they are moved to the radial blanket.

The rather large decrease in the beginning of cycle k_{eff} in the presence of moderator in the internal blankets suggests use of the moderator in internal blanket assemblies as a means to control the excess reactivity of the reactor over a burnup cycle. This possibility will be examined later.

The second point that must be analyzed is the question of the optimum level of moderation in the radial blanket. In this case the objective is to produce as much power from the radial blanket as possible without engendering any peaking problems. To find this optimum moderation level three cases--30%, 40% and 50% moderation of the radial blanket systems were analyzed. As

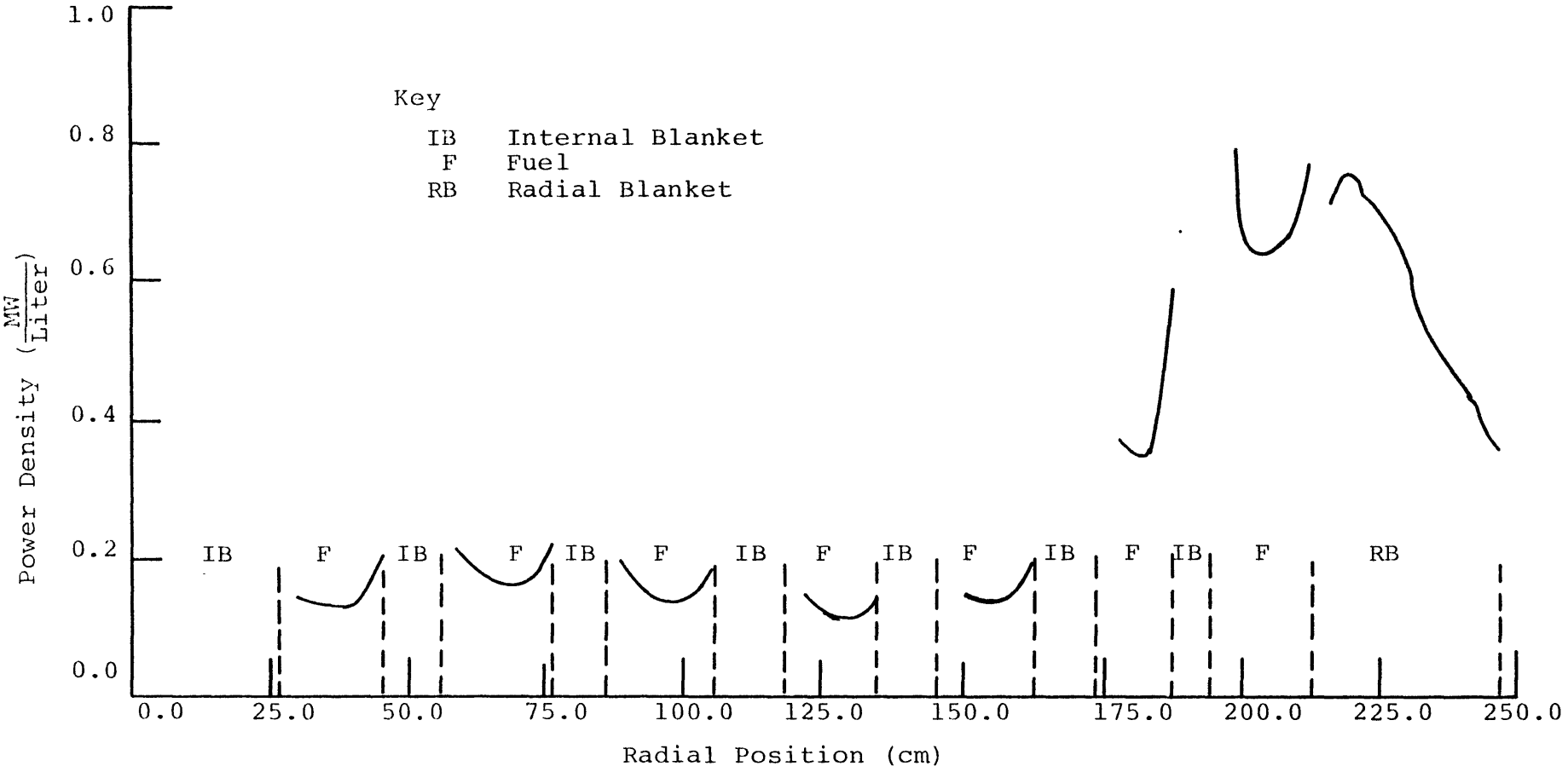

Fig. 3.4 Beginning-of-Equilibrium-Cycle Midplane Power Distribution in the $(U\text{-}Pu)O_2$ Core with 40% Moderated Thorium Internal Blanket Assemblies

discussed in Chapter Two , the fuel management strategy for the cores studied in this work is a two cycle batch burnup of the fuel and internal blankets, i.e., the core and external blanket are depleted for two cycles, then the internal blankets are moved to the radial blanket and the fuel and internal blanket assemblies are replaced with fresh fuel.

For each of the three cases mentioned above,an initial startup core was depleted for two cycles. Next the internal blankets were moved to the blanket and the core and internal blanket assemblies were replaced with fresh fuel. The second core was taken as the steady state core and was depleted for another two cycles.

The BOEC peak core, internal and radial blanket linear heat generation rates (LHGR) were next calculated for each case by combining the two dimensional hexagonal and R-Z calculations as described before. Table 3.14 shows the radial blanket peak LHGRs along with the fraction of the total power produced by the radial blanket in each of the three cases studied.

It can be seen that, as the level of moderation in the radial blanket increases, the fraction of the total power produced by the radial blanket and the peak LHGR increases. At a moderation level of 50% by volume zirconium hydride, the peak LHGR in the radial blanket is greater than the 20 kw/ft limit given in Table 2.3. Thus, the 40% zirconium hydride moderation level was taken as the preliminary optimum value

Table 3.14

Peak LHGRs and the Power Produced by the Radial Blanket Assemblies for Different Levels of Moderation

Radial Blanket Moderation (Volume % $ZrH_{1.6}$)	Peak LHGR (kw/ft)	Contribution to Total Power (%)
30	13.00	16.7
40	17.67	19.0
50	22.74	21.2

for the moderation of radial blanket assemblies. It should be noted that in the case of 50% $ZrH_{1.6}$ moderation, the peaking occurs near the boundary of the first blanket row and the core. Away from the interface, in the second or third row of the blanket the LHGRs are well below the limit. This can be seen by looking at Fig. 3.5 where the BOEC power density in the 50% moderated radial blanket is shown as a function of the radial distance from the blanket-core interface. Note that the power density drops almost linearly from the blanket-core interface. This suggests alternative methods of moderating the radial blanket such as variable moderation, with lower or no moderation of the first row, so that more neutrons can penetrate to the outer rows of the blanket. Several of these ideas will be examined later in this chapter.

This section was primarily devoted to the study of the optimum design of the blanket assemblies. In the next section, a more detailed analysis of the resulting best choice core, i.e., the $(U\text{-}Pu)O_2$ core with 40% voided internal and 40% moderated radial blankets, will be performed.

3.3.3 Startup Core

To start the initial core a $(U\text{-}Pu)O_2$ core with thorium internal blankets(40% voided) and thorium axial and radial blankets was burned for two cycles. The beginning of cycle (BOC) midplane power densities are shown in Fig. 3.6. It can be seen that there is a substantial power peaking in the core. This power peaking is basically due to the fact that the

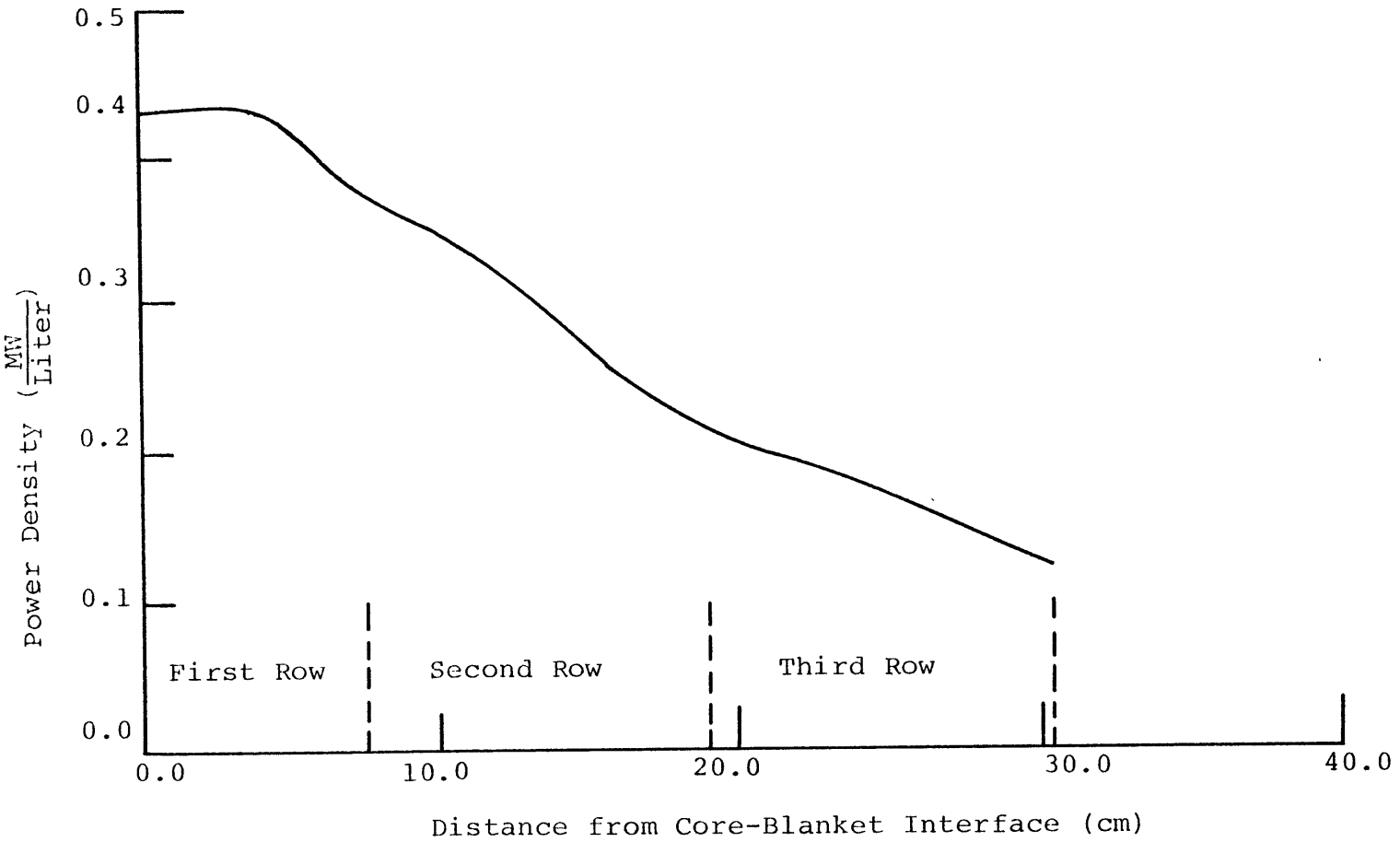

Fig. 3.5 Beginning-of-Equilibrium-Cycle Midplane Power Distribution in the 50% Moderated Thorium Radial Blanket

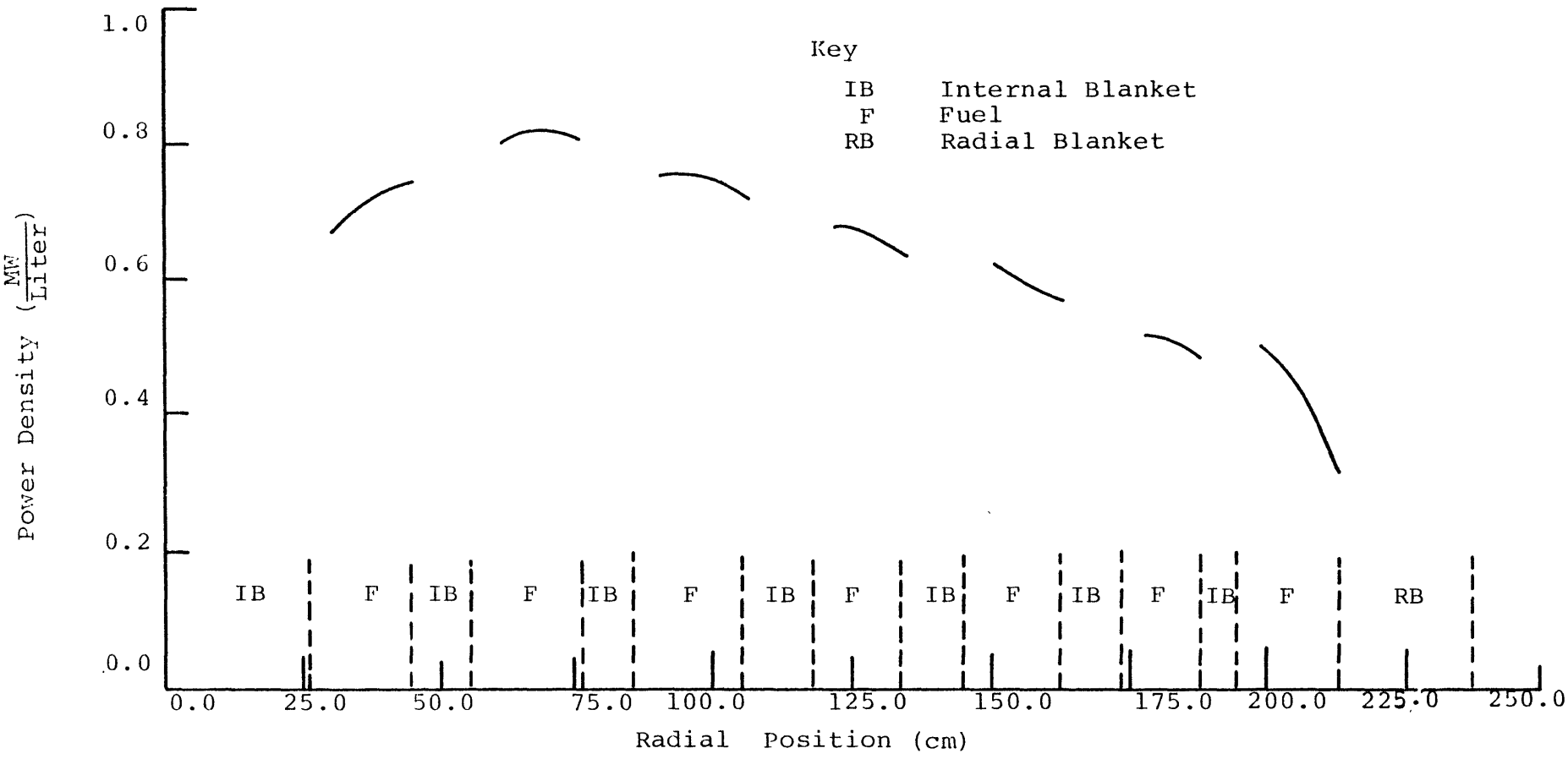

Fig. 3.6 Beginning-of-Cycle Midplane Power Distribution in the $(U\text{-}Pu)O_2$ Startup Core with Thorium Blankets

thorium internal and radial blankets produce very little power at the BOC compared to depleted uranium blanket assemblies which contain 0.2% U235.

Thus, to avoid the core peaking problems of the startup core, the reactor may have to be started up with a radial blanket which is slightly enriched. This would make it neutronically similar to the radial blanket in the steady state core, after the enriched internal blanket assemblies have been moved to the radial blanket. To examine this effect further a $(U\text{-}Pu)O_2$ core with a 40% voided internal blanket and 40% moderated radial blanket which included about 3.3% U233(wt%HM) was burned for two cycles. (It should be noted that the radial blanket of the startup core can be enriched using U235 or plutonium instead of U233. In fact, from a practical point of view, since U233 is not readily available, a 3% to 4% enriched U235 or plutonium radial blanket for the startup core would probably be more suitable.)

The BOC midplane power densities of the startup core with 3.3% U233 in the radial blanket is shown in Fig. 3.7. It is clear that the peaking problem can be solved rather easily using this method of startup. Other strategies not involving blanket pre-enrichment may also be practicable but, such exploration is beyond the scope of the present research effort.

Next, the internal blanket assemblies, after two cycles of burnup, were moved out to the radial blanket, which is

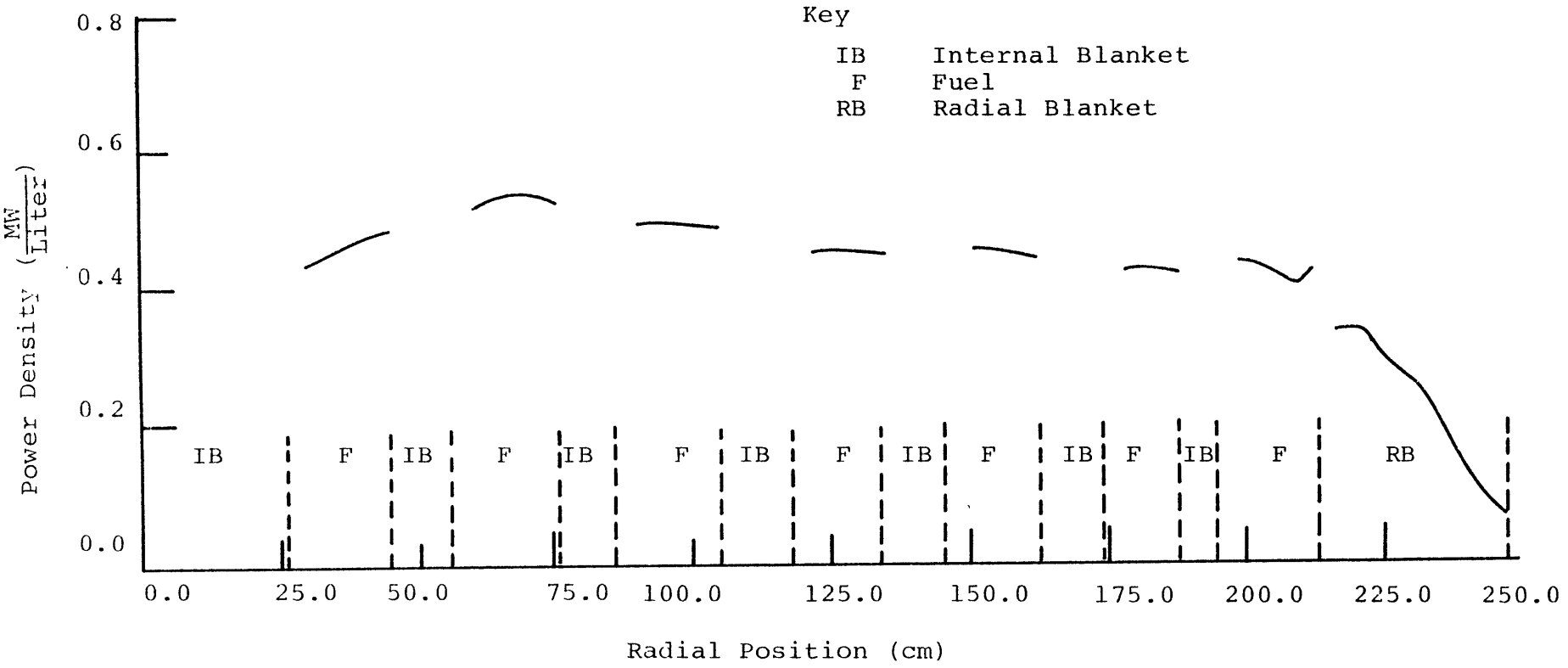

Fig. 3.7 Beginning-of-Cycle Midplane Power Distribution in the (U-Pu)O_2 Startup Core with an Enriched (and Moderated) Thorium Radial Blanket

moderated by 40% zirconium hydride, and the core and internal blanket were replaced with fresh fuel. This core was taken as the steady state core. The properties of this core will be discussed next.

3.3.4 Steady State $(U\text{-}Pu)O_2$ Core with Thorium Internal (40% voided), Axial and Radial (40% Moderated) Blankets

As described in the preceding section, the beginning of equilibrium cycle core consists of fresh $(U\text{-}Pu)O_2$ fuel and fresh thorium internal and axial blankets. The radial blanket consists of the two-cycle depleted, 40% moderated internal blankets shuffled into the radial blanket. The rate of fissile buildup in the internal blanket assemblies is nonuniform, due to the nonuniformity of the flux across the core. This is quite useful in the proposed fuel management scheme since the power production in the radial blanket drops off monotonically as one moves away from the core-blanket interface, because of the flux attenuation. Thus, in moving the internal blankets to the radial blanket, the most highly enriched blanket assemblies are moved into the outermost rows of the radial blanket and the lowest enriched blanket assemblies are moved to the innermost row of the radial blanket. This strategy will help boost the power production in the radial blanket regions farthest away from the core-blanket interface and will help to make the power production in the radial blanket more uniform. As an example, after a two cycle burnup of the core and blanket systems, the U233 production in the internal

blanket assemblies varies between a high of 4.19% U233 and a low of 3.07% U233,about an average of 3.66% U233. After these internal blanket assemblies are moved to the radial blanket, the first, second and third rows of the blanket contain 3.28, 3.45 and 4.12% U233, respectively.

Figures 3.8 and 3.9 show the beginning and end of equilibrium cycle flux and power density distribution in the core and blanket regions.

The powers generated from different regions of the reactor at the beginning and end of the equilibrium cycle are shown in Table 3.15. Comparing the power produced by the radial blanket in this core and the reference core (Table 3.9), it can be seen that the average power produced by the radial blanket in the equilibrium cycle has increased by more than a factor of three. Table 3.16 shows the beginning of equilibrium cycle peak LHGRs in different regions of the reactor. Compared to the peak LHGR in the reference core (Table 3.10), the peak LHGR in the above core has been reduced by 10%. This implies that the total power generated by the core can be increased by another 10% without incurring any core power peaking above that in the reference core. Alternatively, this extra 10% power corresponds to the power produced by approximately 15% of the fuel assemblies. This implies that by using the proposed fuel management strategy it would be possible to redesign a core with 15% fewer fuel assemblies and still

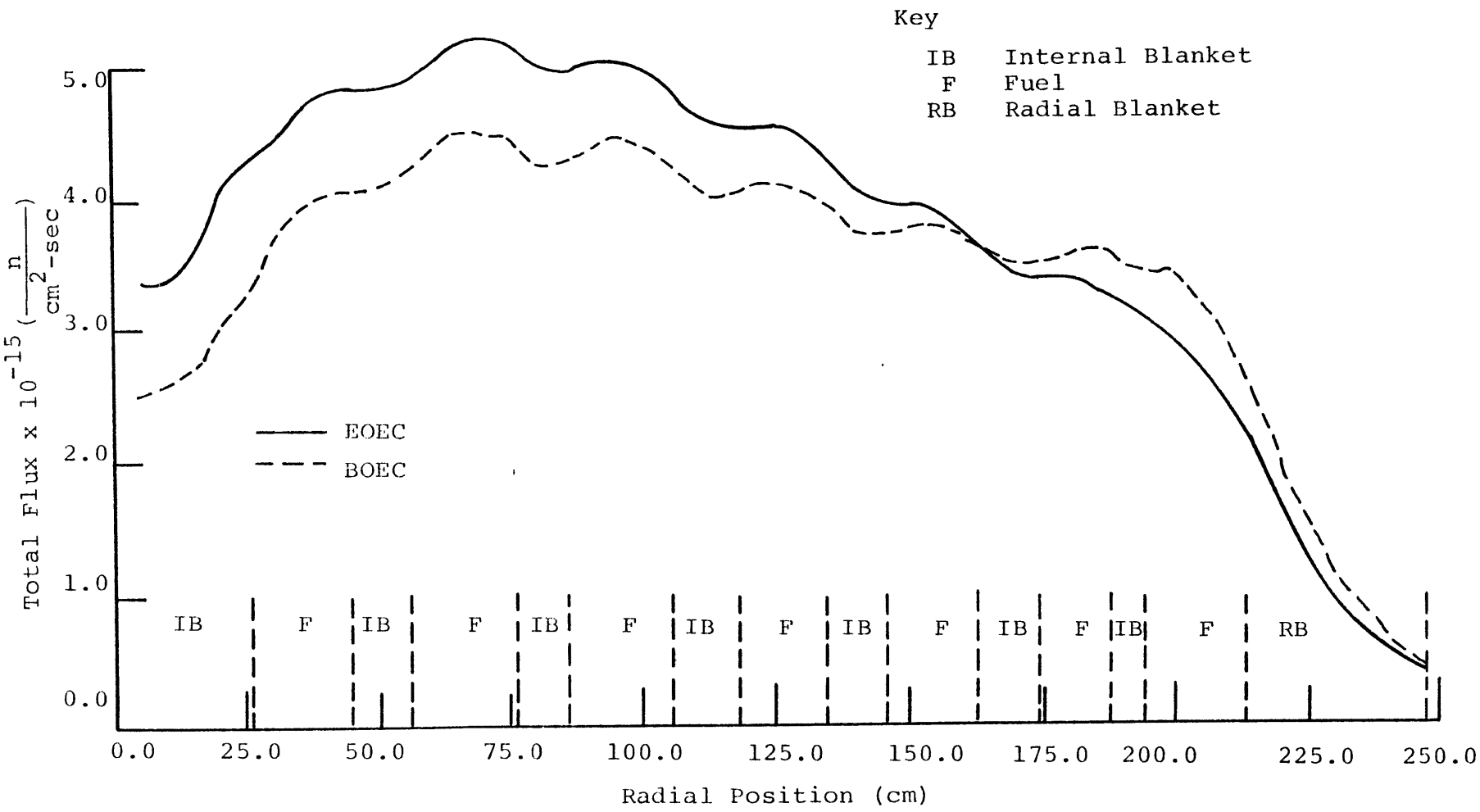

Fig. 3.8 Midplane Total Flux in the (U-Pu)O_2 Core with a 40% Moderated Thorium Radial Blanket

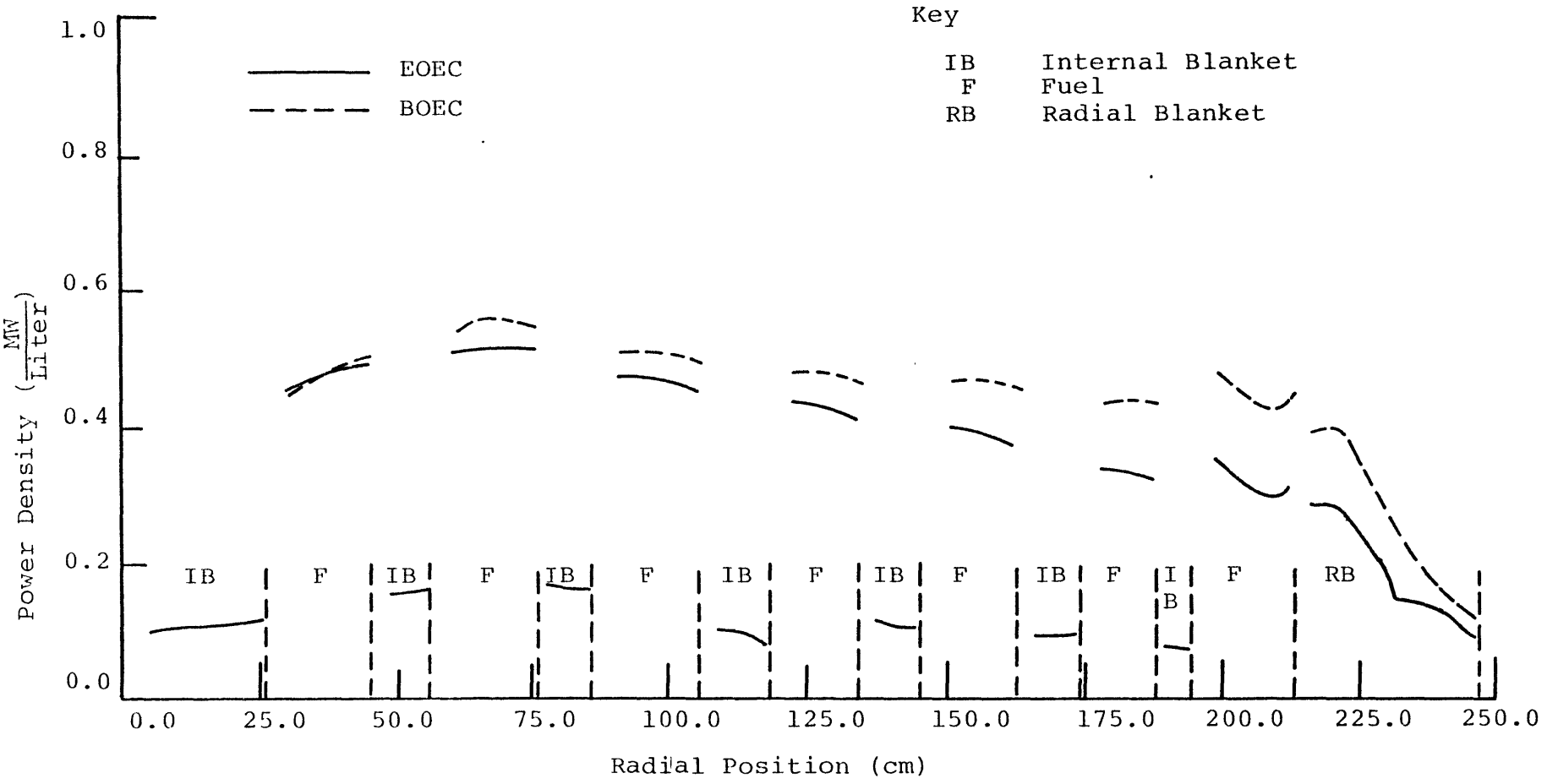

Fig. 3.9 Midplane Power Distribution in the $(U\text{-}Pu)O_2$ Core with a 40% Moderated Thorium Radial Blanket

Table 3.15

Beginning and End of Equilibrium Cycle Power from Different Regions of the $(U\text{-}Pu)O_2$ Core with 40% Moderated Radial Blanket

Reactor Region	Contribution to the Total Power (%)	
	BOEC	EOEC
Core	78.12	68.74
Internal Blanket	0.51	9.64
Axial Blanket	2.32	5.78
Radial Blanket	19.05	15.84

Table 3.16

Beginning of Equilibrium Cycle Peak LHGRs in Different Regions of the $(U\text{-}Pu)O_2$ Core with 40% Moderated Thorium Radial Blanket

Reactor Region	Peak LHGR (kw/ft)
Core	10.13
Internal Blanket	2.68
Radial Blanket	17.67

produce as much power as the reference reactor without exceeding any peaking limits. Also, from Figure 3.9, it can be seen that the shape of the power density profile in the radial blanket at the EOEC is fairly close to the shape at the BOEC. This implies that orificing of the radial blanket assemblies at the beginning of equilibrium cycle is close to the optimum throughout the cycle, which is an added advantage in the above strategy.

Table 3.17 shows the average discharge burnup of the different regions of the reactor. Compared to the average discharge burnups of the reference core (Table 3.11), it can be seen that the core internal and axial blanket burnups are very similar, but the radial blanket burnup in the above core is almost three times higher than that of the reference core. Also note that the internal and radial blankets in the core under study are the same assemblies, i.e., once the blanket assembly is fabricated it stays in the internal and radial blanket positions for four cycles and a total of 42516 $\frac{MWD}{MT}$. As for the number of blanket assemblies that must be fabricated annually, in the reference core, 1/2 of the internal blanket and 1/6 of the radial blanket assemblies are replaced annually. In the core under study all of the internal blankets are replaced every two years which is equivalent to 1/2 of the internal blankets being replaced annually. No separate radial blanket assemblies need be fabricated. Thus in the steady state cycle, there are 252 blanket assemblies that must be

Table 3.17

Average Discharge Burnup of the Different Regions of the $(U\text{-}Pu)O_2$ (with 40% Moderated Thorium Radial Blanket) System

Reactor Region	Average Burnup (MWD/MT)
Core	62,450
Internal Blanket*	10,575
Axial Blanket	2,221
Radial Blanket*	31,941
Radial Plus Internal Blanket	42,516

*same assembly

replaced in the reference core annually and 207 assemblies in the core under study. This difference amounts to approximately 18% lower blanket assembly fabrication requirements. This must be weighed against the lower overall fissile isotope production in the breed/burn fuel management strategy. Whether this tradeoff offers a clear advantage or not is best decided by an economic analysis, which will be presented in Chapter Four.

Another point which is important to note about the $(U\text{-}Pu)O_2$ core with thorium blankets is that the core is not self-sustaining as far as the fissile plutonium requirements are concerned. The fissile plutonium (Pu239 + Pu241) in the fissile-fueled zones of the core depletes to 84.8% of the BOEC inventory in two cycles of residence in the core. The axial blanket extensions of the fuel assemblies produce about 4.9% of the BOEC fissile plutonium requirements. Thus approximately 10% of the BOEC fissile plutonium requirements must be made up by other sources. In any event, the U233 production in the internal and axial blanket assemblies exceeds the plutonium deficit, i.e., the whole core is a net breeder. The difference in the beginning and end of equilibrium cycle plutonium can be made up by either replacing some of the internal blanket assemblies with depleted uranium or by coupling this core to a thermal reactor or advanced converter which would use the U233 produced in the blanket assemblies and provide makeup plutonium to the breeder. The radial blanket at the BOEC

contains an average of 3.66% U233. This average U233 concentration depletes to 3.64% by the end of equilibrium cycle, i.e., the U233 concentration in the radial blanket remains nearly constant.

Finally, the question of irradiation effects on the zirconium hydride in the radial blanket and its ability to withstand the fluence to which the radial blanket is exposed must be discussed. Table 3.18 shows the beginning of equilibrium cycle peak fast fluxes in the radial blanket. As mentioned in Chapter Two, there has been extensive experience with the operating characteristics of zirconium hydride in TRIGA and other experimental reactors, but there has not been much irradiation testing at high fluences. Moreover, most of the irradiation tests that have been performed so far have been mainly performed in an environment more typical of thermal reactors. Also as mentioned in Chapter Two, the highest fluences imposed on zirconium hydride at high neutron energies involved some GCFR fuel irradiation capsules in EBRII where samples of $ZrH_{1.5}$ and $ZrH_{1.7}$ were irradiated at a temperature of 400°C and fluences of 5 to 7 x 10^{22} n/cm^2 (neutron energies greater than 0.1 Mev.) The post irradiation results showed no significant damage to the zirconium hydride. From Table 3.18 it can be seen that the peak fast flux above 0.04 Mev is 0.65 x 10^{15} n/cm^{2}sec. In two years, the peak zirconium hydride rods close to the core-blanket interface experience a fluence of 2.86 x 10^{22}, which is lower than the above

Table 3.18

Beginning of Equilibrium Cycle Peak Fast Fluxes in the Radial Blanket of the $(U\text{-}Pu)O_2$ Core with a 40% Moderated Thorium Radial Blanket

Peak Fast Flux Above 0.49 Mev, $n/cm^2\text{-}sec$	0.24×10^{15}
Fraction of the Total Flux Above 0.49 Mev	0.10
Peak Fast Flux Above 0.04 Mev, $n/cm^2\text{-}sec$	0.65×10^{15}
Fraction of the Total Flux Above 0.04 Mev	0.28

experimental results by a factor of 2 to 3. Therefore the peak moderator rod should be able to stay in the radial blanket for several cycles without any significant hydrogen migration or damage to the rod. Also note that the above calculation is conservative, since the flux above 0.04 Mev is greater than the flux above 0.1 Mev.

In this section the neutronic properties of the $(U\text{-}Pu)O_2$ core with a moderated thorium radial blanket has been discussed. There were two basic objectives in studying the proposed in/out and moderate fuel management scheme. The first objective was to increase the power production from the radial blanket, hence lower the peak linear heat generation rate (LHGR) in the fuel assemblies so that more power can be generated from the reactor. In the core studied in this section, it was shown that approximately 20% of the total power can be generated from the radial blanket, which results in a 10% reduction in the peak fuel LHGR. The second objective in this study was to create a very reactive (and, if possible, critical) radial blanket using the enriched internal blanket assemblies combined with the use of moderation, so that the leakage of core neutrons to the radial blanket can be reduced. The reduction of neutron leakage to the radial blanket would result in lower steady-state core average enrichment. This point will be discussed in some detail in the next section.

3.4 Critical Enrichment of Blanket Assemblies As a Function of Moderation

To study the effect of the radial blanket reactivity on the reactor k_{eff}, the critical enrichment of several Th-U233 and U-Pu239 blanket assemblies was studied as a function of moderation. To do this an R-Z model of the upper half of the blanket assembly shown in Fig. 3.10 was used. The height of the internal blanket, axial extension and the axial shield shown in Fig. 3.14 is exactly the same as the upper half of the blanket assemblies. An arbitrary width of 5 cm, which is approximately equal to one-half of the flat to flat (FTF) thickness of the blanket assembly, was employed. The R-Z model shown in Fig. 3.14 was calculated with reflective boundary conditions on the left, right and bottom boundaries. A vacuum boundary condition was used for the top boundary. These boundary conditions simulate, in a somewhat approximate manner, a critical blanket assembly system located inside a critical environment, or a reactor of these assemblies of infinite radial extent. For radial blanket assemblies, however, the leakage to the radial shield is quite significant, and the reflective boundary condition on the right boundary would not be valid.

For both thorium and uranium blanket systems five separate blanket systems were studied, these include: a regular blanket system with no moderation, and four cases of 30%, 40%, 50% and 70% by volume zirconium hydride moderation: again recall that percent moderation refers to percent of fuel pins replaced by moderator pins of equal volume.

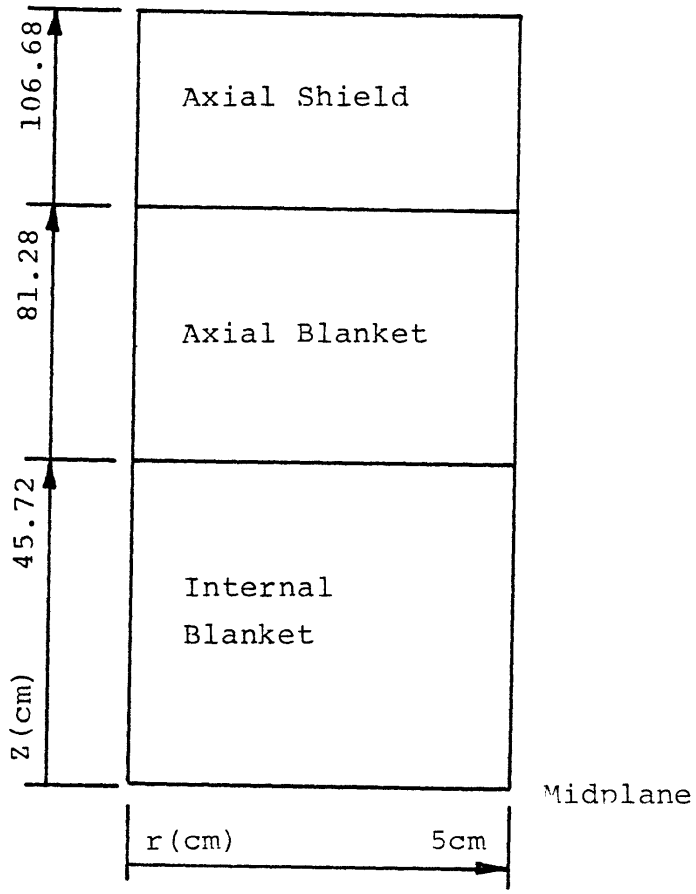

Fig. 3.10 The R-Z Model of the Upper Half of the Blanket Assemblies Used in Blanket Criticality Calculations

In all cases a search on the U233 or Pu239 clean critical enrichment in the blanket region was performed. The axial blanket extension of the assembly was assumed to include either Th232 or depleted uranium depending on the blanket system under consideration. Note that since the search is on clean critical systems with no Pa233, fission products or higher plutonium isotopes, the critical enrichments found in this way are slightly lower than the real-life cases where other elements would also be present in the blanket assemblies.

Table 3.19 shows the results for the Th-U233 blanket system. Also shown is the ratio of capture in Th232 to absorption in U233, which is equivalent to the beginning-of-life breeding ratio. Note that the ratio of captures in fissile nuclei to absorptions in fertile nuclei shown in Table 3.19 are the beginning of cycle clean critical values and are calculated from the relation

$$(BR)_{BOL} = \frac{C_{fertile,IB} + C_{fertile,AB}}{A_{fissile,IB}} \qquad (3.1)$$

where

$C_{fertile,IB}$ is the capture rate in the fertile isotopes (Th232 or U238, depending on the blanket system) in the internal blanket region

$C_{fertile,AB}$ is the capture rate in the fertile isotopes in the axial blanket extension of the internal blanket

Table 3.19

Clean Critical Enrichments and Beginning of Life Breeding Ratios of the Th-U233 Blanket System as a Function of Moderation

Moderation (Volume Percent $ZrH_{1.6}$)	U_{233} Enrichment ($\bar{N}_{U233}/N_{HM}$)	Breeding Ratio C_{Th232}/A_{U233}
0	10.34	1.1821
30	5.82	0.9737
40	4.66	0.8749
50	4.17	0.7559
70	4.71	0.4915

$A_{fissile,IB}$ is the absorption rate in the fissile isotopes (U233 or Pu239 depending on the blanket system) in the internal blanket region. Note that the axial blanket of the internal blanket does not include any fissile isotopes at the beginning-of-life (here we ignore the small amount of U235 in depleted uranium).

The comparable values for the U-Pu239 blanket system are shown in Table 3.20.

The results of the critical enrichment determinations given in Table 3.19 show that as the Th-U233 blanket system is moderated and the spectrum is shifted toward the epithermal energy region; the critical enrichment of the blanket assembly decreases. This is true for the 30%, 40% and 50% moderated systems. But as the moderation increases, the spectrum is shifted toward the lower epithermal and thermal energy regions, where the critical enrichment increases, as is shown for the 70% moderated case. This increase in critical enrichment is attributed to the higher parasitic absorption by the structure and zirconium in the thermal region.

To get the radial blanket critical, sufficient U233 must be bred into the internal blanket assemblies while they reside in the core. Figure 3.11 shows the rate of U233, Pa233 and fission product buildup in the internal blankets as a function of the number of cycles (256 days) the blanket assemblies stay in the core. Comparing these values with the critical enrichments

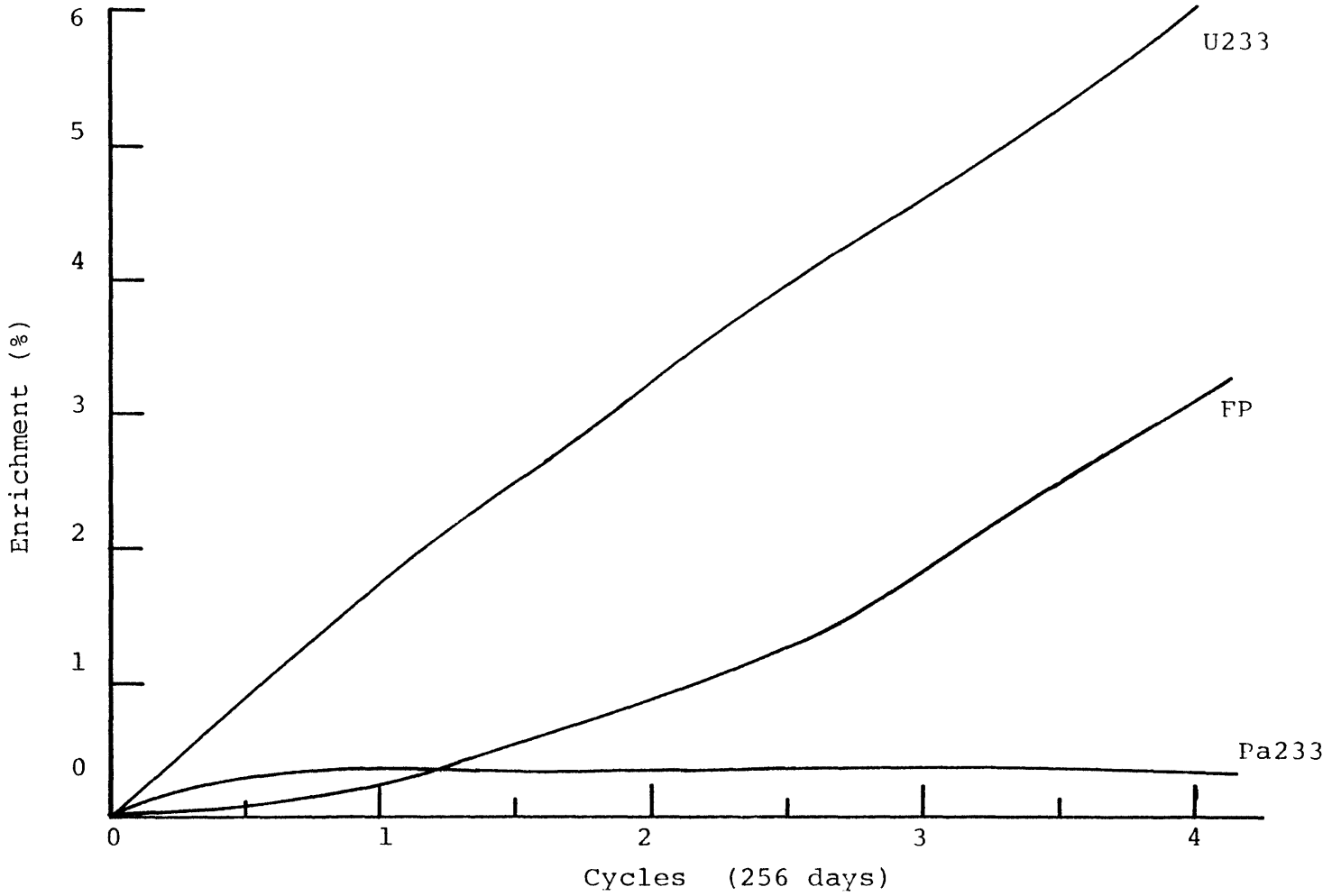

Fig. 3.11 U233, Pa233 and Fission Product Buildup in the Internal Blanket

Table 3.20

Clean Critical Enrichments and Beginning of Life Breeding Ratios of the U-Pu239 Blanket System, as a Function of Moderation

Moderation (Volume percent $ZrH_{1.6}$)	Pu239 Enrichment (N_{U233}/N_{HM})	Breeding Ratio C_{U238}/A_{PU239}
0	9.30	1.2851
30	10.67	0.8269
40	6.98	0.7307
50	5.08	0.6796

of Table 3.19, it can be seen that in four years the U233 buildup is 6.1%, which is higher than the critical enrichment of the 40% moderated blanket assemblies. Thus, to examine the effect of moving the enriched internal blanket assemblies to the moderated radial blanket on the k_{eff} of the system, several beginning-of-equilibrium cycle cases were studied. These cases include shuffling of the internal blanket assemblies after 2, 3 and 4 cycles of residence in the core to the 40% moderated radial blanket. Table 3.21 shows the increase in the BOEC k_{eff} for the three cases mentioned above over the k_{eff} of a (U-Pu)O_2 core with thorium internal and radial blankets with no moderation or enrichment in the radial blanket. It can be seen that the BOEC k_{eff} increases quite substantially using the shuffling fuel management strategy. This results in a sizable reduction in the steady state core enrichment of the thorium blanketed system. As an example, the BOEC average fissile plutonium enrichment of the reference core is 22%. The fissile enrichment of a (U-Pu)O_2 core with thorium blankets is approximately 15% to 20% higher than the (U-Pu)O_2 core with depleted uranium blanket system (H1).

The BOEC average fissile plutonium enrichment of the (U-Pu)O_2 core with a 40% moderated radial blanket studied in the previous section is 23%. Here the shuffling strategy has resulted in a net saving of 2% to 3% average fissile plutonium enrichment in the core. Unfortunately, this saving only helps to bring the (U-Pu)O_2 core with thorium blankets to a competitive level with the reference core and in essence lowers

Table 3.21

Increase in the BOEC k_{eff} of the $(U\text{-}Pu)O_2$ Core with a 40% Moderated Thorium Radial Blanket as a Function of Radial Blanket Enrichment

Radial Blanket Enrichment Average U233	Δk (%)	\$ (β = 0.004)
3.66*	7.66	19.15
4.62*	8.69	21.72
6.10*	10.88	27.2

*U233 build up in the BOEC radial blanket attained after two, three and four cycles of residence in the core, respectively.

the core enrichment penalty that would otherwise result when a thorium blanket system is used.

Another point worth noting in Table 3.20 is that although the enrichment of the internal blanket assemblies that have resided in the core for four cycles and moved to the radial blanket is higher than the critical enrichment of a 40% moderated blanket system, the increase in k_{eff} of the system is not as substantial as might at first be expected. The reason for this is the fact that a large fraction of the neutrons in the radial blanket leak to the radial shield, and so the radial blanket assemblies are in a situation far removed from the no-radial-leakage condition used to determine critical enrichment.

To see if using a better reflector as the radial shield would change the results, the BOEC k_{eff} of a $(U\text{-}Pu)O_2$ core with a 40% voided thorium internal blanket and a 40% moderated radial blanket shuffled from the core after four years of residence was calculated by substituting the radial shield with a zirconium hydride shield. This case is essentially the same as the third case shown in Table 3.21 except for the radial shield which is now zirconium hydride instead of steel. Note that zirconium hydride was chosen as the radial shield to represent a very good reflector, and, in effect, this was an attempt to find an upper limit on the performance of enriched and moderated radial blanket systems. Whether zirconium hydride can be used as the shield material, and what other elements would have to be added to the design of a practical zirconium

Table 3.22

Beginning of Equilibrium Cycle Power Production and Peak LHGRs in Different Regions of the $(U\text{-}Pu)O_2$ Core With a 30% Moderated, 6.1% U233 Enriched Thorium Radial Blanket

Reactor Region	Power Contribution (%)	Peak LHGR (kw/ft)
Core	68.77	9.75
Internal Blanket	0.48	0.43
Radial Blanket	26.04	16.81
Axial Blanket	4.71	--

hydride shield was not considered important at this exploratory stage of the investigation.

Figure 3.12 shows the BOEC midplane power densities in the core and blanket. Note that the power distribution in the core is fairly flat and that the power peaks in the radial blanket. The radial blanket produces about 31% of the total power but there is a power peaking problem in the first row of the radial blanket. Compared to a similar core and blanket system with steel radial blanket shield, there is no noticeable difference in k_{eff}, core power distribution or fraction of the total power produced from the radial blanket between the zirconium hydride and steel reflected systems. The only difference is in the power distribution in the radial blanket, as shown in Figure 3.13. As can be seen, the power density increases next to the zirconium hydride reflector as expected, but the total power produced in the radial blanket does not change. Based on these results there does not seem to be much incentive for using zirconium hydride as the radial shield.

As was mentioned above the steel reflected reactor with a 40% moderated radial blanket that is moved from the core after four cycles of residence, generates 31% of the total power from the radial blanket, but has peaking problems in the first row of the radial blanket. Thus, to examine the neutronic properties of a reactor with a four cycle burned radial blanket system shuffled from the core, but which does not have any radial blanket peaking problems, a lower level of blanket moderation must be employed. To do this, a beginning

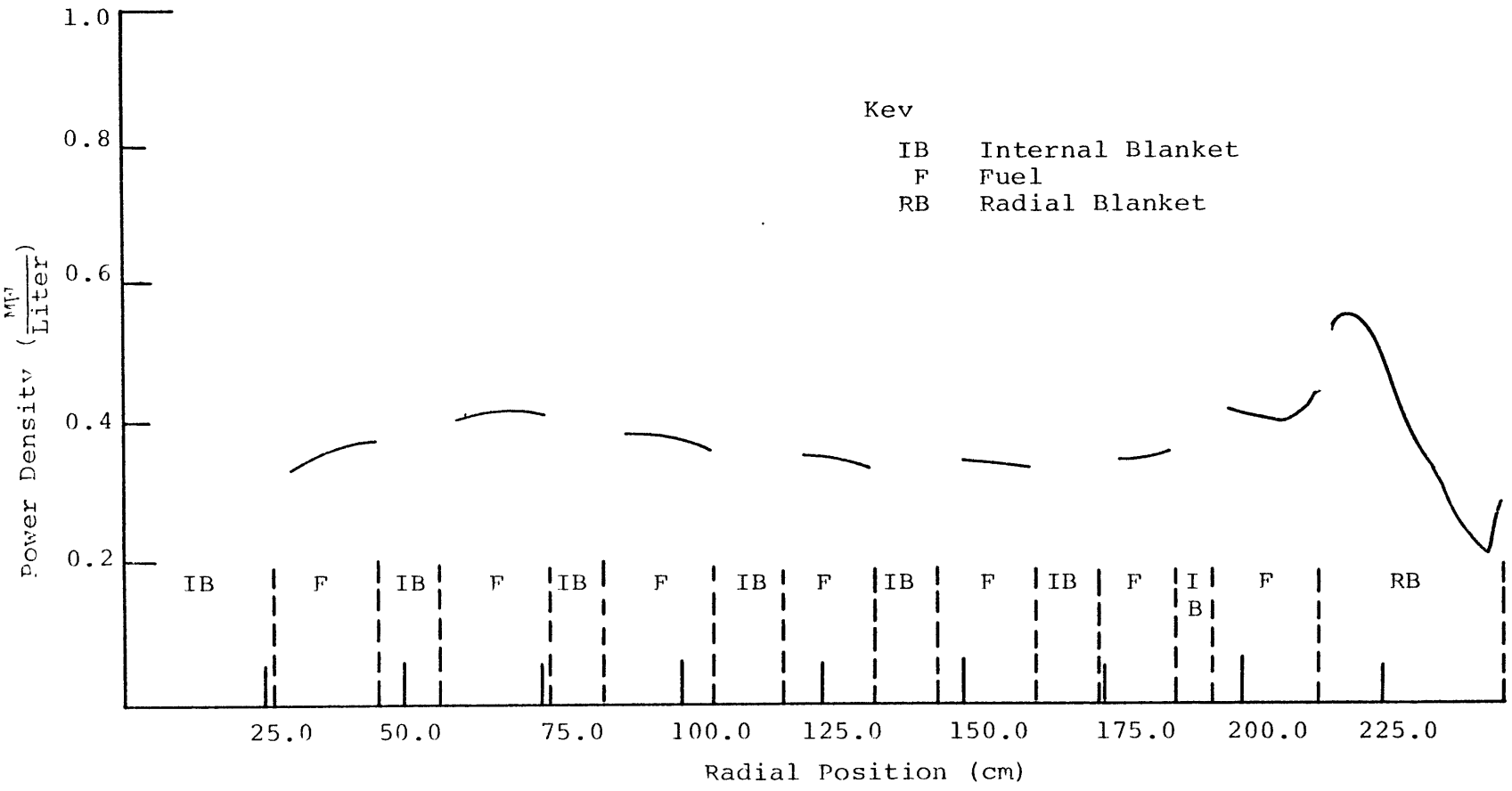

Fig. 3.12 Beginning-of-Equilibrium-Cycle Midplane Power Distribution in the $(U\text{-}Pu)O_2$ Core with a 40% Moderated, 6.1% U233 Enriched Thorium Radial Blanket and Zirconium Hydride Radial Shield

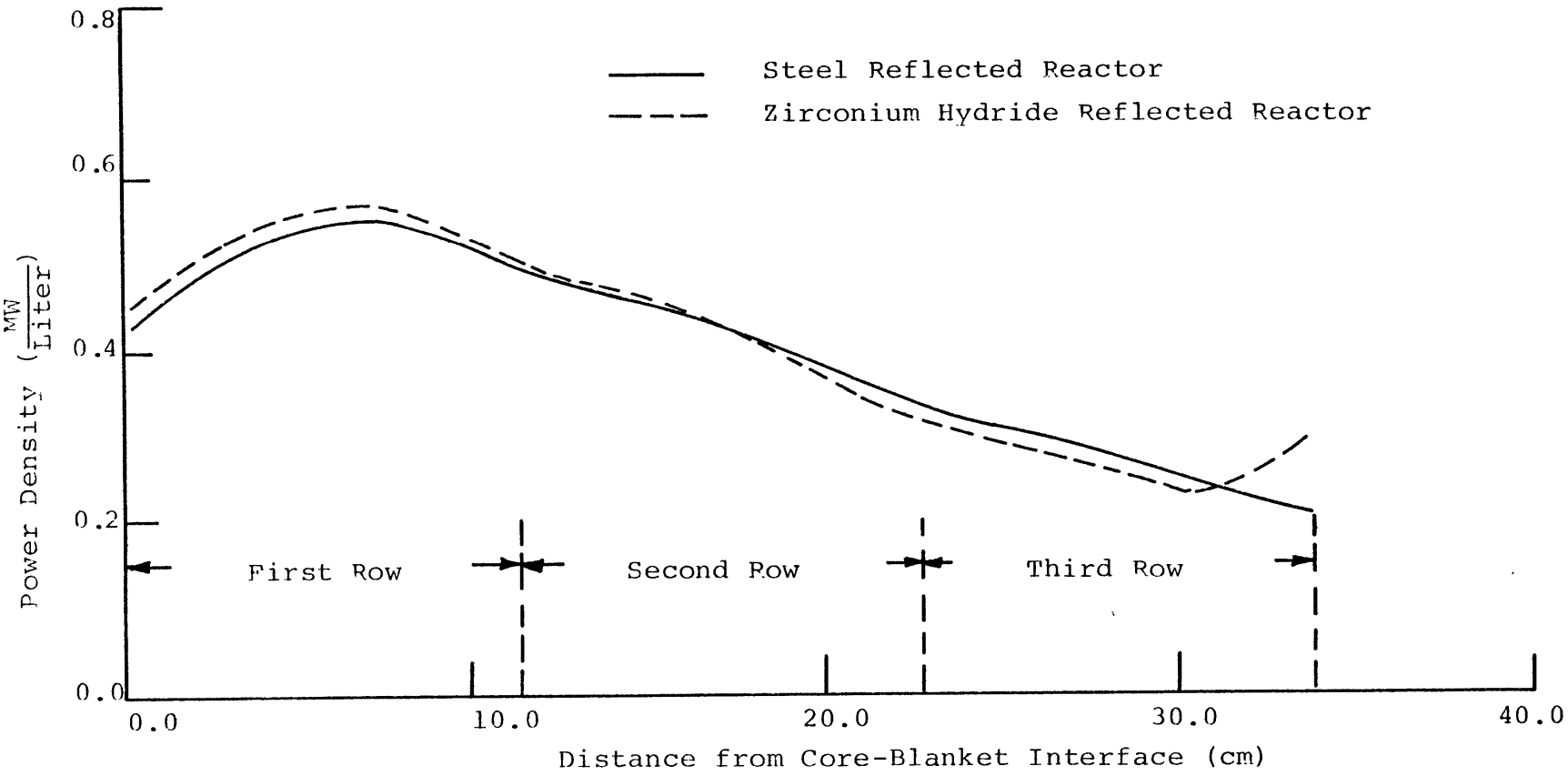

Fig. 3.13 Radial Blanket Power Distribution in the Steel and Zirconium Hydride Reflected Reactors

of equilibrium cycle reactor, consisting of a 30% voided internal blanket system and a 30% moderated radial blanket which has been moved from the core after four cycles of residence was studied. Figure 3.14 shows the BOEC midplane power distribution in the core and blanket. The BOEC power production and peak linear heat generation rates in different regions of the reactor are shown in Table 3.22. Compared to the core with a 40% moderated, two cycle-burned radial blanket system analyzed in Section 3.3, the radial blanket power production at the BOEC has increased from 19.05% to 26.04% and the peak fuel LHGR has dropped by another 5% for a total reduction of approximately 15% compared to the reference core.

Later in this chapter several other core and blanket systems that use the in/out blanket strategy will be analyzed. In these systems the objective is to try to increase the power production from the radial blanket even further by going to larger numbers of radial blanket rows and by variable moderation. It will be shown that although some of these ideas result in a higher power production from the radial blanket, the increases are quite modest and no substantial gains over the system analyzed in Section 3.3 can be achieved.

Thus representative advantages of moving Th-U233 internal blanket assemblies out to a moderated radial blanket (which include production of 20% to 30% of the total core power by the radial blanket, and core power flattening, leading to a reduction of 10% to 15% in the peak fuel linear heat generation rate) have been achieved by the systems analyzed in this

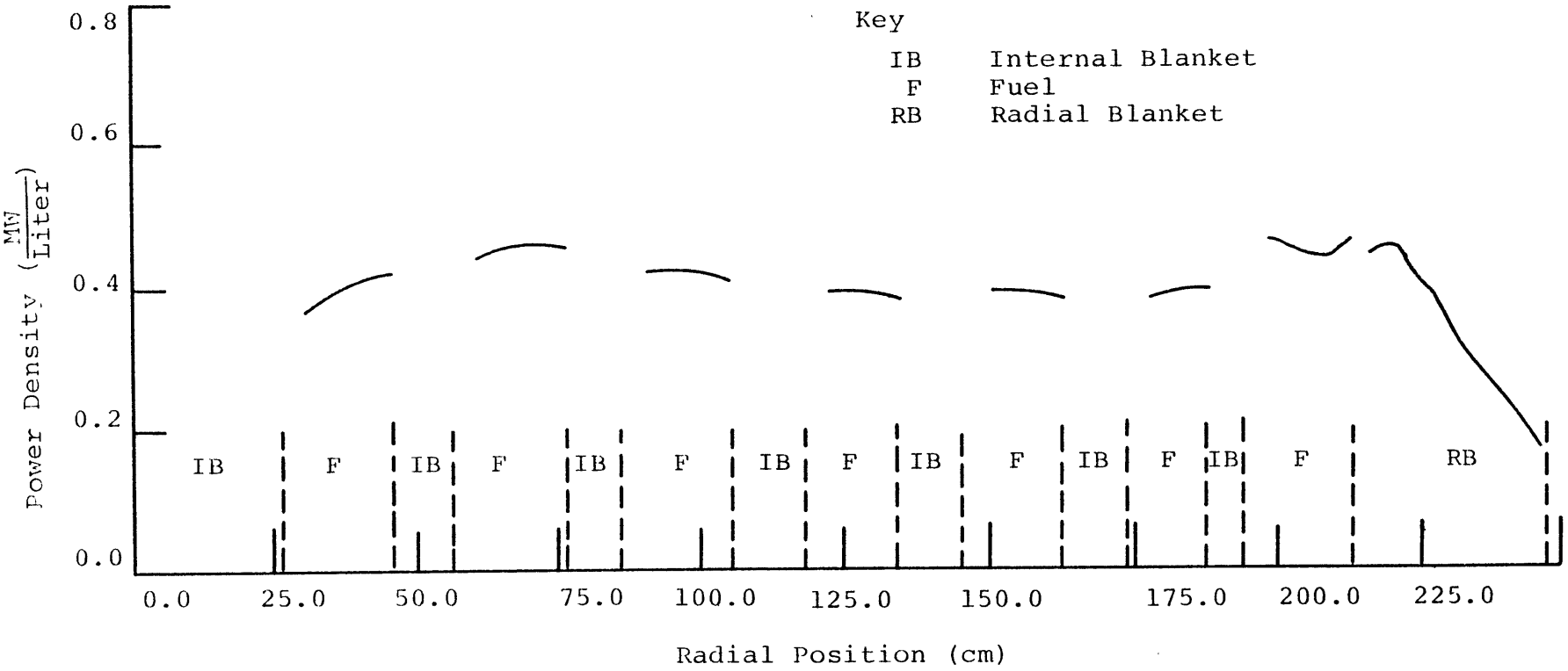

Fig. 3.14 Beginning-of-Equilibrium Cycle Midplane Power Distribution in the $(U\text{-}Pu)O_2$ Core with a 30% Moderated, 6.1% U233 Enriched Thorium Radial Blanket

chapter.. There is hope for more significant improvements, however. The blanket criticality studies discussed earlier indicated that blanket assemblies can be made critical (under a zero flux boundary condition, which simulates a critical internal blanket system) by building up U233 in an internal blanket to a level achievable in about four core cycles (i.e. 4 years) and then moderating the assembly with approximately 40% of the fuel pin positions occupied by zirconium hydride. This finding leads to the idea of moving the internal blanket assemblies inward rather than outward, and creating a critical or near-critical internal blanket "island" in the middle of the core.

To check this idea the reference core was rearranged by replacing the six innermost blanket and fuel rings with 40% moderated blanket assemblies that are moved from the four outer internal blanket rows. The row configuration of the core is shown in Fig. 3.15. The six innermost rings consist of 312 assemblies. The four remaining blanket rings consist of 318 assemblies sandwiched between 564 fissile fueled assemblies. The basic strategy is to build U233 in the outer four rings of the internal blanket and then move these assemblies to the central island where, by using moderation, a critical or near-critical region can be created. Several beginning-of-cycle cases were studied. In all cases the outer blanket assemblies were 40% voided. These blanket assemblies, after several cycles of fissile buildup, are moved to the central island region where they are moderated with 40% zirconium hydride similar

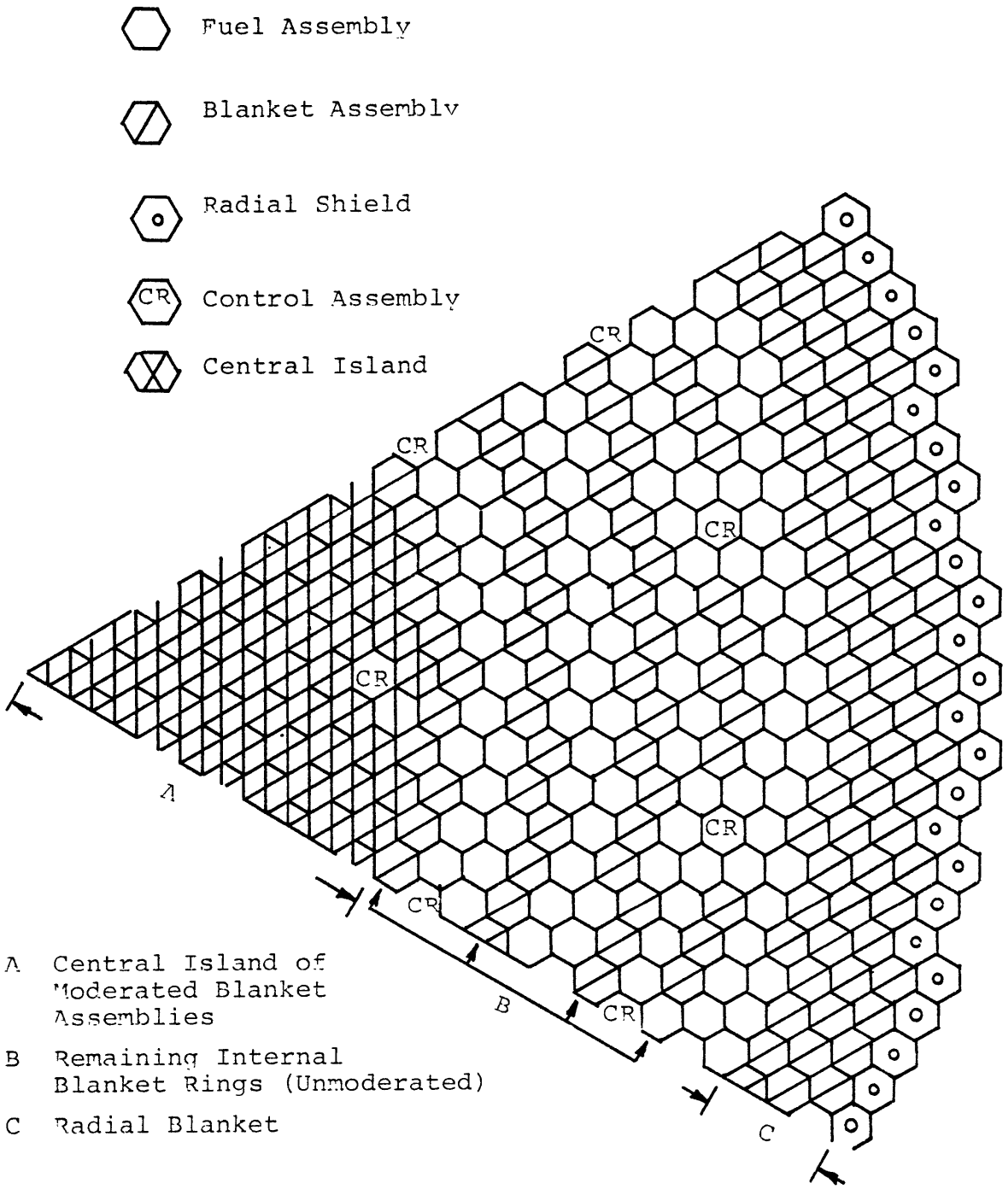

Fig. 3.15 New Core Arrangement Including a Central Island

to the strategy used previously for the radial blanket.

The first case studied consisted of moving the four outer rings of the internal blanket after four cycles of U233 buildup to the central island, which is 40% moderated. The enrichment of the four outer internal blanket rings after 4 cycles of U233 buildup ranges from 4.95% U233 to 6.78% U233 with an average of 5.83% U233. This enrichment is higher than the clean critical enrichment of 4.66% U233 for 40% moderated blanket assemblies given in Table 3.19. The highest enrichment assemblies were moved to the middle of the core and the lower enrichment assemblies to the outer ring of the island. The beginning of cycle k_{eff} for this core was 1.2027 compared to 1.0428 for the beginning of equilibrium cycle k_{eff} for the $(U\text{-}Pu)O_2$ core with 40% moderated radial blanket system studied in Section 3.3. However the power densities in the central region of the core were extremely high, and far above allowable limits. To correct this situation, the enrichment of the central region was reduced by moving the outer four rings of internal blankets after <u>two</u> cycles of U233 buildup to the central island. The enrichment of these blanket assemblies after two cycles of U233 buildup varied from 2.98% to 4.06% with an average of 3.5%, which is lower than the critical enrichment of a 40% moderated blanket system. The beginning of cycle (BOC) k_{eff} in this case was 1.0164. Figure 3.16 shows the BOC midplane power distribution in the core and blanket. Note that the radial blanket of this core consisted of 40%-moderated-two-cycle-burned blanket assemblies, i.e., the internal blanket assemblies must be alternately moved

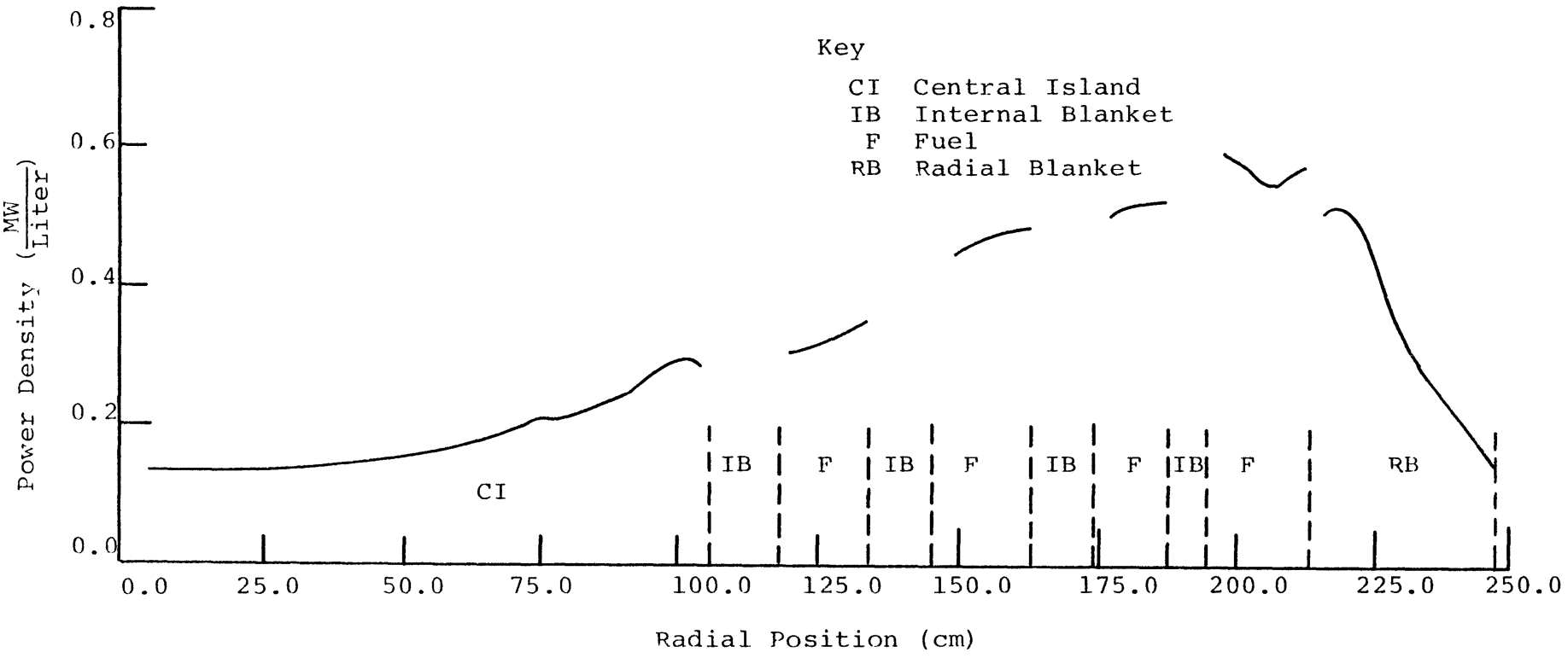

Fig. 3.16 Beginning-of-Cycle Midplane Power Distribution in the $(U\text{-}Pu)O_2$ Core with a 40% Moderated, Two-Cycle-Burned Central Island

to the radial blanket and to the central region. This is necessary both to boost the k_{eff} at the BOC and to flatten the power distribution. If the radial blanket is replaced by fresh thorium assemblies (no enrichment and no moderation) at the BOC the beginning of cycle k_{eff} drops to 0.9963 and the power peaks substantially in the core. In Fig. 3.16, there are no power peaks in the core above the limits given in Table 2.2, despite the fact that the central island region has low power densities and power is pushed to the outer region of the core. However, the power density in the first rows of the radial blanket is very close to the limit. The power density in the radial blanket region next to the core can be reduced by using less moderation or lower enrichment, i.e., moving one-cycle-burned internal blanket assemblies to this row of the radial blanket.

To increase the power density in the central island, the enrichment in this region can be increased by moving the internal blanket assemblies after three cycles of U233 buildup to the central region. The average enrichment of the four outer rings of internal blanket after three cycles of burnup is 4.84% U233. Figure 3.17 shows the beginning-of-cycle power distribution in this core. It can be seen that the power is more uniformly distributed throughout the core and blanket, with no peaks in the radial blanket next to the core blanket interface. Note that up to here the basic fuel management strategy has been a two-cycle batch burnup of the core and blankets. To be able to move a three-cycle-burned internal

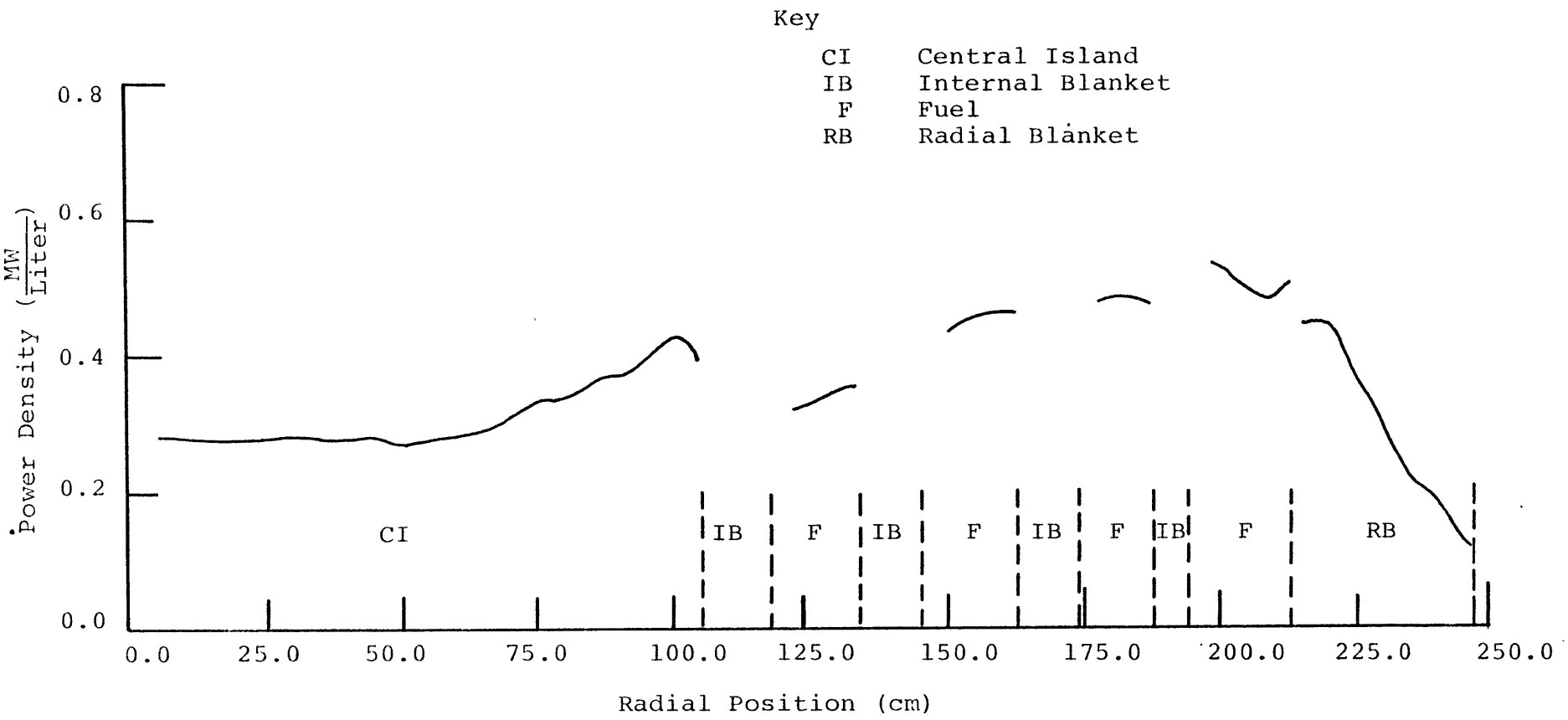

Fig. 3.17 Beginning-of-Cycle Midplane Power Distribution in the $(U\text{-}Pu)O_2$ Core with a 40% Moderated, Three-Cycle-Burned Central Island

blanket to the central island, the fuel management scheme would have to employ annual refuelling.

The preliminary results of the studies on the cores with critical or near critical central islands mentioned in this section are very significant. With respect to the core fissile enrichment, 216 fuel assemblies with an average enrichment of 22% fissile plutonium have been replaced with a Th-U233 moderated system having an average enrichment of only 4.84% U233 (for the three-cycle-burned blanket assemblies). Also, 96 internal blanket assemblies in the middle of the core have been replaced with 4.84% enriched assemblies. If we were to smear the fissile plutonium in the 216 fuel assemblies over 312 fuel and internal blanket assemblies (including an allowance for the difference in fuel volume fractions) the overall smeared fissile plutonium enrichment is about 10.36% fissile plutonium. In effect, by creating a near critical internal blanket island, it has been possible to replace an average fissile plutonium loading of 10.36% in 312 assemblies (or an average fissile plutonium of 22%, in 216 assemblies) with a Th-U233 moderated system containing only 4.84% U233, and still have a core that is almost as reactive as the original core.

Overall, although the studies on the idea of a critical or near critical central island presented here must be regarded as preliminary in nature, enough interesting results are in evidence to suggest further investigation. The biggest advantage of this concept is that a large fraction of the highly

enriched plutonium core assemblies can be replaced by the lower-enriched Th-U233 moderated assemblies, thereby reducing the amount of plutonium involved in the operation of the reactor.

3.5 Use of Internal Blanket Moderation to Control Excess Reactivity

In this section the possibility of using zirconium hydride to control the excess reactivity will be discussed. As was shown in Section 3.3, if the moderator is included in the internal blanket assemblies the beginning of cycle k_{eff} is significantly reduced. Based on this observation, it was concluded at the time that from the physics point of view it is best to leave the internal blanket assemblies in the core without any moderation and add the moderator to the blanket assemblies after they are moved to the radial blanket. However this result also retrospectively initiated the idea of using the moderator in the internal blanket assemblies to control the core's excess reacitivty.

To investigate this possibility, two beginning-of-equilibrium-cycle (BOEC) k_{eff} calculations were performed on the $(U\text{-}Pu)O_2$ core having a 40% moderated thorium radial blanket, studied in Section 3.3. In the first case the four innermost internal blanket rows (see Fig. 2.1) which consist of 163 assemblies out of the total of 415 internal blanket assemblies were filled with 40% zirconium hydride. In the second case the first five innermost internal blanket rows, which consist of 247 out of the total of 415 internal blanket assemblies were filled with 40% zirconium hydride. The beginning-of-equilibrium-cycle k_{eff}'s are given in Table 3.23, and shown in Fig. 3.18. Based on

Table 3.23

Beginning of Equilibrium Cycle k_{eff} as a Function of the Number of Moderated Internal Blanket Assemblies

Number of Internal Blanket Moderated Assemblies	k_{eff}
0	1.0428
163 (Four Rows)	1.0025
247 (Five Rows)	0.9835

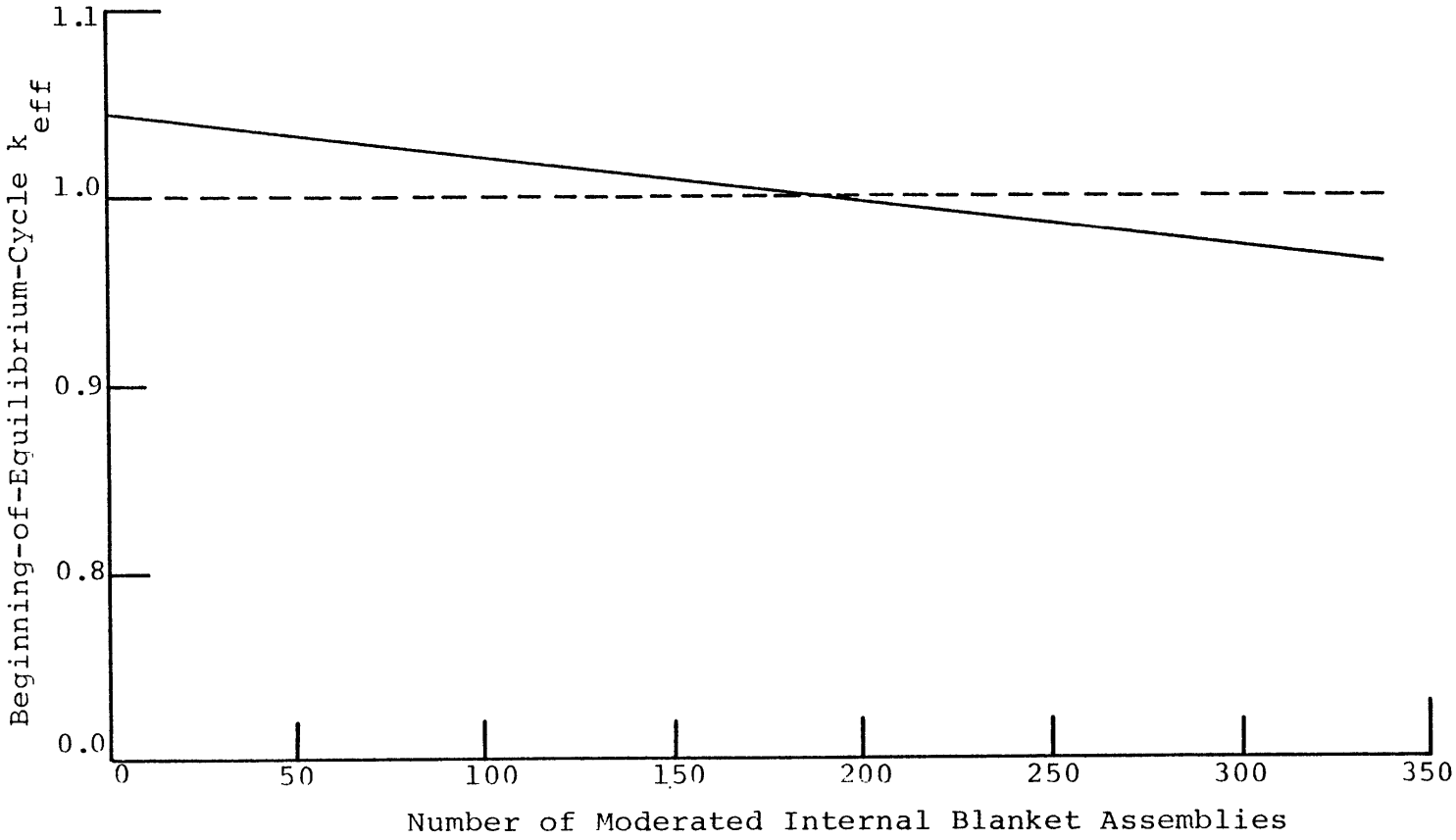

Fig. 3.18 Beginning-of-Equilibrium-Cycle k_{eff} as a Function of the Number of Moderated Internal Blanket Assemblies

Fig. 3.18, if approximately 190 out of the total of 415 internal blanket assemblies include moderator at the BOEC, the reactor will be exactly critical. Note that the beginning-of-equilibrium-cycle k_{eff} of 1.0428 shown in Table 3.23 correponds to an end-of-equilibrium-cycle k_{eff} of 1.0. Thus, by inserting moderator in approximately 190 blanket assemblies the excess reactivity over a two year burnup cycle can be controlled. The required number of moderated blanket assemblies would be much lower if annual refueling, with its lower cycle Δk, were adopted. It should also be noted that a movable mechanism similar to the PWR control system would be necessary to control the excess reactivity throughout the equilibrium cycle, since permanent inclusion of moderator in the internal blanket assemblies would result in a subscritical system as the fuel in the core is depleted.

As shown in the earlier studies related to the moderated internal blankets, complete insertion of the moderator in all of the blanket assemblies will result in a reduction of the flux and power densities in the inner core, and peaking of the flux in the outer region of the core. This of course can be avoided by programming the insertion pattern of the moderator in the blanket assemblies to flatten the power distribution in the core and blanket.

Thus the proposed internal blanket design, which includes empty rod positions to accommodate later moderator addition, can also be used for reactivity control purposes by insertion of moderator in blanket assemblies while they still reside in the core.

3.6 Prompt Neutron Lifetime

In the original study done by Avery (A2) on coupled fast-thermal breeder reactors, the main objective was to create a fast breeder reactor with enhanced safety features by increasing the neutron lifetime to values close to those of thermal reactors and without degrading the neutronic advantages of breeder reactors substantially.

The system proposed by Avery consisted of a fast plutonium-fueled core surrounded by an inner radial blanket consisting of natural uranium, sodium and structure. The inner blanket itself was surrounded by a ring of beryllium. Finally there was an outer blanket consisting of (primarily) depleted uranium. The inner blanket ring behaved essentially as the core for the thermal system. By this method of coupling fast and thermal reactors, it was possible to increase the prompt neutron lifetime from 1.5×10^{-7} seconds (characteristic of an all-fast system) to a value of 2×10^{-5} seconds for the coupled system. This modification resulted in a 10% reduction in the breeding ratio and a 10% increase in the fast core critical mass. In the coupled system approximately 13% of the total power was produced by thermal fission.

To see if coupling of the fast core with moderated blankets as studied in the present work offers any extra safety advantages via longer neutron lifetime, the approach employed by Sheaffer (S6) was used to calculate the neutron lifetime of the reference core discussed in Section 3.2 and the $(U\text{-}Pu)O_2$ core with a 40% moderated thorium blanket discussed in Section 3.3.

The reference core is representative of a heterogeneous all-fast system and the $(U\text{-}Pu)O_2$ core with a 40% moderated radial blanket was taken to represent the coupled system studied in this work.

Sheaffer in his study on fast reactors showed that many fast reactor parameters can be related to two spectrum characterization parameters, S and R, defined as:

$$S = \frac{\bar{\nu}\Sigma_f}{\nu\Sigma_f + \xi\Sigma_{tr}} \tag{3.2}$$

$$R = \frac{S}{1-S} \frac{\Sigma_{tr}}{\Sigma_r} \tag{3.3}$$

where:

$\bar{\nu}$ is the average neutron yield per fission

Σ_f is the macroscopic fission cross section

ξ is the average increase in lethargy per collision

Σ_{tr} is the macroscopic transport cross section

Σ_r is the macroscopic removal cross section

The prompt neutron lifetime was correlated to the spectrum characterization parameter, S, by the relation:

$$L_p = C\ (\bar{\nu}\ \Sigma_f S)^n \tag{3.4}$$

where C and n are constants which were found by matching the above relation against some 45 fast reactor cores having widely different compositions. The best values for C and n resulted in the relation:

$$L_p \doteq 0.1629\ (\nu\Sigma_f S)^{-0.8955} \times 10^{-8}\ \text{sec} \qquad (3.5)$$

This relation will be used in this section to calculate the prompt neutron lifetime of the two cores mentioned earlier. For this purpose a set of one group cross sections for the core, internal and radial blanket were generated for each core. This was done using the 10 group cross sections used in the burnup calculations and the 10 group fluxes from 2DB calculations on each core. To generate a one-group cross section for the whole reactor, the one group fuel, internal and radial blanket cross sections were next flux and volume weighted using the fluxes and volumes of each region.

Table 3.24 shows the final system-average macroscopic cross sections, and the prompt neutron lifetimes, for the two cores under study.

It can be seen that the prompt neutron lifetime in the coupled set is increased by about 13%, which does not constitute any major advantage over the reference system. It is also interesting to note the values shown in Table 3.24, which were found using a one-group model, are fairly close to the typical values reported for fast breeder reactors. As an example, in a study done at Westinghouse (R1) on a particular parfait core, a prompt neutron lifetime of 3.7×10^{-7} seconds was reported, which is fairly close to the values shown in Table 3.24.

The main reason for the short prompt neutron lifetime of the coupled system studied here, compared to Avery's coupled system, is the fact that the moderated blanket studied here is

Table 3.24

Macroscopic Cross Sections and Prompt Neutron Lifetimes of the Reference Heterogeneous and the Coupled Cores

	Reference Heterogeneous Core	Coupled Core
$\nu\Sigma_f$	0.74548E-2*	0.80554E-2
$\xi\Sigma_{tr}$	0.15793E-1	0.23306E-1
L_p	3.6×10^{-7} sec	4.1×10^{-7} sec

*Read as 0.74548×10^{-2}

much less thermalized than the thermal reactor segment of Avery's coupled system. One way to show this is to look at the fraction of the total power produced by thermal fissions. As mentioned earlier, in Avery's coupled system about 13% of the total power was produced by thermal fission. In the coupled system studied here the fraction of power produced by thermal fission (fission induced by neutrons $\leq$ 0.68 ev) in the core and internal blankets is essentially negligible. Focusing next on the radial blanket: the fraction of the power produced by thermal fissions is directly proportional to the thermal fission reaction rate fraction, i.e.,

$$\frac{(\Sigma_f \phi)\,\text{thermal}}{(\Sigma_f \phi)\,\text{total}} \tag{3.6}$$

In the 10 group cross section set used in burnup calculations the upper energy of the last group is 0.68256 ev. Taking this last group as the thermal group the ratio of the fission rate in the last group to the total fission rate is 0.3454, i.e., the thermal fission rate in the radial blanket accounts for about 34% of the total fission rate in the radial blanket. The total power produced by the radial blanket at the beginning of an equilibrium cycle is approximately 20%. Hence the total power produced in the reactor due to thermal fission is approximately 6.9%, which is just over half of the power produced in Avery's coupled system. The fast-to-thermal flux ratio in the radial blanket is 44.6; this ratio in a typicallight water reactor is

around 5 to 6. In review of these findings, it appears that the moderated radial blanket system studied here is much more epithermal than the thermal part of Avery's coupled reactor, which is a plausible reason for the small increase in the neutron lifetime in this system compared to Avery's coupled system.

So far in this chapter the focus on the moderated radial blanket systems has been on two year batch shuffling of internal blanket assemblies to the radial blanket (which is moderated to the extent of 40% zirconium hydride). In the next section several other alternative fuel shuffling and moderation methods will be discussed.

3.7 Neutronic Performance of Several (U-Pu)O_2 Cores with Moderated Thorium Blankets

In this section the neutronic performance of several other (U-Pu)O_2 cores with moderated thorium blankets will be analyzed. The objective in looking at these different systems is to see if the power production from the radial blanket can be increased any further than the reference two cycle batch, 40% moderated radial blanket system studied in Section 3.3. The difference between these systems and the system studied in detail in Section 3.3 is in the number of radial blanket rows, the moderation level, and the blanket residence time.

The first system analyzed consisted of the same core and internal blanket arrangement as the (U-Pu)O_2 core with thorium blanket studied before but with six rows of radial blanket.

In this core the fuel and thorium internal blankets are burned for two cycles after which the internal blankets are moved to the radial blanket and fuel and internal blanket assemblies are replaced by fresh fuel. The number of internal blanket assemblies is only one half of the number of radial blanket assemblies, so that in the second two-cycle burnup step, the radial blanket consists of half two-cycle-burned internal blankets and half two-cycle-burned radial blanket assemblies. The third two-cycle-burnup step represents the steady state core and blanket system. So, at the beginning of equilibrium cycle (BOEC) the fuel and internal blanket consists of fresh fuel and the radial blanket includes half two-cycle-burned blanket assemblies and half four-cycle-burned assemblies. Thus, the blanket assemblies stay in the core for six years, two years in the core proper and four years in the radial blanket. Figure 3.19 shows the BOEC midplane power distribution in this core. (The BOEC power density curves for different cores shown in this section should be compared with Fig. 3.8, which is for the standard two-cycle, 40% moderated case). Table 3.25 gives the BOEC power fractions in different regions of the reactor. Note that the fraction of the power from radial blanket has increased from about 19% in the system studied in Section 3.3 to over 24% in this system, but this increase is not high enough to justify incorporation of over a factor of two bigger radial blanket system. From Fig. 3.19, it can be seen that the power production from the last few rows of the radial blanket is very low.

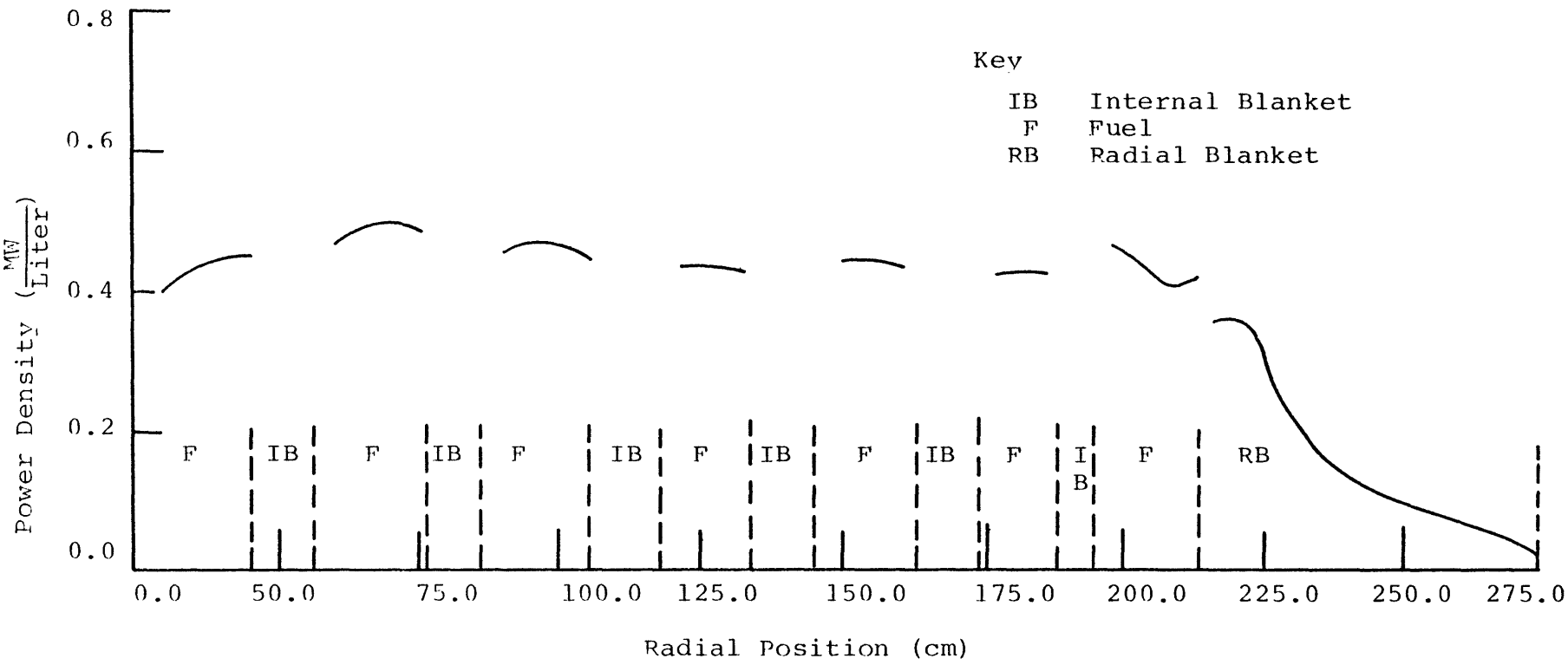

Fig. 3.19 Beginning-of-Equilibrium Cycle Midplane Power Distribution in the $(U\text{-}Pu)O_2$ Core with a Six Row, 40% Moderated Radial Blanket

Table 3.25

Beginning of Equilibrium-Cycle Power Production From Different Regions of the $(U\text{-}Pu)O_2$ Core with a 40% Moderated, Six Row Radial Blanket

Reactor Region	Power Contribution (%)
Fuel	72.94
Internal Blanket	0.46
Axial Blanket	2.56
Radial Blanket	24.04

In an attempt to increase the power production from the last few rows of the radial blanket two other cases were analyzed. In one case the first three rows of the radial blanket were left unmoderated and the last three were moderated with 40% zirconium hydride. This was done to see if flux attenuation can be reduced in the first few rows of the radial blanket so that more neutrons can get to the outermost rows of the radial blanket. Table 3.26 gives the power fractions of different regions of the core at the BOEC. It can be seen that the results are fairly similar to the results of the preceding case just presented in Table 3.25.

In the second case a variable moderation procedure was employed. It was thought that if the last rows of the radial blanket are more moderated than the first rows, the power production from the last rows might increase. In this case the first two rows of the radial blanket were moderated with 40% zirconium hydride, the next two rows with 50% zirconium hydride and the last two rows with 60% zirconium hydride. The BOEC power fractions are given in Table 3.27. Again it can be seen that the results are similar to previous cases. This was to be expected, since, in all of the cases described in this section, the first two rows of the radial blanket generate almost 80% of the total power produced by the radial blanket; thus in effect there is only 20% of the radial blanket power to be improved upon. This is also true with regard to the three-row blanket system where several variable enrichment

Table 3.26

Beginning-of-Equilibrium-Cycle Power Production in Different Regions of the $(U\text{-}Pu)O_2$ Core with Six Rows of Radial Blanket: First Three Rows UnModerated, Last Three Rows 40% Moderated

Reactor Region	Power Contribution (%)
Fuel	72.91
Internal Blanket	0.48
Axial Blanket	2.87
Radial Blanket	23.74

Table 3.27

Beginning-of-Equilibrium-Cycle Power Production from Different Regions of the (U-Pu)O_2 Core with Six Rows of Radial Blankets: First Two 40% Moderated, Next Two 50% Moderated and the Last Two 60% Moderated

Reactor Region	Power Contribution (%)
Fuel	73.15
Internal Blanket	0.48
Axial Blanket	2.75
Radial Blanket	23.64

and moderation cases were analyzed. The results did not show much improvement over the two-cycle-40% moderated case studied before.

Finally, a core with half as many internal blanket assemblies as the cases studied before and three rows of radial blanket was studied. In this case U233 was bred into the internal blanket assemblies for two cycles and then the assemblies were moved to the radial blanket. Since the number of internal blanket assemblies is half of the number of radial blanket assemblies, the blanket assemblies remain in the radial blanket for four cycles. Figure 3.20 shows the BOEC midplane power densities in this core. Table 3.28 gives the fraction of the power produced by different regions of the reactor. The average enrichment of the core has dropped from about 23% fissile plutonium to about 18% fissile plutonium, due to removal of half of the internal blanket assemblies. This of course results in a higher positive sodium void coefficient compared to cores with more internal blanket assemblies, so that the neutronic advantages should be judged against possible safety disadvantages. From Fig. 3.20 it can be seen that the power density distribution in the core is quite flat, and the fraction of power produced by the radial blanket is again very similar to the cases previously studied.

So far in this chapter, all the studies related to the in/out fuel management strategy have been on the thorium internal and radial blanket system because of the superior

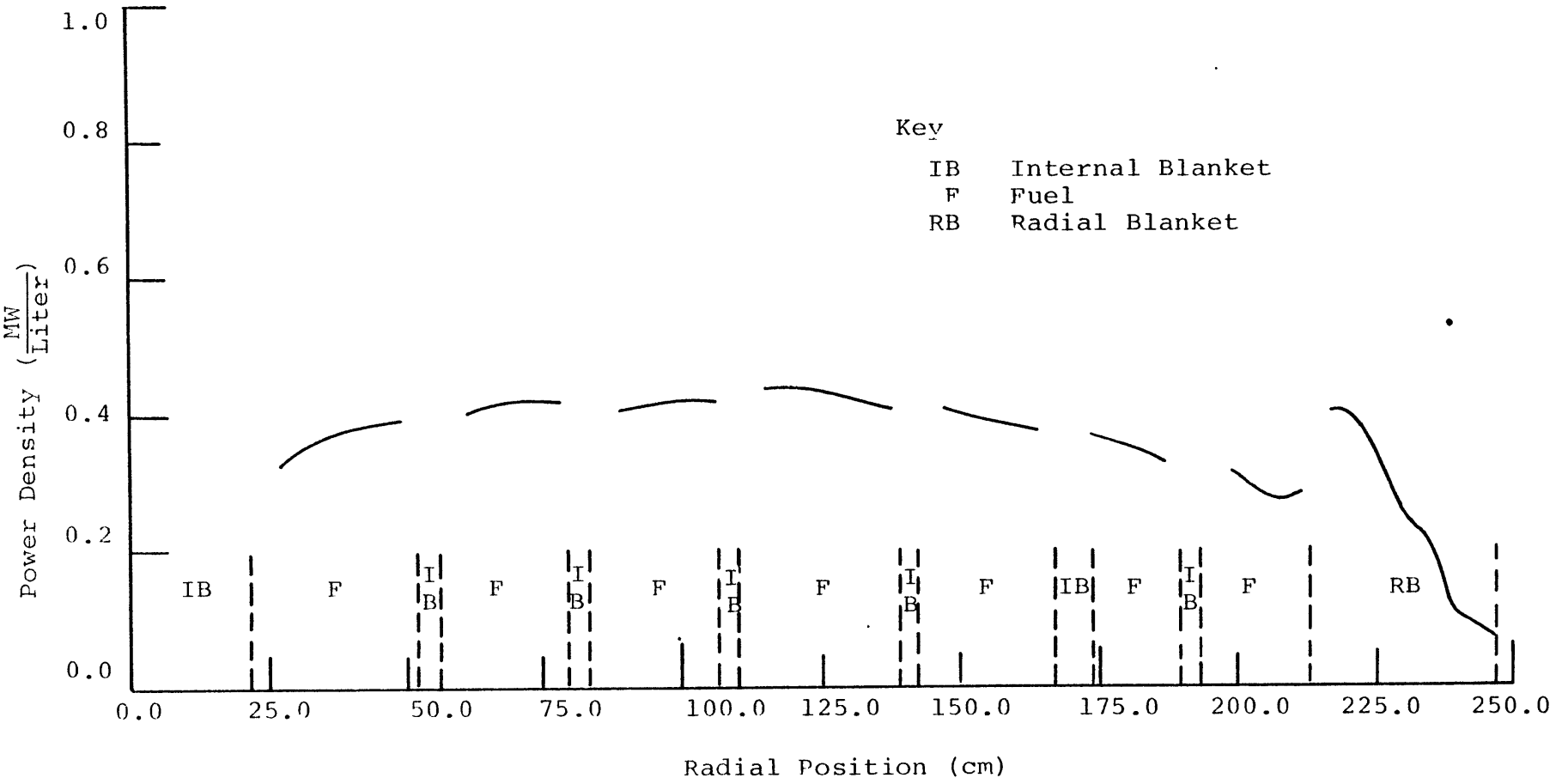

Fig. 3.20 Beginning-of-Equilibrium-Cycle Midplane Power Distribution in the $(U\text{-}Pu)O_2$ Core with Half as Many Internal Blanket Assemblies as in the Reference Core and a 40% Moderated Thorium Radial Blanket

Table 3.28

Beginning-of-Equilibrium-Cycle Power Production in Different Regions of the (U-Pu)O_2 Core With Half as Many Internal Blanket Assemblies in the Core and a 40% Moderated Thorium Radial Blanket

Reactor Region	Power Contribution (%)
Fuel	84.1%
Internal Blanket	0.5
Axial Blanket	0.8
Radial Blanket	19.17

neutronic characteristics of the epithermal Th-U233 system. In the next section, a brief study on the effects of using the in/out strategy on the neutronic performance of a $(U\text{-}Pu)O_2$ core having depleted uranium blankets will be presented.

3.8 Burnup Analysis of the $(U\text{-}Pu)O_2$ Core with Depleted Uranium Blankets, Employing an In/Out Fuel Management Strategy

3.8.1 Introduction

In this section a brief discussion on the neutronic properties of the $(U\text{-}Pu)O_2$ core with depleted uranium blankets and using the in/out shuffling strategy, will be presented. The primary purpose of this phase of the work was to see if there are any advantages in using the breed/burn strategy in an all-uranium blanket system. For this purpose two steady state cores were analyzed. The first system consists of a $(U\text{-}Pu)O_2$ core with depleted uranium internal, axial and radial blankets without any moderation. The second system consists of a $(U\text{-}Pu)O_2$ core with a 40% voided depleted uranium internal blanket and a 40% moderated radial blanket similar to the case studied in Section 3.3. In both cases the core and blankets were depleted for two cycles after which the internal blanket assemblies are moved to the radial blanket. The second two-cycle depletion was taken as the steady state core, which is described next.

3.8.2 Burnup Analysis of the Steady State (U-Pu)O_2 Core with Depleted Uranium Blankets and In/Out Fuel Management

As was mentioned earlier, to see the effect of the in/out shuffling strategy on the neutronic properties of the (U-Pu)O_2 core with depleted uranium blankets two cases were considered. In the first case internal blanket assemblies, after two cycles of plutonium buildup were moved to the radial blanket. Figure 3.21 shows the beginning-of-equilibrium cycle core and blanket power distribution. The fraction of the power produced by different regions of the reactor are given in Table 3.29. The beginning-of-equilibrium-cycle k_{eff} is 1.0223 (compared to 1.0079 for the reference core). The power produced by the radial blanket is slightly higher than the reference core and power is pushed more toward the outer region of the core. Overall there is not much difference in the neutronic performance of this core compared to the reference core.

The second core studied consists of a 40%-voided depleted uranium internal blanket, which after two cycles of plutonium build-up is moved to the radial blanket, where it is moderated using 40% zirconium hydride. It should be noted that the 40% moderation was selected because it was used in most of the cases studied for the thorium blanket system and no attempt was made to optimize the moderator content of the radial blanket, particularly in view of the fact that the performance of a U-Pu epithermal system is not expected to provide any substantial gains in radial blanket performance. Figure 3.22 shows the beginning-of-equilibrium-cycle power distribution in

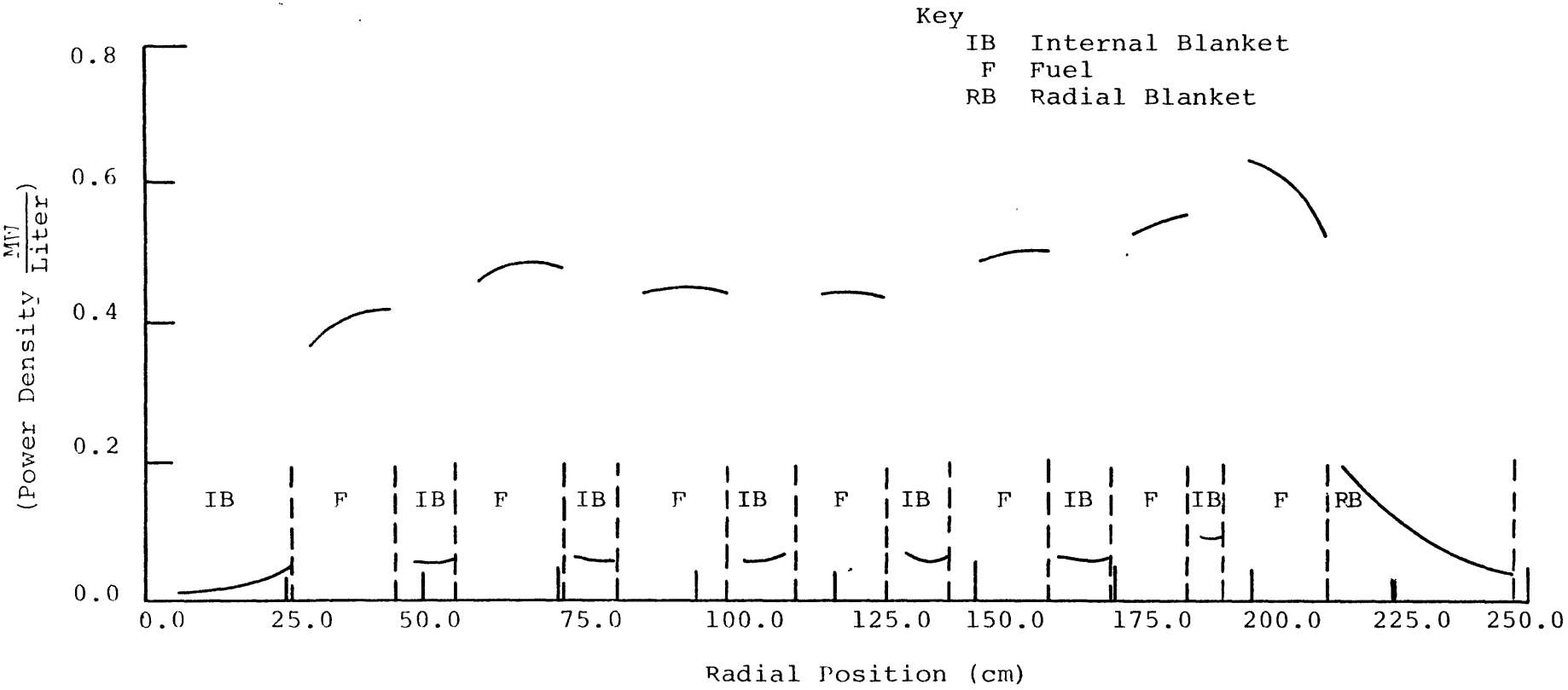

Fig. 3.21 Beginning of Equilibrium Cycle Midplane Power Distribution in the $(U\text{-}Pu)O_2$ Core with Depleted Uranium Internal Blanket and a Two Cycle Burned In/Out Shuffled Radial Blanket

Table 3.29

Beginning of Equilibrium Cycle Power Production in Different Regions of the $(U\text{-}Pu)O_2$ Core with a Depleted Uranium Internal Blanket and a Two-Cycle-Burned In/Out-Shuffled Radial Blanket

Reactor Region	Power Contribution (%)
Fuel	84.87
Internal Blanket	5.08
Axial Blanket	2.45
Radial Blanket	7.60

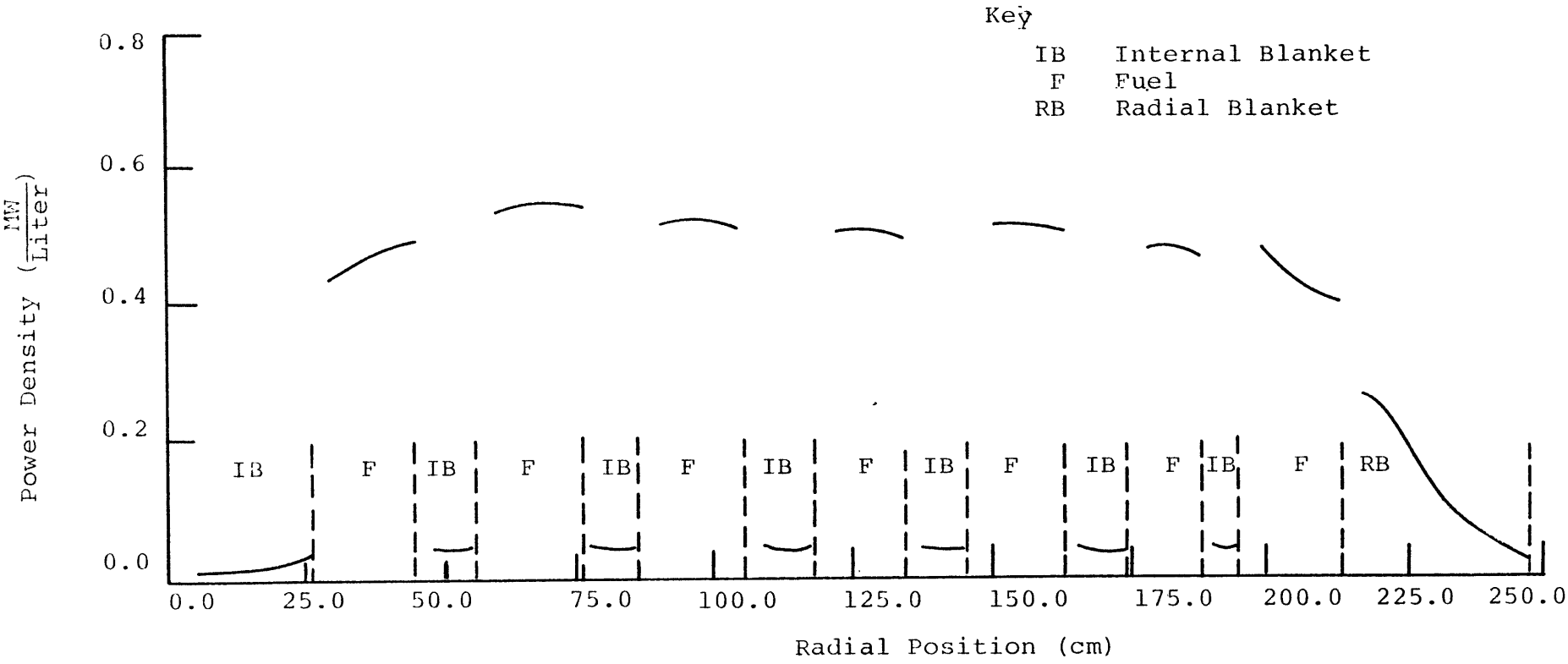

Fig. 3.22 Beginning-of-Equilibrium-Cycle Midplane Power Distribution in the $(U\text{-}Pu)O_2$ Core with a 40% Voided Depleted Uranium Internal Blanket and a Two Cycle Burned, 40% Moderated, In/Out Shuffled Radial Blanket

the core and blanket. Table 3.30 gives the fraction of the power produced by different regions of the reactor. The beginning-of-equilibrium-cycle k_{eff} is 1.0547. Compared to the reference core the power production from the radial blanket is nearly doubled and the power is fairly flat in the core. From the non-proliferation point of view the advantage of using this method of in/out shuffling is in the lower annual plutonium production. This implies that if the objective in utilizing fast breeder reactors is to have a self-sufficient system from the fissile production point of view, with a minimum amount of excess plutonium in the external phases of the fuel cycle, the above strategy could be used effectively.

3.9 Summary and Conclusions

In this chapter the neutronic and burnup properties of the proposed in/out-moderated fuel management strategy were studied. To do this several core and blanket systems were analyzed. These systems were divided into three categories:

1. The reference $(U\text{-}Pu)O_2$ core with depleted uranium internal, axial and radial blankets
2. $(U\text{-}Pu)O_2$ cores with thorium blankets employing an in/out fuel management scheme where the internal blanket assemblies after several cycles of fissile buildup are moved into a moderated radial blanket
3. $(U\text{-}Pu)O_2$ cores with depleted uranium blanket systems employing the in/out fuel management strategy.

Table 3.30

Beginning of Equilibrium Cycle Power Production in Different Regions of the (U-Pu)O_2 Core with a 40% Voided Internal Blanket and a Two-Cycle-Burned, 40% Moderated, In/Out Shuffled Radial Blanket

Reactor Region	Power Contribution (%)
Fuel	82.04
Internal Blanket	3.56
Axial Blanket	3.08
Radial Blanket	11.32

The basic objective in adopting the in/out-moderated fuel management strategy has been to create a reactive radial blanket so that:

a) A substantial portion of the total reactor power can be produced by the radial blanket leading to a reduction in the peak core linear heat generation rate (at fixed total system power)

b) The core neutron leakage to the radial blanket can be reduced, resulting in a lower steady state core fissile enrichment

With respect to the first objective, several (U-Pu)O_2 cores with thorium blankets were analyzed. It was found that the best configuration of the core included an internal blanket system which is 40% voided (i.e., 40% of the blanket pins are left empty) and a radial blanket system which is 40% moderated (filled with zirconium hydride). In these cores the 40% voided internal blanket assemblies, after two to four cycles of residence in the core, were moved to the radial blanket, which is moderated using 40% zirconium hydride. The results showed that approximately 20% to 25% of the total reactor power can be produced by the radial blankets, resulting in a 10-15% reduction in the peak core linear heat generation rate (LHGR). This reduction of the peak LHGR translates to either 10-15% higher power from the same core, or a 15 to 20% smaller core for the same amount of power as delivered by the original core. The studies on the (U-Pu)O_2 core with depleted uranium blankets and employing the in/out fuel management strategy

did not indicate any substantial advantages.

With respect to the second objective, it was found that, although U233 production in the internal blankets is high enough to create an infinite critical epithermal system when moderator is added, the leakage of the neutrons from the radial blanket to the radial shield limits the advantages of this strategy. For the $(U\text{-}Pu)O_2$ core with a 40% moderated blanket system this strategy resulted in a 15% reduction in the core fissile enrichment. Since the critical enrichment of $(U\text{-}Pu)O_2$ cores with thorium internal and external blankets is 10-15% higher than that of $(U\text{-}Pu)O_2$ cores with uranium blankets, the above savings brings the cores with thorium blankets down to a competitive level with uranium blanketed cores.

To take greater advantage of the potentially critical blanket assemblies a different blanket shuffling strategy involving creation of a critical or near-critical central blanket island was examined. It was shown that almost 1/3 of the fuel assemblies (216 assemblies) having an enrichment of 22% fissile plutonium can be replaced by 312 Th-U233 moderated blanket assemblies containing only 4.8% U233. It was concluded that this system offers some interesting possibilities for further investigation.

The results of the blanket criticality calculations as a function of moderation (Tables 3.19 and 3.20) indicate that a once-through breeder reactor similar to the Fast Mixed Spectrum Reactor (FMSR) described in Chapter 1 cannot be developed from

a moderated system of the present type due to the low breeding ratio of the moderated assemblies (i.e., when $k_\infty > 1.0$, BR $\leq$ 1.0). Among the systems shown in Tables 3.19 and 3.20, only unmoderated U-Pu and Th-U233 systems have breeding ratios above one, with the U-Pu system having the highest breeding ratio as expected. The critical enrichment of the unmoderated U-Pu system is about 9%-10% fissile plutonium. Since the plutonium production rate in the core starts at about 1%-2% fissile plutonium per year and levels off at higher enrichments, it takes a very long time to build in plutonium close to the critical enrichment level, and this is the reason for the long (17 years) fuel residence requirement in the FMSR. While U-233 need only be built up to half the plutonium level (to achieve $k_\infty = 1$ in a moderated environment)--which can take place in roughly half the time--the breeding ratio suffers greatly.

Finally, the idea of using moderator in the internal blankets for the control of excess reactivity was examined, and it was found that this method can be used effectively to control excess reactivity over a one or two-year burnup cycle.

CHAPTER FOUR

ECONOMIC ANALYSIS

4.1 Introduction

In this chapter the economic performance of the cores studied in Chapter 3 will be evaluated. To do so, first an economic environment consisting of the unit costs and other related parameters necessary for the fuel cycle cost calculations will be defined. In reviewing the literature for the latest values of economic parameters used in fast breeder reactor fuel cycle cost calculations, a wide range of values and uncertainties were found for different components of the fuel cycle cost. The most noticeable and controversial parameter in this category is the unit price of fissile plutonium. As will be shown later in the fuel cycle cost calculations, depending on the price of fissile plutonium, the cost of buying plutonium and its carrying charges constitute one of the largest portions of the fuel cycle cost. Thus in comparing the fuel cycle cost of a fast breeder reactor with any other type of reactor, such as a light water reactor or in fuel cycle cost comparisons between homogeneous and heterogeneous cores, the assumed price of plutonium has a major impact on the results. For example, when comparing homogeneous against heterogeneous fast breeder reactors, heterogeneous cores have considerably higher fissile inventories, which gives rise to an economic penalty; but they also have lower

total fuel fabrication costs, due to the smaller number of high-fabrication-cost fuel assemblies. Depending on the price of plutonium, the importance of the saving due to lower fuel assembly fabrication costs has a different net impact. If the price of plutonium is high, fabrication costs constitute a small portion of the total fuel cycle cost, and the savings associated with lower fuel assembly fabrication costs cannot make up for the higher fissile inventory costs. But if the price of plutonium is sufficiently low, then the fuel assembly fabrication cost is a major part of the fuel cycle cost, and the net saving associated with a heterogeneous core could be higher than the penalties associated with higher fissile inventory. So it can be seen that the uncertainties in some of the parameters used in fuel cycle cost calculations can have a decisive effect on the results and conclusions of a given analysis.

In many economic analyses in the nuclear field, and especially in fuel cost calculations for LMFBRs, where the actual product is not commercially available and most of the cost components (especially from the back-end of the fuel cycle) are estimated, there is a large degree of uncertainty associated with the final results. Realizing the existence of this band of uncertainty, what is important in fuel cycle cost calculations such as those performed in this study is to use a consistent set of parameters and assumptions in making comparisons.

In this chapter a short description of the simple model (A4, B6) used for the calculation of the levelized fuel cycle cost will be given. This will be followed by a listing of the reference economic parameters necessary for the fuel cycle cost calculations. Using the simple model and the assumed economic environment, the levelized fuel cycle cost of the reference core and the breed/burn cores will be calculated. An analysis of the results and a comparison between the economic performance of the cores studied will be presented, followed by a summary of the results and conclusions.

4.2 Fuel Cycle Cost Model

As was mentioned in Chapter Two, the fuel cycle cost calculations in this study are performed using Abbaspour's simple model (A4), which in turn is a follow-on to earlier work by Brewer (B6). In this model all the batches of fuel (or blanket) are assumed to be steady state batches, i.e., the start up and shutdown batches at the beginning and end of the plant life are not explicitly accounted for. Also, the revenues from the sale of electricity are assumed to be received at the middle of the cycle, at which time the depreciation is also credited. Abbaspour (A4) compared this model and the above assumptions with a more sophisticated fuel cycle cost code, MITCOST (C7), and found good agreement.

The levelized fuel cycle cost e (mills/kwhe) derived using the simple model approximations can be written in the form:

$$e = \frac{1}{E} \sum_i M_i C_i F_i G_i \qquad (4.1)$$

where

E is the total electricity generated by a batch of fuel (or blanket) during its residence in the reactor, (Mwhe)

M_i is the mass flow in stream i, (Kg)

C_i is the unit cost of the material in step i, ($/Kg)

F_i is a "financial weighting factor," and for the case in which all fuel cycle expenses, and credits, are capitalized and depreciated is given by

$$F_i = \left[\frac{1}{1-\tau} \frac{(P/F, x, t_i)}{(P/F, x, t_r/2)} - \frac{\tau}{1-\tau} \right] \qquad (4.2)$$

τ is the tax rate

x is the discount rate, and is given by

$$x = (1 - \tau) r_b f_b + r_s f_s \qquad (4.3)$$

r_b is the fraction of the total investment from bonds

r_s is the rate of return to the stockholders

f_s is the fraction of the total investment from stocks; $f_s + f_b = 1.0$

t_i is the lag or lead time for transaction i, measured from the beginning of the batch irradiation, (yr)

t_r is the total residence time for a batch of fuel (or blanket) in the reactor, (yr)

$(P/F, x, t)$ is the present worth factor for transactions which occur t years from the reference time (beginning

of batch irradiation in the present calculations)

G_i is the escalation factor, given by

$$G_i = \left\{ \frac{(P/F,\ y,\ t_r/2)\left[1-\frac{(P/F,\ x,\ N\cdot t_c)}{(P/F, y_i,\ N\cdot t_c)}\right]\left[1-\frac{(P/F,\ x,\ t_c)}{(P/F,\ y,\ t_c)}\right]}{(P/F,\ y_i,\ t_i)\left[1-\frac{(P/F,\ x,\ N\cdot t_c)}{(P/F,\ y,\ N\cdot t_c)}\right]\left[1-\frac{(P/F,\ x,\ t_c)}{(P/F,\ y_i,\ t_c)}\right]} \right\} \tag{4.4}$$

y is the escalation rate allowed by the rate commission for the price of electricity

y_i is the escalation rate for transaction i

N is the total number of batches of fuel (or blanket) that will be irradiated throughout the life of the plant

t_c is the cycle duration, and is the time between successive refuelings of a batch of fuel (or blanket) assemblies. Assuming the escalation rate for the price of electricity is equal to the escalation rate for other transactions, i.e., $y_i = y$, G_i reduces to:

$$G_i = \frac{(P/F, y,\ t_r/2)}{(P/F, y,\ t_i)} \tag{4.5}$$

The simple model assumption that the revenues from the sale of electricity are received and depreciation is credited at the middle of the cycle can be improved by assuming a continuous

cash flow rather than a lumped sum payment in the middle of the cycle. This can be done by substituting for $(P/F, x, t_r/2)$ and $(P/F, y, t_r/2)$ in Eqs. (4.2) and (4.5) by $\frac{1}{tr}(P/\bar{A}, x, t_r)$ and $\frac{1}{tr}(P/\bar{A}, y, t_r)$, respectively. The factor $(P/\bar{A}, x, t)$ is the present worth factor for a uniform cash flow of magnitude $\bar{A}$ over the period t.

Having defined the relationship for the levelized fuel cycle cost calculations, in the next section the unit prices for various parameters used in the fuel cycle cost calculations will be presented.

4.3 The Economic Environment

To obtain a reference economic environment, an effort was made to compile the latest consistent set of values used in fuel cycle cost analyses. Table 4.1 shows the list of unit costs identified for the relevant transactions (N3). The financial parameters used in the fuel cycle cost calculations are given in Table 4.2. The only unit costs not shown in Table 4.1 are the price of fissile plutonium and U233. As was mentioned earlier, the price of plutonium has a major effect on the levelized fuel cycle cost of fast breeder reactors, and at this time there is no unified consensus on the best method for assigning a unit price for fissile plutonium. There are several methods that can be used to calculate a unit price for plutonium in a nuclear economy that includes a mixture of light water and breeder reactors. In one method the cost of plutonium is assumed to be equal to the cost of

Table 4.1

List of Unit Cost Values Used
In the Fuel Cycle Cost Calculations

Transaction	Unit Cost ($/Kg HM)
Fabrication	
$(U\text{-}Pu)O_2$ Fuel Assembly	650
UO_2 Blanket Assembly	140
ThO_2 Blanket Assembly	150
Zirconium Hydride Rods	65 $/Kg zirconium hydride
Spent Fuel Shipping	
$(U\text{-}Pu)O_2$	90
$(U\text{-}Th)O_2$	100
Reprocessing	
$(U\text{-}Pu)O_2$ Fuel Assembly	450
UO_2 Blanket Assembly	390
ThO_2 Blanket Assembly	430
Waste Shipping and Storage	
$(U\text{-}Pu)O_2$	125
$(U\text{-}Th)O_2$	125

Table 4.2

Financial Parameters Used in Fuel Cycle Cost Calculations

	Uninflated	Actual*
Bond (debt) rate of return	2.5%/yr	8.1%/yr
Bond fraction	0.55	
Stock (equity) rate of return	7.0%/yr	12.9%/yr
Stock fraction	0.45	
Income tax fraction, τ	0.5	
Discount rate, x**	3.83%/yr	8.03%/yr

* Based on an inflation rate of 5.5% per year

** $x = (1 - \tau) f_b r_b + f_s r_s$

the recovery of fissile plutonium from light water spent fuel with no additional value attached to the plutonium (T3, N4). Table 4.3 shows the price of plutonium based on the recovery costs from typical PWR discharge fuel as a function of reprocessing cost. Note that based on this approach, once the breeder reactors constitute a sizeable fraction of the total nuclear power installed, the unit cost of plutonium might logically be based on recovery charges from breeder reactor irradiated fuel; this would reduce the cost of plutonium to 6.5 - 10$/gr due to the high fissile plutonium concentration (on the order of 7 - 10%, including the axial blanket) in the breeder's spent fuel.

A second method of calculating the unit price of plutonium is based on the indifference value of plutonium in light water reactors. The indifference value of plutonium in light water reactors is the value of plutonium that results in equal fuel cycle cost between a plutonium-fueled LWR and a conventional low enrichment U235 fueled LWR. In other words, at the indifference price of plutonium a utility owning a light water reactor can either use low enrichment U235 to operate the reactor, or buy plutonium at the indifference value (instead of low enrichment U235) and end up with the same levelized fuel cycle cost. To find the indifference value of plutonium in LWRs, Abbaspour (A4) looked at a combination of plutonium producer reactors operating on the U235/U238 cycle and plutonium consumer reactors operating on the Pu/U238 cycle.

Table 4.3

Unit Cost of Fissile Plutonium
Based on the Recovery Costs from PWR Spent Fuel

Unit Cost of Reprocessing ($/Kg HM)	Source	Unit Price of Fissile Plutonium ($/gr) *
150	Ref. S8	23.11
250	Semi-Remote "AGNS" Type Facility Ref. N3	38.51
370	Fully Remote "Canyon" Type Facility Ref. N3	57.00

* Based on a fissile plutonium concentration of 0.6556% in the LWR discharged fuel and 1% reprocessing losses (N3).

The indifference value of plutonium as a function of ore and separative work unit costs was found to be:

$$C_{p_u} = 0.578C_{U_3O_8} + 0.178C_{SWU} - 13.9 \qquad (4.6)$$

where

C_{p_u} is the unit price of fissile plutonium, ($/gr)

$C_{u_3O_8}$ is the unit price of U_3O_8, ($/lb)

C_{swu} is the unit price of separative work, ($/Kg).

Table 4.4 shows the unit price of plutonium based on this relationship.

Finally, due to the uncertainties in the price of plutinium and lack of an acceptable method of pricing the plutonium, it has been suggested that in the economics analysis no value should be assigned to plutonium (B8, R2). In this case the comparative economic analysis will be performed by calculating the fuel cycle cost contribution of the rest of the fuel cycle excluding plutonium carrying charges. The final decision on the comparative performance of the reactors of current interest will be made based on a combination of the economic and neutronic performance characteristics of the reactors. The argument in favor of the exclusion of plutonium price is that in a nuclear economy consisting of a mixture of light water and breeder reactors, the same utilities that own the light water reactors will also own the breeder reactors. Thus, in effect, the plutonium transactions between light water reactors and breeders, or vice versa, will not go beyond the accounting boundary of a utility that owns the mixture of fast

Table 4.4

Unit Price of Plutonium
Based on the Indifference Value
Of Fissile Plutonium in Light Water Reactors

Commodity	Unit Price
U_3O_8	40 $/lb
SWU	100 $/Kg
Fissile Plutonium	27 $/gr

and thermal reactors. Since the plutonium is produced and recycled in the same utility, assigning an artificial price to the plutonium and including a plutonium carrying charge in the fuel cycle cost calculations is not meaningful, or indeed, correct. This argument is valid if one assumes that all utilities own a mixture of thermal and fast reactors and they are individually large enough to be self sufficient with respect to plutonium needs. If this is not the case then the price of plutonium would be at least equal to the indifference value of plutonium in light water reactors, since if reprocessing and recycling of plutonium in LWRs is permitted, a utility owning LWRs should be willing to buy plutonium at its indifference value and to run the LWRs on the plutonium cycle. If recycling of plutonium in light water reactors in not permitted by the government due to safeguards or resource-requirement considerations, then the plutonium would be available only for breeder use, and the argument favoring a low-value of plutonium would be valid. In fact, this appears to be the policy that the government of France has adopted with respect to plutonium recycling.

Finally, in the very long term, when learning curve effects bring the capital cost of breeder reactors sufficiently low, and breeders dominate the nuclear economy, one can define an indifference cost of plutonium based on equating the total busbar cost of electricity between LWRs and breeder reactors (S9). Under these circumstances, the breeder operator could afford to pay a higher price than the LWR-only indifference

price. Since this circumstance will probably not apply in the near term, when breeders must make their initial market penetration, we will not employ this convention here.

Considering the above arguments related to the price of plutonium, for the comparative economic analysis in this work, it is assumed that once breeder reactors are commercially available and reprocessing and plutonium recycle is allowed, the plutonium market would be free to fluctuate, i.e., the plutonium would be allowed to be used in either light water or breeder reactors. Based on this the breeder reactor should be able to pay at least as much as the indifference value of the plutonium in the LWRs to be able to be competitive in the plutonium market. Thus for the economic calculations in this chapter, a LWR indifference plutonium value of 27 $/gr (Table 4.4) was assumed. For completeness, however, we will also comment on the effect of cheap plutonium on the resulting comparisons.

With respect to the price of U233, Abbaspour (A4) also studied the indifference value of U233 in LWRs. The following relationship was found.

$$C_{U233} = 0.678C_{U_3O_8} + 0.318C_{SWU} - 13.72 \qquad (4.7)$$

where

C_{U233} is the indifference value of U233 in light water reactors, ($/gr).

Based on a unit price of $40/lb for U_3O_8 and $100/KG for SWU, the unit price of U233 was found to equal 45.2 $/gr. As a point of interest we note that the indifference value of U233 in HTGR's

is reported to be 1.25 times the price of 93% enriched U235 (A5, R3). At the above unit costs for U_3O_8 and SWU, 93% enriched U235 costs 39.6 \$/gr. Based on this, the indifference value of U233 in HTGR's is \$49.5/gr, which is close to the indifference value of U233 in LWR's found using Eq. (4.7) above.

In the next section the unit costs and parameters chosen in this section will be used to calculate the levelized fuel cycle cost for the reference core and the $(U - Pu)O_2$ cores with in/out - moderated radial blankets.

4.4 Levelized Fuel Cycle Cost of the Reference Core and $(U - Pu)O_2$ Cores with In/Out-Moderated Radial Blankets

As was discussed in the cost section, there is a considerable uncertainty associated with the economic parameters used in the fuel cycle cost calculations, which obviously propagates into the final results. Thus it is important to look upon the final fuel cycle costs with a clear understanding of how the components of the fuel cycle cost break down, and the sensitivity of the fuel cycle cost to each of these parameters.

Tables 4.5 through 4.7 show the cash flows associated with the fuel, internal and radial blanket transactions in the reference core. Note that the cash flows associated with the axial blanket extensions of each of the above assemblies are included in the corresponding table. Based on a capacity factor of 0.7 and the results summarized in these tables, the levelized fuel cycle cost for the reference core is calculated to equal 7.94 mills/Kwhe. It should be noted that the reference

Table 4.5

Cash Flows Associated With the Fuel Assemblies
And Their Axial Blanket Extensions for the Reference Core*

	Transaction	Time** (yr)	C_i ($/Kg)	M_i (Kg)	G_i	F_i	$(CMFG)_i X10^6$ ($)
1.	Plutonium Purchase	-1	$27x10^3$	2739.4	0.87	1.42	91.47
2.	Fabrication (Fuel)	-0.5	650	12421.2	0.90	1.32	9.59
3.	Fabrication (Axial Blanket Extensions)	-0.5	150	10835.3	0.90	1.32	1.93
4.	Spent Fuel Shipping	3.0	90	23256.5	1.08	0.77	1.74
5.	Reprocessing	3.5	450	23256.5	1.11	0.71	8.24
6.	Waste Shipping and Storage	5.0	125	23256.5	1.20	0.52	1.81
7.	Plutonium Credit	3.5	$27x10^3$	2542.2	1.11	0.71	-54.13
	Total						55.78

* Mass flows for 1/2 of the fuel assemblies, for a residence time, t_r, of two years.

** Lead or lag time measured from the beginning of the batch irradiation

Table 4.6

Cash Flows Associated With the Internal Blanket Assemblies And Their Axial Blanket Extensions for the Reference Core*

	Transaction	Time (yr)	C_i ($/Kg)	M_i (Kg)	G_i	F_i	$(CMFG)_i X10^{-6}$ ($)
1.	Fabrication	-0.5	140	18532.3	0.90	1.32	3.20
2.	Spent Fuel Shipping	3.0	90	18532.3	1.08	0.77	1.38
3.	Reprocessing	3.5	390	18532.3	1.11	0.71	5.69
4.	Waste Shipping	5.0	125	18532.3	1.20	0.52	1.44
	and Storage	5.0	125	18532.3	1.20	0.52	1.44
5.	Plutonium Credit	3.5	$27x10^3$	408.0	1.11	0.71	-8.68
	Total						3.03

* Mass flows for 1/2 of the internal blanket assemblies for a residence time, t_r, of two years.

Table 4.7

Cash Flows Associated With the Radial Blanket Assemblies
And Their Axial Blanket Extensions for the Reference Core*

	Transaction	Time (yr)	C_i ($/Kg)	M_i (Kg)	G_i	F_i	$(CMFG)_i X10^{-6}$ ($)
1.	Fabrication	-0.5	140	3592.8	0.82	1.70	0.7
2.	Spent Fuel Shipping	7.0	90	3592.8	1.23	0.51	0.20
3.	Reprocessing	7.5	390	3592.8	1.27	0.45	0.8
4.	Waste Shipping and Storage	9.0	125	3592.8	1.37	0.29	0.17
5.	Plutonium Credit	7.5	$27x10^3$	144.09	1.27	0.45	-2.22
	Total						-0.35

* Mass flows for 1/6 of the radial blanket, for a residence time, t_r, of 6 years.

design represents a conservative LMFBR design because of its low thermal efficiency (≈30%). Also, the design of the core includes a very large number of internal blankets, so that the positive sodium void coefficient can be reduced to a very small value. The combined effect of these design choices is an increase in the fissile inventory of the core, which results in higher fuel cycle costs than one might expect for homogeneous core designs.

In the above levelized fuel cycle cost calculations, almost half of the fuel cycle cost is due to plutonium charges, i.e., plutonium purchase minus plutonium credit accounts for approximately 50% of the total fuel cycle cost. The fuel assembly fabrication costs account for about 16% of the total fuel cycle cost. Thus it can be seen that the plutonium price has the largest effect on the levelized fuel cycle cost, and the need for a more detailed analysis of plutonium pricing issues, leading to a unified method for the calculation of the price of plutonium is obvious. The preceding tables also illustrate another important point. Note that the escalation factor, G_i, is considerably larger for the credit transactions than for the purchase transactions. Since the discount rate employed is a real world market rate (which includes the inflation allowance) it is important to allow for monetary inflation (via the G_i factor) in all transactions. Otherwise the calculated overall fuel cycle cost would be unrealistically high becuase of the underestimation of the credit transactions.

The cash flows for the various components of the fuel cycle cost of the $(U\text{-}Pu)O_2$ core with a two-cycle-burned, in/out - 40% moderated, radial blanket is shown in Tables 4.8 and 4.9. Based on a capacity factor of 0.7 and a 10% increase in total power generation by the breed/burn core, the levelized fuel cycle cost was calculated to equal 7.79 mills/KWhe, which is slightly lower than the fuel cycle cost for the reference core (7.99 mills/KWhe). Again note that fissile charges,i.e. purchase of plutonium minus plutonium and U233 credit, constitutes a little over 50% of the fuel cycle costs. If we were instead to assign a zero value to plutonium, to represent the other end of the spectrum of pricing conventions, the fuel cycle costs would be: 5.01 mills/KWhe for the reference core and 3.74 mills/KWhe for the breed/burn core. Based on these results it would appear that there is a major economic incentive in going to lower fissile inventory cores.

One of the cores that was analyzed in Chapter 3 was the core with a central "island" (Fig. 3.15). In this core, the six innermost rows of fuel and internal blanket assemblies were substituted with moderated internal blanket assemblies that have been moved from the rest of the internal blanket positions after several cycles of fissile build up. As was described in Chapter 3, this strategy

Table 4.8

Cash Flows Associated With the Fuel Assemblies and their Axial Blanket Extensions of the $(U\text{-}Pu)O_2$ Core With a Two-Cycle-Burned, In/Out - 40% Moderated Radial Blanket*

	Transaction	Time (Yr)	C_i ($/Kg)	M_i (Kg)	G_i	F_i	$(CMFG)_i X10^{-6}$ ($)
1.	Plutonium Purchase	-1	$27x10^3$	5726.58	0.87	1.42	191.01
2.	Fabrication (Fuel)	-0.5	650	24842.4	0.90	1.32	19.18
3.	Fabrication (Axial Blanket Extensions)	-0.5	150	21670.6	0.90	1.32	3.86
4.	Spent Fuel Shipping	3.0	90	46513.0	1.08	0.77	3.48
5.	Reprocessing	3.5	450	46513.0	1.11	0.71	16.49
6.	Waste Shipping and Storage	5.0	125	46513.0	1.20	0.52	3.62
7.	Plutonium Credit	3.5	$27x10^3$	5041.0	1.11	0.71	-107.26
	Total						130.38

*Mass flows for all the fuel assemblies, for a residence time, t_r, of two years.

Table 4.9

Cash Flows Associated With the Internal and Radial Blanket Assemblies and their Axial Blanket Extensions of the $(U\text{-}Pu)O_2$ Core With a Two-Cycle-Burned, In/Out - 40% Moderated Radial Blanket*

	Transaction	Time (Yr)	C_i ($/Kg)	M_i (Kg)	G_i	F_i	$(CMFG)_i X10^{-6}$ ($)
1.	Fabrication (Blanket Rods)	-0.5	160	20656.1	0.87	1.51	4.34
2.	Fabrication (Moderator Rods)	-0.5	65	5362.9	0.87	1.51	0.45
3.	Spent Fuel Shipping	5.0	90	20656.1	1.17	0.64	1.39
4.	Reprocessing	5.5	430	20656.1	1.20	0.58	6.18
5.	Waste Shipping and Storage	6.0	125	20656.1	1.23	0.52	1.65
6.	U233 Credit	5.5	$45.2x10^3$	578.9	1.20	0.58	-18.21
	Total						-4.20

*Mass flows for the internal blankets (which later become the radial blanket) with a total residence time, t_r, of four years.

results in replacing 216 fuel assemblies with their high plutonium enrichment by moderated blanket assemblies which have much lower U233 enrichment, and with the additional advantage that all the fissile material, i.e. U233 for these assemblies is produced in the core. The proposed fuel management strategy for this core consists of annual refueling of the fuel assemblies, and shuffling of the three-cycle-burned internal blanket assemblies to the radial blanket. Thus in the steady state operation the fresh internal blanket assemblies build U233 for three cycles after which these assemblies are moved to the central island and fresh internal blanket assemblies are loaded into the core. This batch of internal blanket assemblies will build U233 for two cycles after which they are moved to the radial blanket, and this alternating movement continues. In this way the blanket assemblies remain in different regions of the reactor for a total of five years.

Tables 4.10 and 4.11 show the cash flows for the fuel and blanket regions of this core. Note that based on the fuel management strategy described before, the U233 concentration in the five-year-burned internal blanket assemblies would be different depending on whether the blanket assemblies were moved to the central island or the radial

Table 4.10

Cash Flows Associated With the Fuel Assemblies and their Axial Blanket Extensions of the Breed/Burn Core With the Central Island*

	Transaction	Time (Yr)	C_i ($/Kg)	M_i (Kg)	G_i	F_i	$(CMFG)_i X10^{-6}$ ($)
1.	Plutonium Purchase	-1	$27x10^3$	2129.7	0.87	1.42	71.04
2.	Fabrication (Blanket)	-0.5	650	9239.2	0.90	1.32	7.13
3.	Fabrication (Axial Blanket Extensions)	-0.5	150	8059.6	0.90	1.32	1.43
4.	Spent Fuel Shipping	3.0	90	17298.8	1.08	0.77	1.29
5.	Reprocessing	3.5	450	17298.8	1.11	0.71	6.13
6.	Waste Shipping and Storage	5.0	125	17298.8	1.20	0.52	1.34
7.	Plutonium Credit	3.5	$27x10^3$	3749.6	1.11	0.71	-39.89
	Total						48.46

*Mass flow for half of the core assemblies, for a residence time, t_r, of two years.

Table 4.11

Cash Flows Associated With the Blanket Assemblies and their Axial Blanket Extensions of the Breed/Burn Core With the Central Island*

	Transaction	Time (Yr)	C_i ($/Kg)	M_i (Kg)	G_i	F_i	$(CMFG)_i X10^{-6}$ ($)
1.	Fabrication (Blanket)	-0.5	160	16362.0	0.87	1.51	3.43
2.	Fabrication (Zirconium-Hydride)	-0.5	65	5362.9	0.87	1.51	0.45
3.	Spent Fuel Shipping	6.0	90	16362.0	1.20	0.57	1.0
4.	Reprocessing	6.5	430	16362.0	1.23	0.51	4.41
5.	Waste Shipping and Storage	7.0	125	16362.0	1.27	0.45	1.16
6.	U233 Credit	6.5	$45.2x10^3$	319.52	1.23	0.51	-9.05
	Total						1.39

*Mass flows for the blanket assemblies, for a residence time, t_r, of five years.

blanket. Since the mass flows in both branches of the blanket flow paths were essentially the same, all were treated as following the central island route in compiling Table 4.10. Based on these results the levelized fuel cycle cost is 6.15 mills/KWhe, which is approximately 20% lower than that of the two cores studied previously. Note that the fuel management and the design of the central island core is rather preliminary and no effort was spent on optimization of the core design or blanket shuffling strategy. Thus some additional benefits might be gained by further work on optimization of the core configuration and fuel management strategy.

4.5 Summary and Conclusions

In this chapter the levelized fuel cycle costs for the reference core and for two breed/burn cores was calculated using the simple models developed by Abbaspour (A4) and Brewer (B6). In the first part of the chapter a reference economic environment consisting of the unit costs and financial parameters necessary for the fuel cycle cost calculations was chosen. Relative to these values, it was indicated that there is a considerable uncertainty associated with the economic parameters, and in some cases (such as establishment of the price of plutonium) the effect of these uncertainties on the fuel cycle cost is substantial.

Using the values chosen for the reference economic environment and the simple model, the levelized fuel cycle cost of the reference core and a $(U\text{-}Pu)O_2$ core with the two-cycle-burned, in/out, 40% moderated radial blanket was calculated. The breed/burn core was found to have a slightly lower fuel cycle cost (7.79 vs. 7.94 mills/KWhe). In both cores the plutonium transactions accounted for almost half of the total fuel cycle cost. This result emphasizes the importance of the price of the plutonium and its effect on the fuel cycle cost.

Finally a third core, consisting of a $(U\text{-}Pu)O_2$ core with a central island of moderated blanket assemblies moved inward from the heterogeneous internal blanket, as studied in Chapter 3, was analyzed. It was shown that this core has an approximate 20% lower fuel cycle cost due to its lower fissile inventory. This core has some interesting features and has sufficient potential to warrant further studies.

With respect to the fuel cycle cost calculations in general, based on the study done here it is concluded that there is an urgent need for a complete and thorough analysis of the issues related to plutonium pricing. This is necessary because of the large effect of the price of plutonium on the fuel cycle cost (almost 50% in the cores

analyzed in this chapter) and the lack of a unified consensus on the best method of plutonium pricing among different research organizations. Finally, the fast breeder reactor fuel cycle cost calculations and their relation to the co-existing light water reactor fuel cycle cost must be clarified since the competition for plutonium has a direct and major effect on many decisions related to construction of fast breeder reactors.

With respect to the cores analyzed in the present work the representative breed/burn core has a number of nonproliferation advantages, such as lower total reprocessing requirements and lower plutonium bearing fuel assembly transportation and reprocessing requirements. It also has a slightly lower fuel cycle cost. Thus using the proposed design has not resulted in any economic penalty.

Finally, the preliminary studies on the core with the central island has indicated that an attractive economic gain could be obtained by going to lower fissile inventory cores such as the breed/burn, central island concept.

CHAPTER FIVE

GAMMA AND NEUTRON HEATING

5.1 Introduction

A large portion of the energy produced in the blanket assemblies of fast breeder reactors at the beginning of cycle (BOC) is due to gamma and neutron heating. This is due to the fact that, at the BOC, the blanket assemblies contain very little (or no) fissile materials, and fertile fissions are less important than in the core, due to fast neutron attenuation. The relative importance of gamma and neutron heating in the blanket assemblies is reduced as fissile isotopes are produced in the assemblies during their residence in the reactor. However, to establish coolant orifice settings at the end of cycle and to establish overcooling at the beginning of cycle, it is necessary to evaluate the contribution of the gamma and neutron heating to the total heating rate in the blanket assemblies.

Gamma heating is considerably more important than neutron heating in conventional blanket assemblies. Gamma heating in the blanket assemblies consists of local gamma heating and that due to photons transported from the fissile fueled assemblies in the core to the blanket assemblies. The contribution of gamma heating to the total blanket heating varies with the fissile content of the blanket assembly and

its distance from the core-blanket interface. As an example: in the radial blanket next to the core-blanket interface gamma heating could be comparable to the fission heating at the beginning of cycle (W1, K4). But away from the interface, in the second and third rows of the blanket, gamma heating can be several orders of magnitude larger than the fission heating.

Similar considerations apply to internal blanket assemblies at the beginning of cycle, but here fast fissions are sustained at an important level.

Neutron heating's contribution to the total heating rate in conventional blanket assemblies is much smaller than both the gamma and fission heating. Typically, in a depleted uranium radial blanket at the BOC, neutron heating's contribution is about a factor of 50-100 less than fission heating in the first row of the radial blanket and increases to about 10% of the fission heating away from the core-blanket interface (W1).

In the moderated blanket assemblies studied in this work, neutron heating associated with scattering of the neutrons by hydrogen constitutes the major source of heating in the zirconium hydride moderator. Thus, a neutron heating analysis of the moderated blanket assemblies, and especially the determination of the heat generation rate in the moderator pins, must be addressed to insure that the temperatures to which the moderator will be exposed are within acceptable operating limits.

In this chapter the gamma and neutron heating in the reference core and the $(U\text{-}Pu)O_2$ core with the two-cycle-burned, In/Out, 40% moderated radial blanket will be analyzed. A gamma heating analysis of the above cores will be presented first. This will be followed by neutron heating studies for these cores. Using the results of the gamma and neutron heating determinations for the moderated radial blanket assemblies, the power density and temperatures that would result in zirconium hydride rods will be calculated. Finally, a summary of the results and conclusions will be presented.

5.2 Gamma Heating Analysis

5.2.1 Introduction

There are several reactions that result in production of gamma photons. A brief review follows: see Kalra's analysis for a more detailed review (K4). Sources of gamma include:

1. Gamma production associated with fission including prompt fission gammas and short and long lived fission product decay gammas.
2. Gamma production associated with capture, which includes prompt and post-capture decay gammas.
3. Gamma production due to inelastic scattering.
4. Gamma production due to (n,2n) and (n, charged particle) reactions.
5. Gamma production due to annihilation.
6. Gamma production due Bremsstrahlung.

Each of the above reactions contribute to the total gamma production but with varying degrees of importance. The

prompt fission gammas and short lived fission product gammas, which are essentially produced at the same time, are very important as far as the contribution to the total gamma production is concerned. The long lived fission product gammas are important in post-shutdown heating calculations and do not contribute much to gamma heating during reactor operation. Capture gammas and annihilation gammas are also important sources of gammas. Gamma production due to (n, 2n), (n,α) and (n,p) are not too important because of the very high neutron threshold energies required for these interactions. Bremsstrahlung gammas do not contribute much to the total gamma production either.

The gamma photons produced by the above reactions are deposited in the core and blanket materials by three mechanisms: 1) pair production, 2) Compton scattering, and 3) the photoelectric effect.

Pair production can occur if the energy of the gammas is higher than 1.02 Mev, which is the minimum energy required to create an electron-positron pair. Any extra gamma energy is carried off as kinetic energy of the pair produced.

Compton scattering is important in the energy range of 0.1 t0 2.0 Mev. In this reaction gamma energy is transferred to electrons through scattering of gamma photons by electrons.

The photoelectric effect is important in the energy range below 100 kev, and consists of absorption of the gamma photons by the electrons.

5.2.2 Method of Calculation

Gamma heating calculations were performed using a 40 group coupled neutron-gamma cross section set (O1) and the one dimensional transport-code ANISN (E2). The 40 group neutron-gamma coupled set consists of 22 neutron groups and 18 gamma groups. The gamma production cross sections are included in the set as downscattering terms from the 22 neutron groups to the 18 gamma groups. The groupwise gamma absorptions are included as $\overline{E\sigma a}$ (Mev-barn) in groups 18 to 40.

To calculate the gamma heating in the core and blanket regions, the group and pointwise gamma fluxes ($\frac{\text{Photons}}{\text{cm}^2\text{-sec}}$) were first calculated using the 40 group coupled set and the transport code ANISN on the one dimensional model of the core and blanket used previously for cross section collapsing, as shown in Fig. 2.1.

Using a one dimensional transport code rather than a diffusion code is necessary to account for the transport of the gammas from the core zones to the blanket zones with sufficient accuracy. It has been shown that due to the leakage of gammas from the core zones to the internal and radial blanket zones, the total power produced by gamma heating in the blanket regions can be underpredicted by 22 to 35% if diffusion theory (and in situ gamma absorption) is used instead of transport theory calculations (L7).

The gamma flux produced by the ANISN calculation and the gamma absorption cross sections ($\overline{E\sigma a}$) from the 40 group coupled set were next used to calculate the gamma heating as a function

of position using the relation:

$$Q'''_{GH}(r) = \sum_j \phi_j(r) \left[\sum_i N_i(r) \; (\overline{E\sigma a})_{ij} \right] \qquad (5.1)$$

where

$Q'''_{GH}(r)$ is the volumetric heat generation rate due to gamma heating as a function of position (KW/liter)

$\phi_j(r)$ is the gamma flux ($\frac{\text{photons}}{\text{cm}^2\text{-sec}}$) in group j as a function of position

$N_i(r)$ is the number density of material i as a function of position

$(\overline{E\sigma a})_{ij}$ is the gamma absorption cross section for material i in energy group j.

The results of the calculations for the two cores mentioned above are presented in the next section.

5.2.3 Gamma Heating in the Reference Core and the (U-Pu)O_2 Core with Two-Cycle-Burned, In/Out, 40% Moderated Radial Blankets

To get the actual value of the power densities produced by gamma heating, the power densities produced by gamma deposition calculated using Eq. (5.1) for each core, and the fission densities from the same ANISN calculations were combined and normalized to the midplane power densities of the corresponding 2DB calculations. In these normalizations a value of 183 Mev/fission was assumed for plutonium fission (K5). Figures

5.1 and 5.2 show the ratio of gamma to fission heating in different regions of the two reactors. In the fuel zones of both reactors, the gamma heating rate is about 5% of the fission heating rate. In the blanket zones of the reference reactor, gamma heating is about 20% of the fission heating. This ratio is much higher in the internal blanket zones of the breed/burn core (Fig. 5.2) due to the absence of any fissile isotopes and the low fast fission cross section of thorium. In the radial blanket of the breed/burn core, the gamma heating rate is about 10% of the fission heating, which is more typical of fissile-fueled core assemblies, due to the high bred-in fissile content of the radial blanket assemblies. As was mentioned earlier, the relative gamma heating rate in the blanket zones decreases as a function of the duration of assembly residence in the core, due to the buildup of fissile istopes and the correspondingly higher fission rates.

Figure 5.3 shows the volumetric heat generation rates (KW/liter) due to gamma deposition in different regions of the two reactors. The heating rates in the two reactors are fairly close in magnitude. The small differences in heating rates between the two reactors can be mostly attributed to the difference in neutron flux in the regions of concern. For example, gamma heating rates in most of the

internal blanket regions of the reference core are higher than those of the breed/burn core, whereas in the fissile-fueled zones the reverse is true.

To provide an idea of the contribution of the gamma heating to the linear heat generation rates (LHGR), we note that at a gamma heating rate of 20 KW/liter the contribution of gamma heating to the blanket LHGRs is about 0.56KW/ft. Since the blanket LHGRs at the BOEC and throughout their residence in the core are well below specified limits, the gamma heating contribution is not very significant as far as the peak LHGRs are concerned. The importance of gamma heating calculations is related to the orificing and the need to provide enough coolant for the maximum heat generation rate at the EOC. The peak LHGR in the radial blanket of the breed/burn core is much closer to the allowable limit as compared to a conventional radial blanket. In Chapter Three it was shown that for the 40% moderated radial blanket, shuffled into the radial blanket from the core, the peak LHGR is 17.67 KW/ft. Addition of the gamma heating contribution (~ 0.2 KW/ft) to this

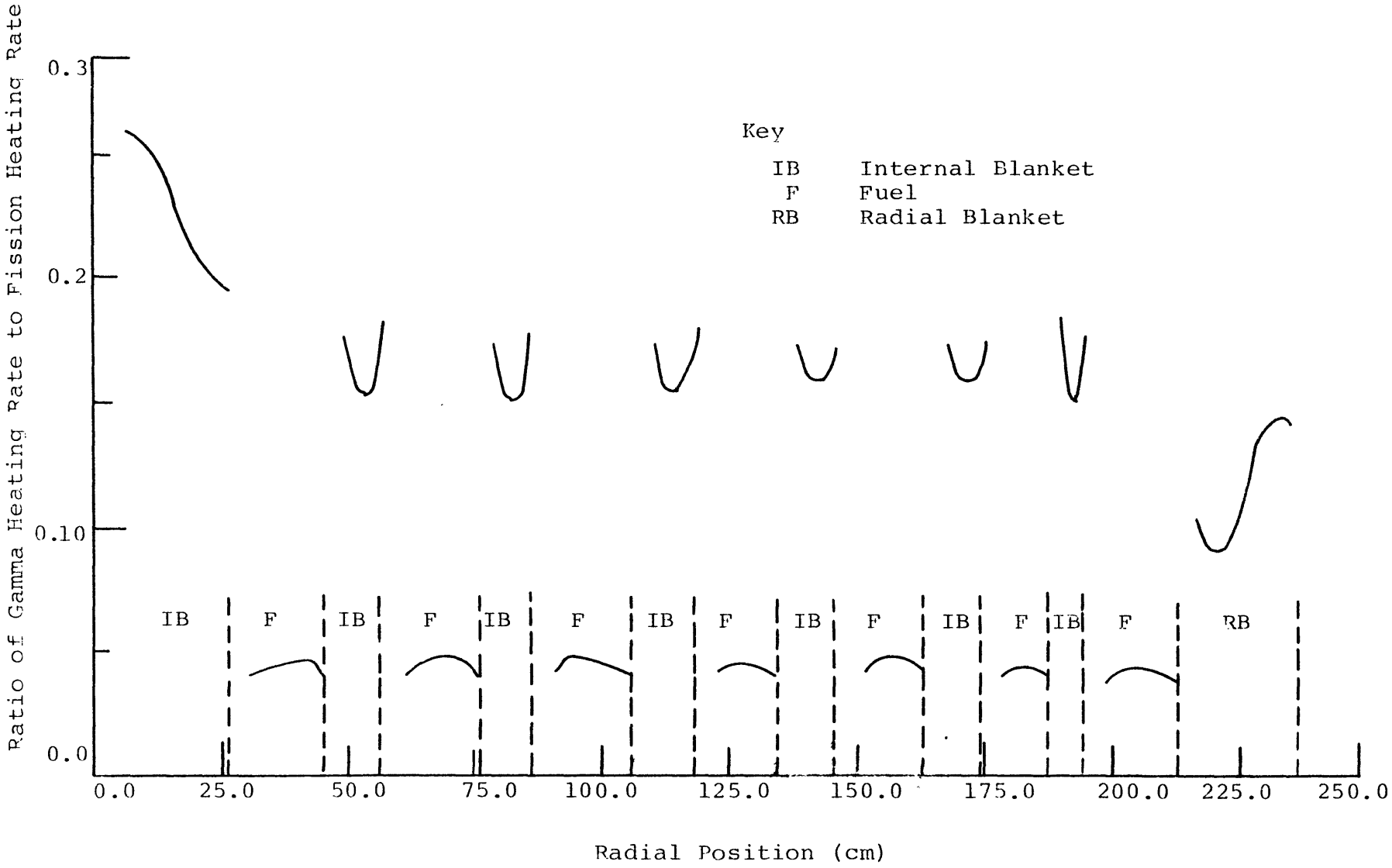

Fig. 5.1 Gamma-to-Fission Heating Rate Ratios in the Reference Core

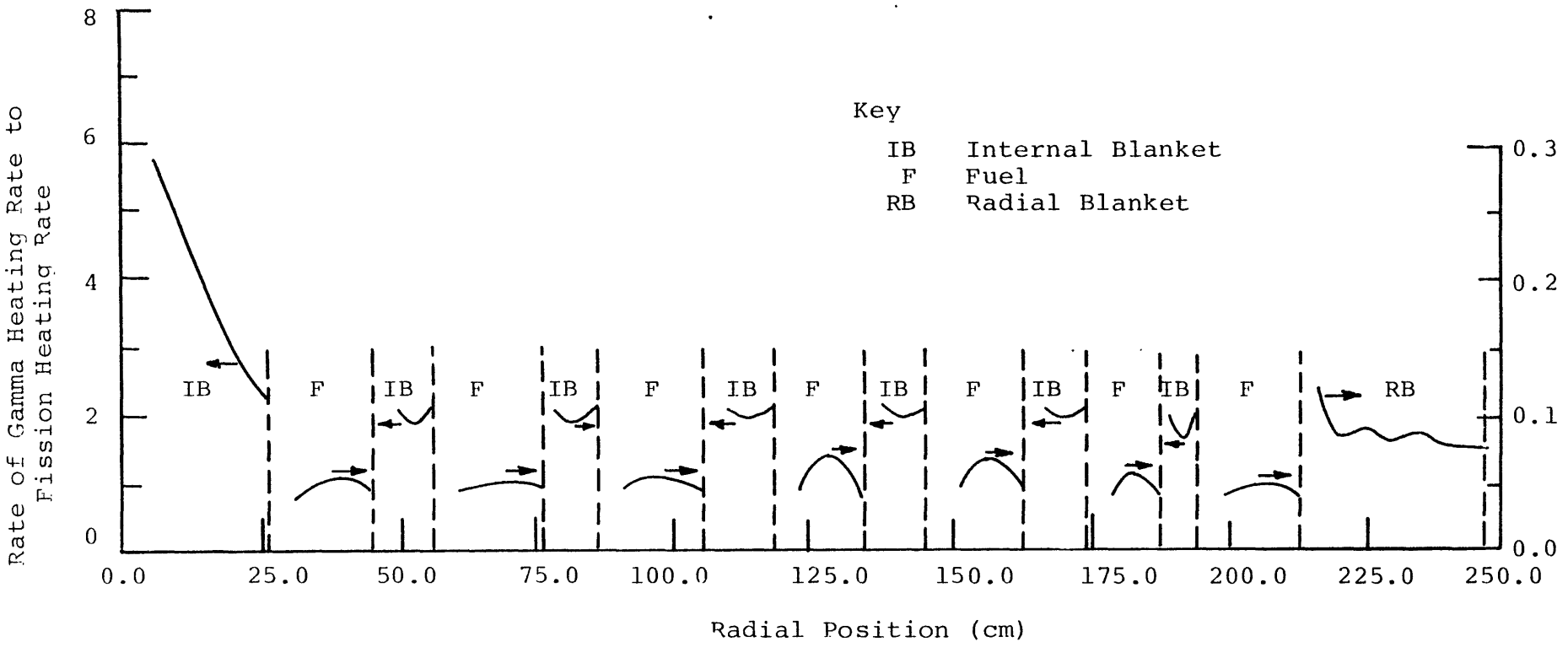

Fig. 5.2 Gamma-to-Fission Heating Ratio in the (U-Pu)O_2 Core with a Two-Cycle-Burned, In/Out 40% Moderated Thorium Radial Blanket

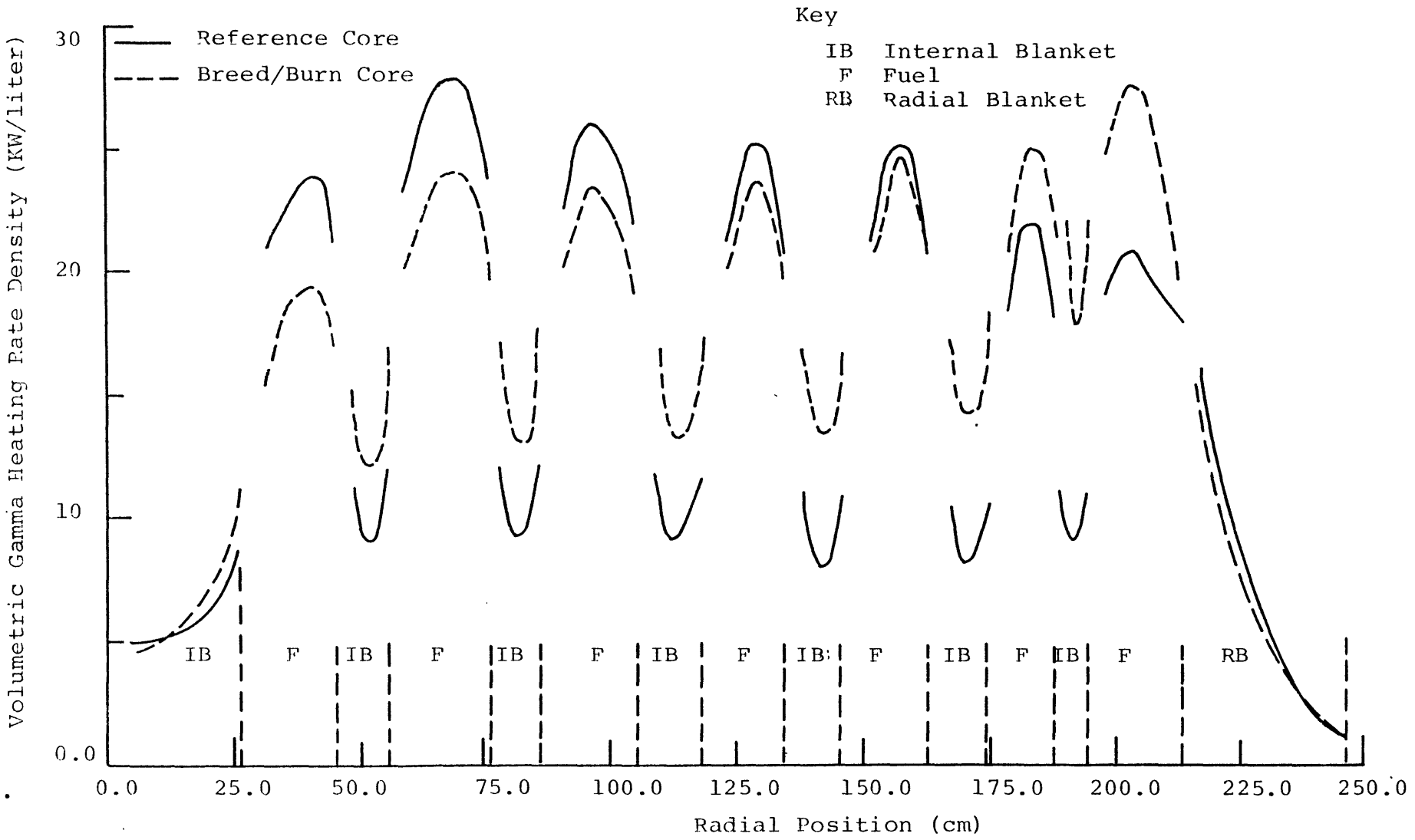

Fig. 5.3 Volumetric Gamma Heating in the Reference Core and the $(U\text{-}Pu)O_2$ Core having a Two-Cycle-Burned, In/Out-40%, Moderated Radial Blanket

value will result in a value (~17.87) which is still below the peak limit of 20 KW/ft specified in Table 2.3. Note that the LHGR contribution due to gamma heating estimated above should not be directly added to the value found from 2DB studies, since this will result in double counting of that part of the gamma heating. This is due to the fact that in the 2DB calculations the contribution of gamma heating is accounted for in power density calculations by assuming 215 Mev per fission. What is not accounted for in 2DB is the transport of gammas from the fuel zones to the blanket zones. As was mentioned earlier, it has been shown that using diffusion calculations (coupled with the assumption of in situ gamma absorption) could result in a 22 to 35% underprediction of the gamma heating in the blanket zones. Hence the increase in the LHGR due to gamma transport, which is not accounted for in the 2DB calculations, is about 0.2 KW/ft.

Overall the gamma heating contribution to the total heating rates in the fuel and blanket regions is not very significant. In the case of the breed/burn core, since the peak LHGR in the radial blanket is much closer to the allowable limit than in the conventional cores, it is important to have a good estimate of the gamma heating contribution so that we can be assured that the peak LHGR is always below the specified limit.

5.3 Neutron Heating

5.3.1 Introduction

As was discussed earlier, the contribution of neutron heating to the total energy generation rate in the core and blanket regions is less than that of gamma heating. The importance of neutron heating in the present work arises from the fact that the radial blanket is moderated, and neutron heating constitutes the most important source of heating in the zirconium hydride pins due to the large scattering cross section and low mass of the hydrogen.

Neutron heating is generated by energy deposition in elastic scattering, inelastic scattering, and capture. Among these reactions, elastic scattering is the most important and contributes most to the total neutron heating rate.

In the next section the methods and relationships used to calculate neutron heating will be discussed.

5.3.2 Method of Calculation

The neutron heating in the two cores under study was calculated using the 26 group Bondarenko-format cross section set ABN-FTR-200 (B7, N2) and the one-dimensional diffusion code 1DX(H4). To do this, the group and pointwise fluxes in each reactor were found by performing a diffusion calculation on the one dimensional model of the core and blanket zones of each reactor. These fluxes and the 26 group cross sections were next used to calculate the neutron heating due to each of the reactions mentioned earlier.

The elastic scattering contribution to the neutron heating can be found from the relation (W1):

$$Q'''_{ES}(r) = \sum_j \phi_j(r) \left[\sum_i N_i(r)\sigma^e_{ij} \overline{\Delta E_{ij}}^e\right] \qquad (5.2)$$

where

$Q'''_{ES}(r)$ is the volumetric heat generation rate due to elastic scattering as a function of position

$\phi_j(r)$ is the neutron flux in group j as a function of position

$N_i(r)$ is the number density of material i as a function of position

σ^e_{ij} is the elastic scattering cross section of material i in group j

$\overline{\Delta E_{ij}}$ is the average energy lost in elastic scattering of a neutron in group j with material i

The average energy loss due to elastic scattering can be written as (L8):

$$\overline{\Delta E_j}^e = E_j(1-e^{-\xi}) \qquad (5.3)$$

where $\overline{E_j}$ is the average energy of the group j and ξ is the average increase in lethargy per collision. Assuming a 1/E spectrum, the average energy of group j is equal to:

$$\overline{E}_j = (E_j - E_{j+1})/\ln(E_j/E_{j+1}) \qquad (5.4)$$

where E_j is the upper energy of group j and E_{j+1} is the lower

energy of group j. The 26 group cross section set was generated using a fission spectrum for the top three groups and a 1/E spectrum for the remaining 23 groups. Since elastic scattering is not very prominent in the top three groups, the later assumption of a 1/E spectrum for these groups introduces a very small error.

The next source of neutron heating is inelastic scattering. In the inelastic scattering process energy is deposited through recoil of the struck nucleus. There are two recoil mechanisms that result in heating (W1). The first one is associated with the recoil of the nucleus when the compound nucleus is formed. The second recoiling action occurs when the low energy neutron is emitted. Using conservation of linear momentum the energy deposited due to the above processes is found to be:

$$E_{RC} = \frac{1}{A+1} \bar{E}_j \tag{5.4}$$

$$E_{RD} = \frac{1}{A} \bar{E}_k \tag{5.5}$$

where

E_{RC} is the recoil energy due to formation of the compound nucleus by an incident neutron of energy $\bar{E}_j$

E_{RE} is the recoil energy due to emission of a neutron of energy $\bar{E}_k$

A is the atomic weight of the initial nucleus

$\bar{E}_j$ is the average energy of the incident neutron

$\bar{E}_k$ is the average energy of the scattered neutron

The total energy deposition rate due to inelastic scattering can be written as:

$$Q'''_{INS}(r) = \sum_j \phi_j(r) \sum_i N_i(r)\sigma_{ij}^{in} E_{RC} + \sum_j \phi_j(r) \sum_i N_i(r) \sum_k \sigma_{(j\to k)}^{in} E_{RD} \quad (5.6)$$

where

$Q'''_{INS}(r)$ is the volumetric heat generation rate due to inelastic scattering as a function of position

σ_{ij}^{in} is the total inelastic scattering cross section of material i in group j

$\sigma_{i(j\to k)}^{in}$ is the inelastic scattering cross section from group j to group k of material i

Next consider the neutron heating due to capture. The energy deposition due to recoil of the compound nucleus in the capture is the same as the recoil energy associated with compound nucleus formation of inelastic scattering, given by Eq. (5.4). Thus, the energy deposition rate due to capture is equal to:

$$Q'''_C(r) = \sum_j \phi_j(r) \sum_i N_i(r) \sigma_{ij}^{C} E_{RC} \quad (5.7)$$

where

$Q'''_C(r)$ is the volumetric heat generation rate due to capture as a function of position

σ^c_{ij} is the capture cross section of material i in group j

Finally, the last component categorized here under "neutron heating" is the nuclear recoil due to emission of a gamma photon following an (n,γ) reaction. This is the least important of the reactions described here, and contributes very little to the total neutron heating. Hence, in our calculation of neutron heating this component was neglected. The results of the neutron heating calculations for the two cores under study are presented in the next section.

5.3.3 Neutron Heating in the Reference Core and the $(U\text{-}Pu)O_2$ Core with a Two-Cycle-Burned, In/Out-40% Moderated, Radial Blanket

The neutron heating in the two cores under study was calculated using the group and pointwise fluxes found from the one dimensional calculation on the two cores, the 26 group Bondarenko-format cross sections and Eqs. (5.2), (5.6) and (5.7) for each component of the neutron heating.

Figures 5.4 and 5.5 show the neutron to fission heating ratios in different regions of the two cores under study. As can be seen, in the fuel regions of the two cores the neutron heating is only about 0.5% of the fission heating. In

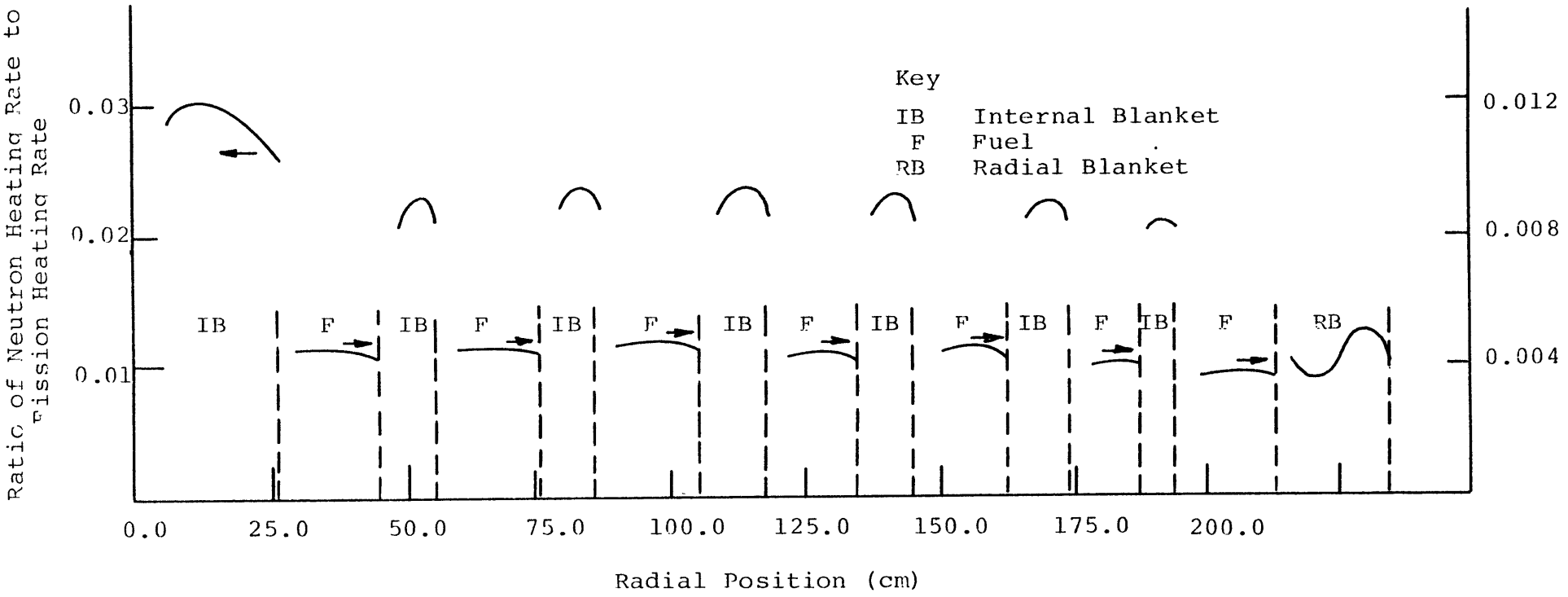

Fig. 5.4 Ratio of Neutron to Fission Heating Rates in the Reference Core

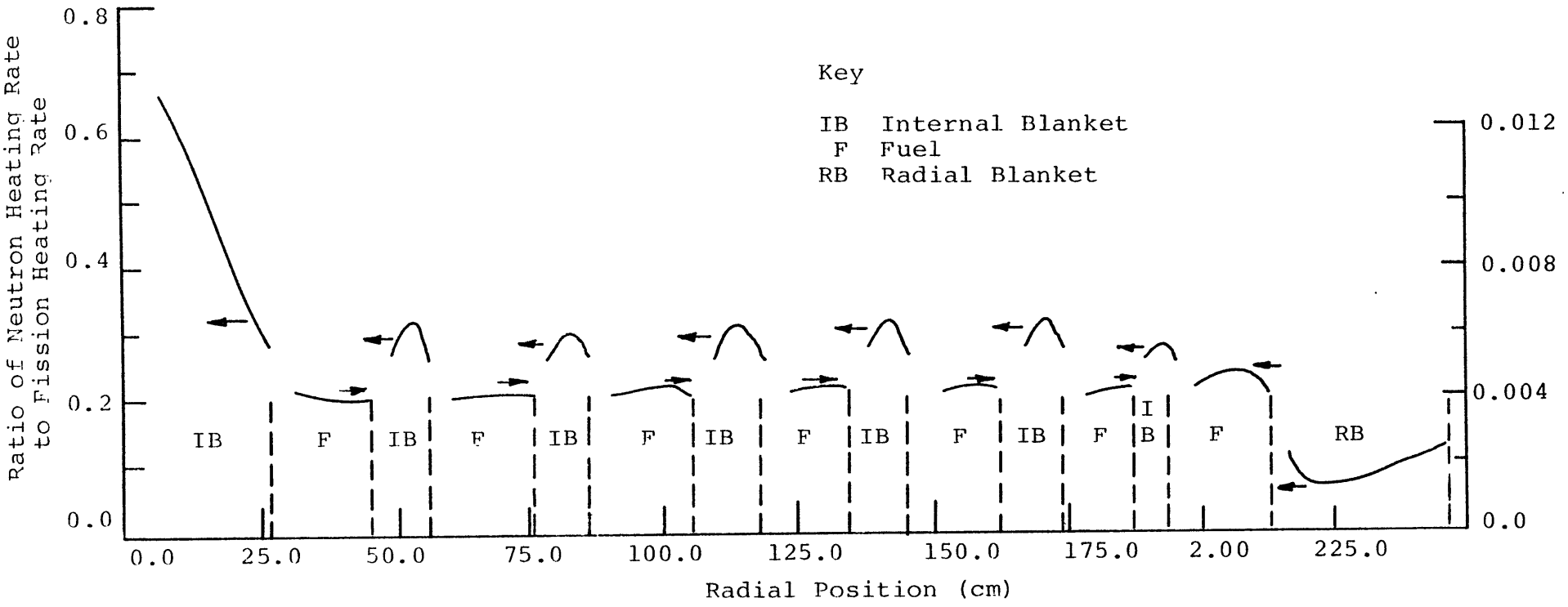

Fig. 5.5 Ratio of Neutron to Fission Heating Rates in the (U-Pu)O_2 Core with a Two-Cycle-Burned, In/Out-40% Moderated, Radial Blanket

the blanket regions of the reference core, neutron heating is about 2-3% of the fission heating. This ratio is much higher in the internal blankets of the breed/burn core. Figure 5.6 shows the volumetric neutron heating rate (KW/liter) in the two cores under study. As can be seen, in both cores the neutron volumetric heat generation rate is about 2 KW/liter. This value increases to abou 12 KW/liter in the moderated radial blanket of the breed/burn reactor.

Overall, neutron heating's contribution to the total heating rate in the core and blanket regions of the conventional fast reactor cores is not very significant. In the next section the results of the gamma and neutron heating calculations for the radial blanket of the breed/burn core will be used to estimate the peak power densities and temperatures in the zirconium hydride moderator rods.

5.4 Energy Deposition and Temperature in the Zirconium Hydride Moderator Pins

In this section the peak volumetric heat generation rates produced in the zirconium hydride moderator rods due to gamma and neutron heating will be calculated. The basic objective in this analysis is to assure that the power densities and temperatures of the moderator pins are within acceptable operating limits for zirconium hydride. Based on the peak volumetric heat generation rate, the peak centerline zirconium hydride temperatures will be calculated as a function of moderator pin diameter.

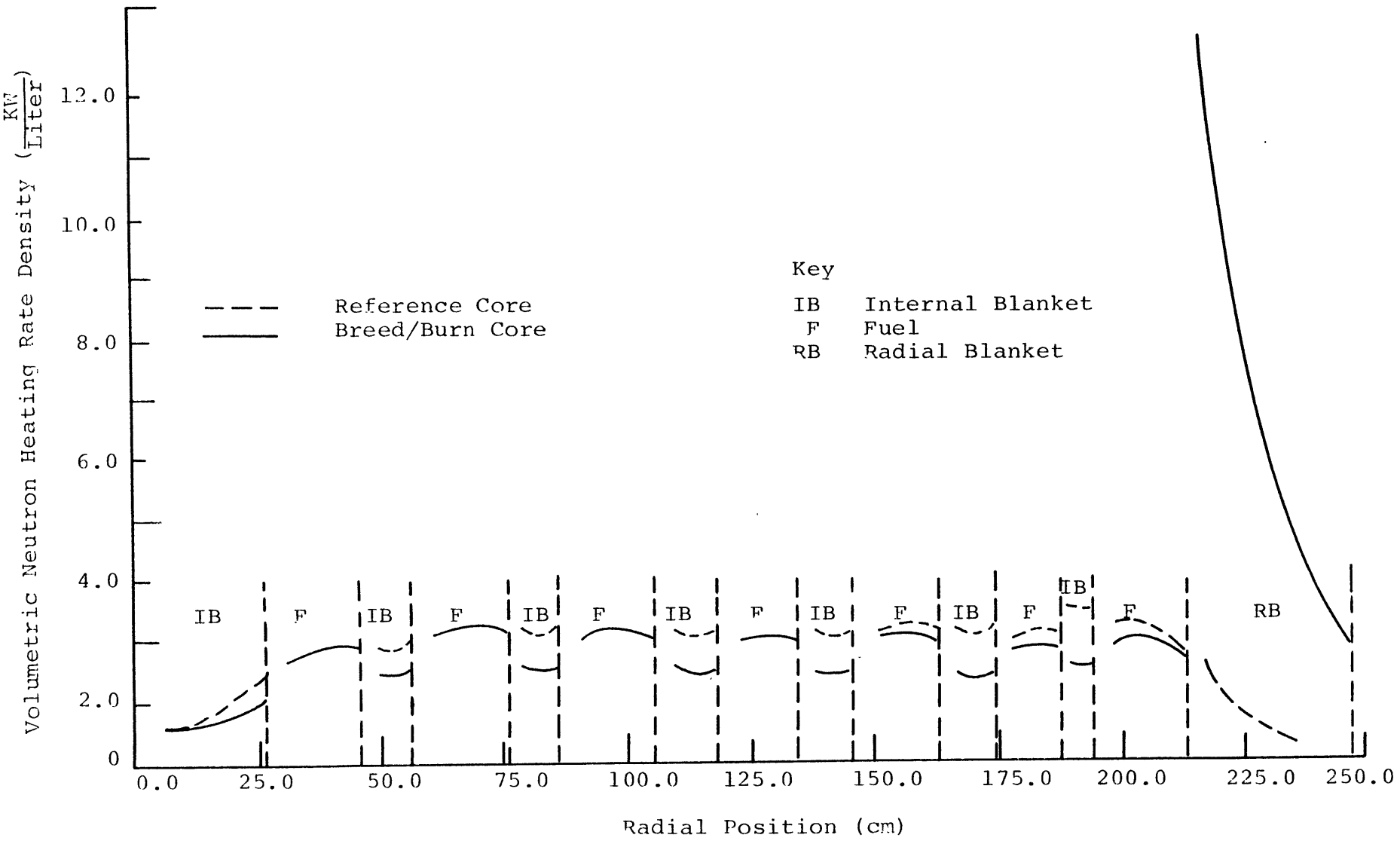

Fig. 5.6 Volumetric Neutron Heating Rates in the Reference Core and the $(U\text{-}Pu)O_2$ Core with a Two-Cycle-Burned, In/Out-40% Moderated, Radial Blanket

Figure 5.7 shows the volumetric heat generation rate in the zirconium hydride due to gamma and neutron heating, as a function of distance from the core-blanket interface. The peak total volumetric heat generation rate (the value at the core midplane) is 11.53 KW/liter. Using this value, the peak temperature increase across the zirconium hydride rod can be found as a function of diameter using the definition of the heat generation rate:

$$q' = 4\pi \int_{T_S}^{T_{CL}} K dT \qquad (5.8)$$

where

q' is the linear heat generation rate, which is related to the volumetric heat generation rate by the relation:

$$q' = \pi r^2 q''' \qquad (5.9)$$

r is the radius of the pin, (ft)

q''' is the volumetric heat generation rate, (Btu/hr ft^3)

K is the thermal conductivity, (Btu/hrft°F)

T_S is the pin surface temperature, and

T_{CL} is the pin centerline temperature

The thermal conductivity of the zirconium hydride as a function of temperature is given by (S3):

$$K = 0.042 + 1.79 \times 10^{-5} \; T \text{ cal/sec-cm-C} \qquad (5.10)$$

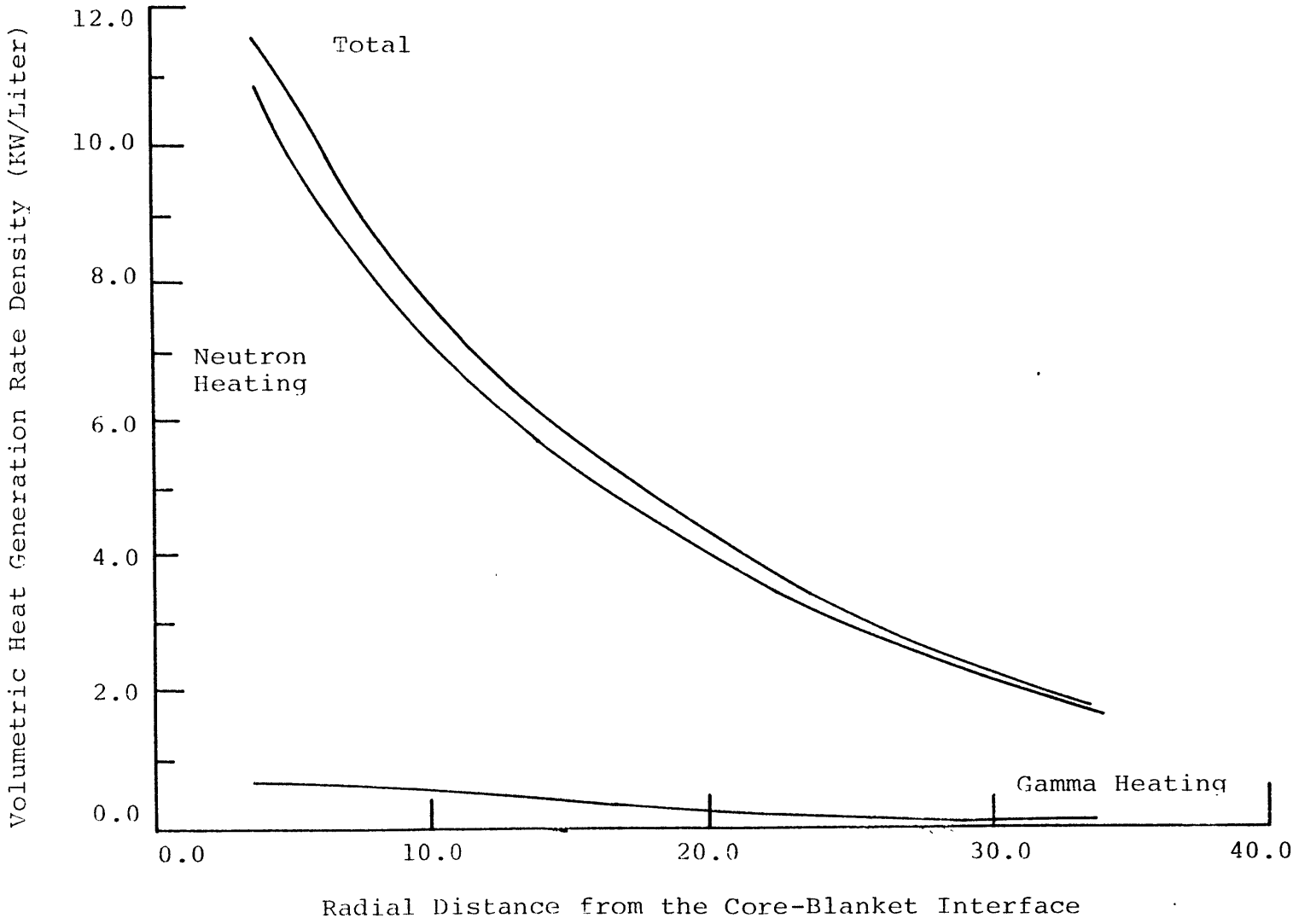

Fig. 5.7 Gamma and Neutron Volumetric Heat Generation Rates in Zirconium Hydride

For comparison purposes,at 500°C, zirconium hydride's thermal conductivity is 0.0509 cal/sec-cm-°C, which can be compared to K = 0.0097 cal/sec-cm-°C for UO_2.

Table 5.1 shows the zirconium hydride centerline temperature as a function of rod diameter. In these calculations a coolant bulk temperature of 895°F, the core exit temperature, was assumed to insure conservatism. Again to be conservative, the temperature rise across the clad, gap and hydride pellet radius were calculated at the core midplane, where the peak axial heat rate occurs. Note in Table 5.1 that the temperature rise from the coolant to the zirconium hydride centerline is very small, due to the low heat generation rate in the moderator pins. As far as the peak allowable zirconium hydride temperature is concerned, previous experience with SNAP reactors (L3), and other sources (S7), have indicated that zirconium hydride can be operated at temperatures up to 750°C (1382°F) without any problems. At higher temperatures hydrogen will be released resulting in a buildup of pressure, and stress on the cladding.

The results shown in Table 5.1 show that due to the very small heat generation rates in the zirconium hydride, the centerline temperatures of even very large pins are well below the allowable limits. Thus the moderated blanket assemblies can be designed using large moderator pins without exceeding any zirconium hydride temperature limitations.

Table 5.1

Peak Zirconium Hydride Centerline Temperature as a Function of Pin Diameter

Moderator Pin Diameter (cm)	Maximum Centerline Temperature (°F)	(°C)
1.0	908.78	487.10
2.0	916.42	491.34
4.0	933.14	500.63

5.5 Summary and Conclusions

In this chapter the contribution of the gamma and neutron heating rates to the total power production in different regions of the reference core and the $(U\text{-}Pu)O_2$ core with a two-cycle-burned, in/out-40% moderated, blanket was analyzed. It was shown that the gamma heating contribution to the total heating rate is much higher than the neutron heating contribution. The combined total increment of the linear heat generation rate (LHGR) in the blanket assemblies due to gamma and neutron heating is about 0.61 KW/ft. Overall the gamma and neutron heating are not significant in peak LHGR studies but are necessary for the blanket orificing and overcooling calculations.

Using the results of gamma and neutron heating calculations in the zirconium hydride, a conservative estimate of the peak centerline temperature in the moderator pins was made. Based on these calculations it was shown that due to low power generation in the zirconium hydride rods, very large moderator pins can be used in the moderated radial blanket assembly without exceeding the allowable operating temperature of zirconium hydride.

CHAPTER SIX

SUMMARY, CONCLUSIONS AND RECOMMENDATIONS

6.1 Introduction

The motivation for deployment of fast breeder reactors comes from the fact that most of the non-renewable resources, such as oil and uranium, used today for the production of electricity are being depleted at a rate which engenders concern (K1). Coal, which is abundant in the United States, and is expected to contribute substantially to the United States' electricity production, has many adverse effects associated with it. Other alternatives such as solar-generated electricity and fusion are not expected to contribute on a large scale to electricity requirements before well into the twenty-first century (B1).

Breeder reactors with their unique ability to produce more fissile fuel than they consume could provide for the electricity needs of the world essentially indefinitely. Currently, breeder reactors suffer from a general concern over the use of plutonium as the primary fuel and the possibility that with deployment of a large number of breeder reactors diversion of the plutonium for terrorist activities or national weapons programs would occur.

With regard to this concern, the objective of the present work is to study a fuel management scheme that

enhances the non-proliferation characteristics of fast breeder reactors, while at the same time offering the potential for economic advantages.

In the proposed fuel management strategy the internal blankets, of a heterogeneous FBR core, after several cycles of residence in the core (and fissile buildup), are moved to a moderated radial blanket. The combination of the several-percent-enriched blankets and the moderation will result in a very reactive radial blanket system capable of producing a large fraction of the total power. The large power production from the radial blanket, plus improved radial power flattening, will result in the ability to produce more power from the core without violating fuel thermal or materials limits. The second objective in the proposed shuffling strategy is to create a critical or near critical radial blanket so that the leakage of the core neutrons to the radial blanket can be reduced, and consequently the average fissile enrichment of the core can be lowered.

This summary is organized in the following manner: first a description of methods and models used for the depletion calculations will be presented. This will be followed by a discussion of the depletion analysis of the reference core and the breed/burn cores studied in this work. The economic analyses of these cores are presented next, followed by a neutron and gamma heating study of the core and blankets. Finally recommendations for further work will be made.

6.2 Burnup Methods and Models

6.2.1 Reference Reactor

To study the proposed fuel management strategy, a reference heterogeneous core examined at Argonne National Laboratory was chosen as a reference case (B5). This core consists of 780 fissile-fueled assemblies, and 415 internal blanket assemblies. The reference core has a two-row radial blanket (270 assemblies). In our study three rows of radial blanket (414 assemblies) were employed so that when the internal blanket assemblies were shuffled into the radial blanket, the number of internal and radial blanket assemblies would match. Table 6.1 gives some general data about the reference core and fuel and blanket assemblies. The fuel assemblies in the reference core are constructed of $(U\text{-}Pu)O_2$ fuel pins, while the internal, radial and axial blankets contain depleted uranium fuel rods. The cladding and other structural material in the core is 20% cold worked stainless steel 316. In studying the breed/burn concept both a $(U\text{-}Pu)O_2$ core with depleted uranium blankets and a $(U\text{-}Pu)O_2$ core with thorium blankets were analyzed, although most of the emphasis was put on the $(U\text{-}Pu)O_2$ core with thorium internal blankets because of the expected superior performance of the Th-U233 system in the epithermal spectrum created in the moderated radial blanket.

6.2.2 Cross Section Preparation and Reactor Model

The basic cross section set used for all the

Table 6.1

General Characteristics of the Reference Core and Fuel and Blanket Assemblies

Core	
Reactor Power, MWt	4124
Plant Electrical Power, MWe	1200
Full Power Capacity Factor, %	70
Active Core Height, in	36
Axial Blanket Height, in	14
Fuel Assembly	
No. of Assemblies	780
Assembly Pitch, in	4.682
Pins per Assembly	217
Pin OD, in	0.23
Clad Thickness, in	0.015
Oxide Smear Density, %TD	85.5
Axial Blanket Pellet Density, %TD	95.9
Peak Pellet Linear Power, (3σ, 15% Overpower) KW/ft	14.4
Volume Fractions	
Fuel	0.3591
Structure	0.2436
Coolant	0.3973
Blanket Assembly	
No. of Assemblies	
Internal	415
Radial	414
Assembly Pitch, in	4.682
Pins per Assembly	127
Pin OD, in	0.506
Clad Thickness, in	0.015
Oxide Smear Density, %TD	93.7
Peak Linear Pin Power, (3σ, 15% Overpower) KW/ft	20
Volume Fractions	
Fuel	0.5278
Structure	0.2638
Coolant	0.2088

calculations in this work is the 50 group LIB-IV microscopic cross section set (K2). For burnup calculations this set was corrected for resonance self-shielding and temperature dependence and collapsed to 10 groups using the one dimensional code SPHINX (D1) applied to a one dimensional model of the reactor. Due to some confusion and uncertainty about the appropriateness of the LIB-IV fission product set, a new set of 50 group fission product cross sections were generated from a 70 group fission product set endorsed by the Japanese Nuclear Data Committee (JNDC) (K3). Benchmark calculations performed by JNDC for some integral measurements has showed better agreement than other fission product sets, including ENDFB/4-derived sets. The JNDC cross section set does not include a lumped fission product cross section set for U233 fission products. These cross sections were generated from the JNDC's fission product sets for U235 and U238 by fitting group-by-group σ values to a linear function of atomic mass--a procedure shown to have a plausible theoretical basis, and to be justified by fission product yield data. This linear hypothesis was also tested for a set of one-group lumped fission products for U233, U235 and U238 collapsed in a Gas Cooled Fast Breeder Reactor (GCFR) spectrum. The results are shown in Fig. 6.1. As can be seen, lumped fission product cross sections are fairly linear as a function of atomic mass. Based on this evidence, a 70 group U233 fission product set was generated from the

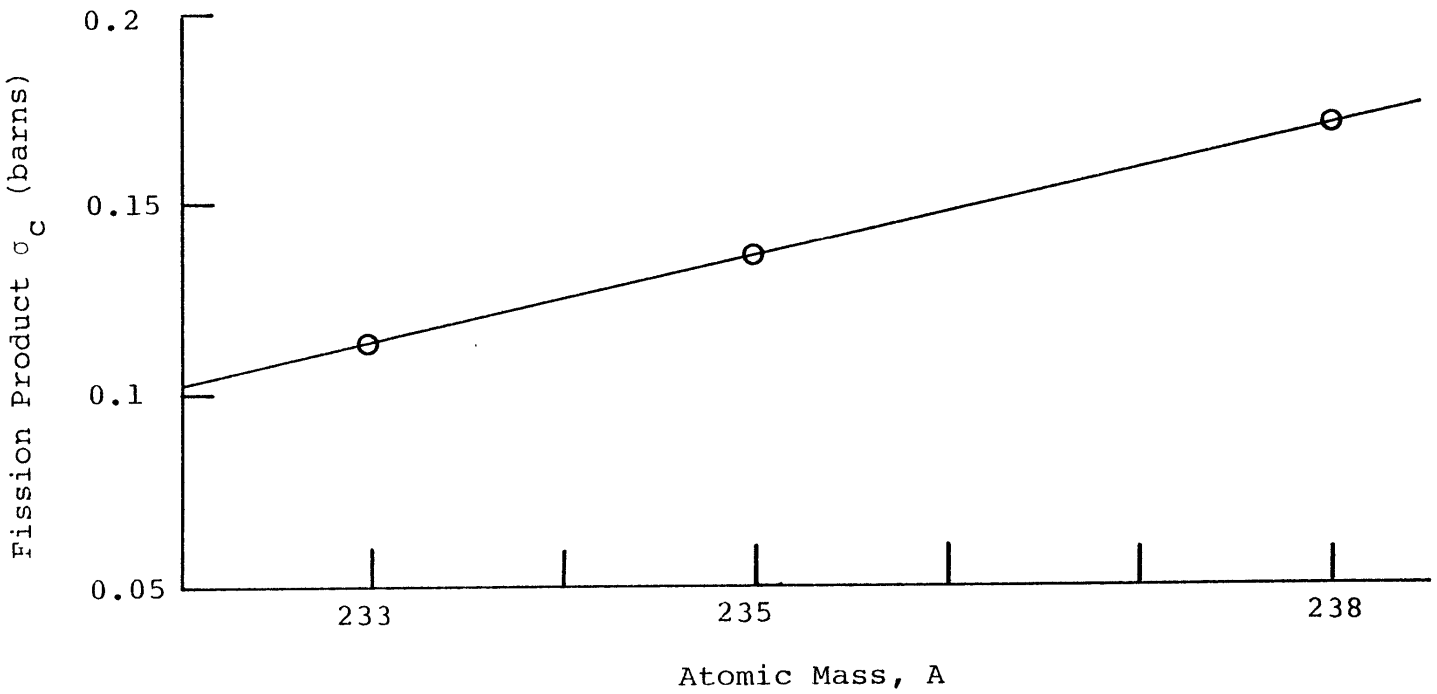

Fig. 6.1 One Group Capture Cross Section for Uranium Fission Products Collapsed in a GCFR Spectrum, as a Function of Atomic Mass

U235 and U238 Japanese fission product sets, and was then collapsed to 50 groups to fit into the LIB-IV structure. Finally the fission product set was collapsed to 10 groups for burnup analysis.

The burnup calculations were performed using 10 group cross sections in the two dimensional burnup code 2DB (L4). Figure 6.2 shows the R-Z model of the core used in 2DB burnup calculations. In all burnup calculations the beginning of cycle core enrichment requirement was found by assuring that the k_{eff} equals 1.0 at the end of cycle. In the burnup calculations no partial control rod insertion was assumed, and all the control positions were assumed to be filled with sodium. This assumption will result in a slightly higher breeding ratio compared to the real case, where the control rods are partially inserted. But since the excess reactivity throughout the cycle is very small due to the excellent breeding characteristic of the core, the error in omission of control rod insertion is very small. Note that in the design of the core enough control rod positions are included to guarantee the safe shutdown of the reactor with one control bank completely stuck.

6.2.3 Moderator Properties and Moderated Blanket Design

The proposed moderator used in the moderated radial blankets is zirconium hydride (S3). The advantage of this moderator over other solid moderators is its high moderating power, which is approximately the same as that of water. The

Key

IB	Internal Blanket	ABI	Axial Blanket Extension of Internal Blanket
F	Fuel	ABF	Axial Blanket Extensions of the Fuel
RB	Radial Blanket	SH	Shield

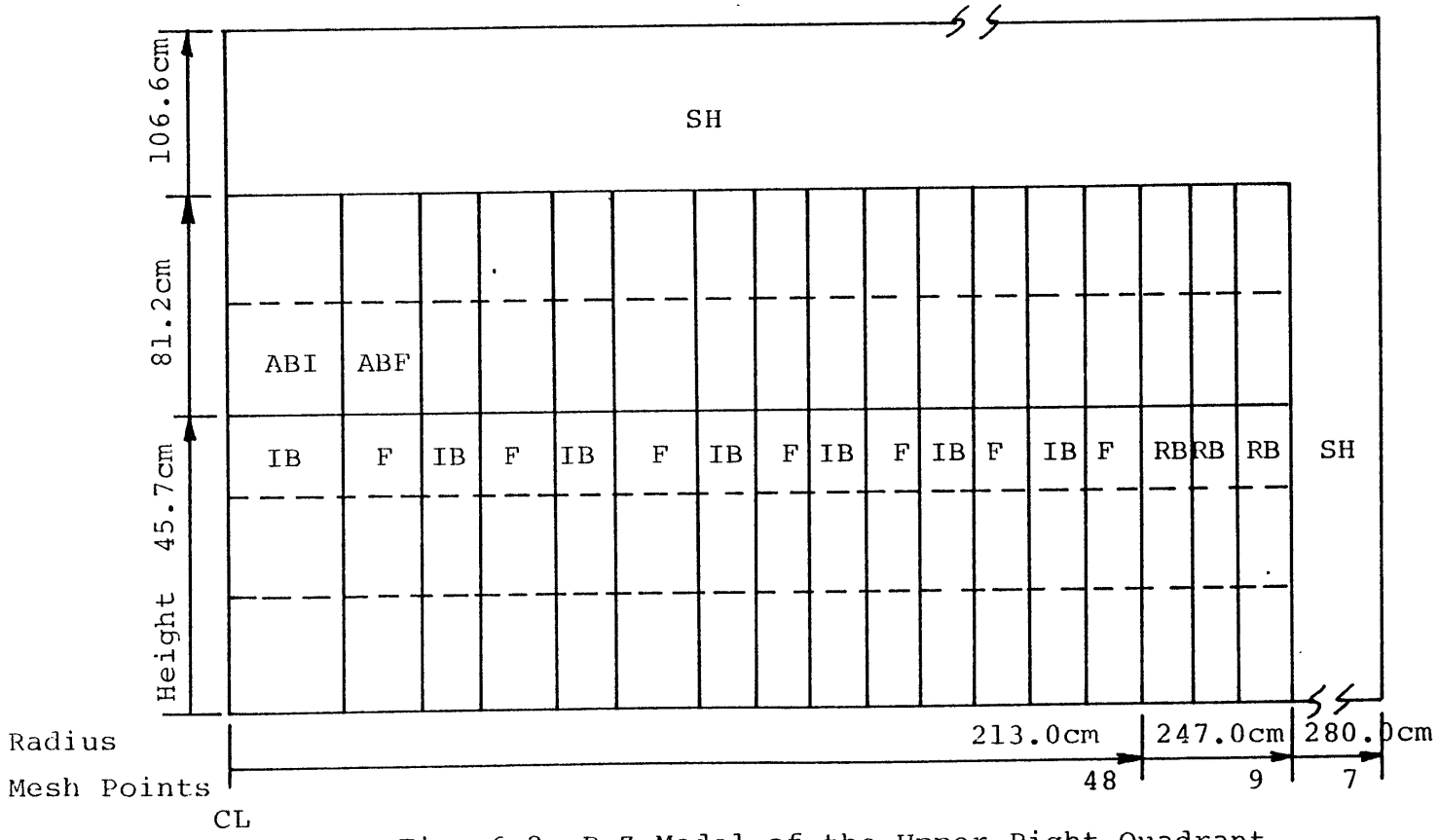

Fig. 6.2 R-Z Model of the Upper Right Quadrant of the Reactor Used for Burnup Calculations

high moderating power of zirconium hydride results in a large degree of spectrum softening without taking up too much space. This permits the design of the moderated blanket assemblies and the host core to be compact.

The experience with zirconium hydride behavior in a reactor environment includes: 1) using zirconium hydride as the moderator for an experimental thermal reactor fueled with U-Pu oxide and cooled with sodium (H3). 2) Using zirconium hydride mixed with the fuel in combined fuel-moderator elements in SNAP (L3) and TRIGA (S4, S5) reactors.

In all of the above cases zirconium hydride has behaved satisfactorily, with no hydrogen migration or other problems.

With respect to zirconium hydride's behavior under irradiation, besides the above experience there have been some specific experiments performed. In one set of experiments samples of zirconium hydride were irradiated at fluences of up to 1.15×10^{24} n/m^2 ($E > 1$ Mev) at a temperature of 580°C. In another set of experiments samples of zirconium hydride were irradiated in EBR II at 400° C up to fluences of 5 to 7×10^{26} n/m^2 ($E > 0.1$ Mev). In both cases post irradiation examinations indicated no hydrogen migration or any significant damage to the zirconium hydride.

In the present application the moderated blanket assemblies can be designed to include as many zirconium hydride rods as necessary for the desired level of moderation. The moderator pin can be designed to be much larger than the

blanket fuel pins due to the relatively low energy deposition in, and relatively high thermal conductivity of zirconium hydride.

6.3 Depletion Analysis

6.3.1 Depletion Analysis of the Reference Core and the $(U-Pu)O_2$ Cores with Thorium Blankets, Employing the In/Out-Moderated Blanket Strategy

Depletion analyses were performed for three sets of reactors. To be able to make a consistent comparison of the neutronic performance of the different cores under study, a complete burnup analysis was first performed on the reference cores. The fuel management strategy for the reference core includes an annual refueling of half of the fuel and internal blanket assemblies and a one-sixth refueling of the radial blanket. Several core parameters were compared with the values reported by ANL for the same core (B5). These included the volume averaged fuel assembly fissile plutonium enrichment (22.0% (MIT) vs 21.93% (ANL)), breeding ratio (1.26 vs 1.30) and the peak core linear heat generation rate (11.10 vs 11.23). The above agreement validated the methods and procedures used in this study to within state-of-the-art capabilities.

To find the optimum configuration of the thorium-blanketed $(U-Pu)O_2$ cores in which the internal blankets were shuffled out into the radial blankets, an initial physics study was performed on several parameters, to find the

optimum level of moderation and to determine whether moderator should be incorporated in the internal blankets from the outset or added after an assembly is shuffled to the radial blanket. A final objective was to determine the number of cycles spent by the internal blanket assemblies in the core and radial blanket. The fuel management strategy ultimately evolved for these cores included a two year batch burnup of the fissile-fueled assemblies and a concurrent two year burnup of the admixed internal blanket assemblies, following which the latter are moved to the radial blanket for an additional two cycles (two years) of burnup. With respect to the moderation of the blanket assemblies, in the absence of any detailed thermal-hydraulic-mechanical design analysis the simplest method for considering different levels of blanket moderation was to assume that a certain percentage by number of the blanket fuel pins, such as 30, 40 or 50% are replaced by moderator rods. In practice, once the desired level of moderation is found from neutronic calculations, a detailed thermal-hydraulic analysis of the blanket assembly, including an optimization of moderator pin diameter, would be carried out to determine the actual intra-assembly arrangement of the fuel and moderator pins.

To examine whether the moderator should be included in the internal blankets or added after the internal blankets are moved to the radial blanket, three cases were studied. In the first case all the internal blanket assemblies included

40% zirconium hydride. In the second case the 40% by number of moderator pin positions in the internal blankets were assumed to be filled with sodium, and in the third case they were left empty. Note that in the second and third cases it is assumed that once the internal blanket assemblies are moved to the radial blanket, moderator will be added to them. The beginning of the equilibrium cycle k_{eff} for the three cases of 40% moderation, 40% sodium-filled and 40% voided were 0.9001, 1.0375 and 1.0428, respectively. As can be seen, the inclusion of the moderator in the internal blanket results in a substantial reduction in k_{eff}. In fact, this large reduction prompted the idea of using moderation in the internal blankets as a means to control the excess reactivity of the core--an option which will be re-examined later. Based on these results it was concluded that to get the highest k_{eff} at the beginning-of-cycle the best strategy is to leave the moderator pins in the blanket assemblies empty, while the blanket assemblies reside in the core. The moderator can be added to the assemblies when they are moved to the radial blanket using a movable mechanism similar to a PWR control rod mechanism, i.e., an empty control rod cluster can be removed and replaced with a moderator-filled cluster.

The second parameter examined was the optimum level of moderation of the radial blanket. In this case the objective is to produce as much power from the radial blanket as

possible without exceeding the specified peak LHGR of 20 KW/ft. To do this three cores with 30, 40 and 50% voided internal blankets were depleted for two years. Next the internal blankets were moved to the radial blanket where moderator was added to the radial blanket assemblies. The fuel and internal blanket assemblies were replaced by fresh fuel. The results showed that as the level of moderation was increased the contribution of the radial blanket power to the total power in the above three cases increased from 16.7% to 19.0% to 21.2%. At the same time the peak LHGR increased: from 13.0 KW/ft to 17.67 KW/ft to 22.74 KW/ft, respectively. At the 50% moderation level the peak LHGR is above the specified limit of 20.0 KW/ft, and so the 40% moderation level was taken as the optimum for the radial blanket. Thus, the first representative breed/burn core consists of a $(U\text{-}Pu)O_2$ core with a 40%-voided thorium internal blanket system, and a 40%-moderated radial blanket system. The fuel management of the core and blankets consists of two year batch burnup of the fuel and internal blanket assemblies, after which the internal blankets are moved to the radial blanket for an additional two years of burnup, and the fuel and internal blanket assemblies are replaced by fresh fuel. Note that since the flux is not flat in the core, the rate of fissile build up in the internal blankets is a function of blanket assembly position. This is quite beneficial in the proposed strategy since higher-enrichment

blanket assemblies will be moved to the outer rows of the radial blanket to help flatten the power in the radial blanket. Figures 6.3 and 6.4 show the beginning and end of equilibrium cycle power densities in the reference core and the $(U\text{-}Pu)O_2$ core with the two-cycle-burned, in/out, moderated radial blanket. Note that the reference core has two rows of radial blanket assemblies but that the power density at the boundary of the second row and the shield is so small that addition of a third row does not contribute much to the total power production from the radial blanket. Table 6.2 shows the beginning-of-equilibrium-cycle power contributions and peak LHGRs in different regions of the reference core and the breed/burn core. Note that the peak LHGR in the breed/burn core is 10% lower. This implies that the total power generated by the core can be increased by 10% without any LHGRs being higher than in the reference core. This extra power corresponds to the power produced by 15% of the fuel assemblies. Thus the core could instead be redesigned with 15% fewer fuel assemblies and produce as much power as the reference core without exceeding any thermal limits imposed upon the reference core.

Table 6.3 shows the average discharge burnups of the reference core and the $(U\text{-}Pu)O_2$ core with a two-cycle-burned, in/out, moderated radial blanket. Note that the core, internal and axial blanket burnups are fairly similar, whereas the radial blanket burnup in the breed/burn core

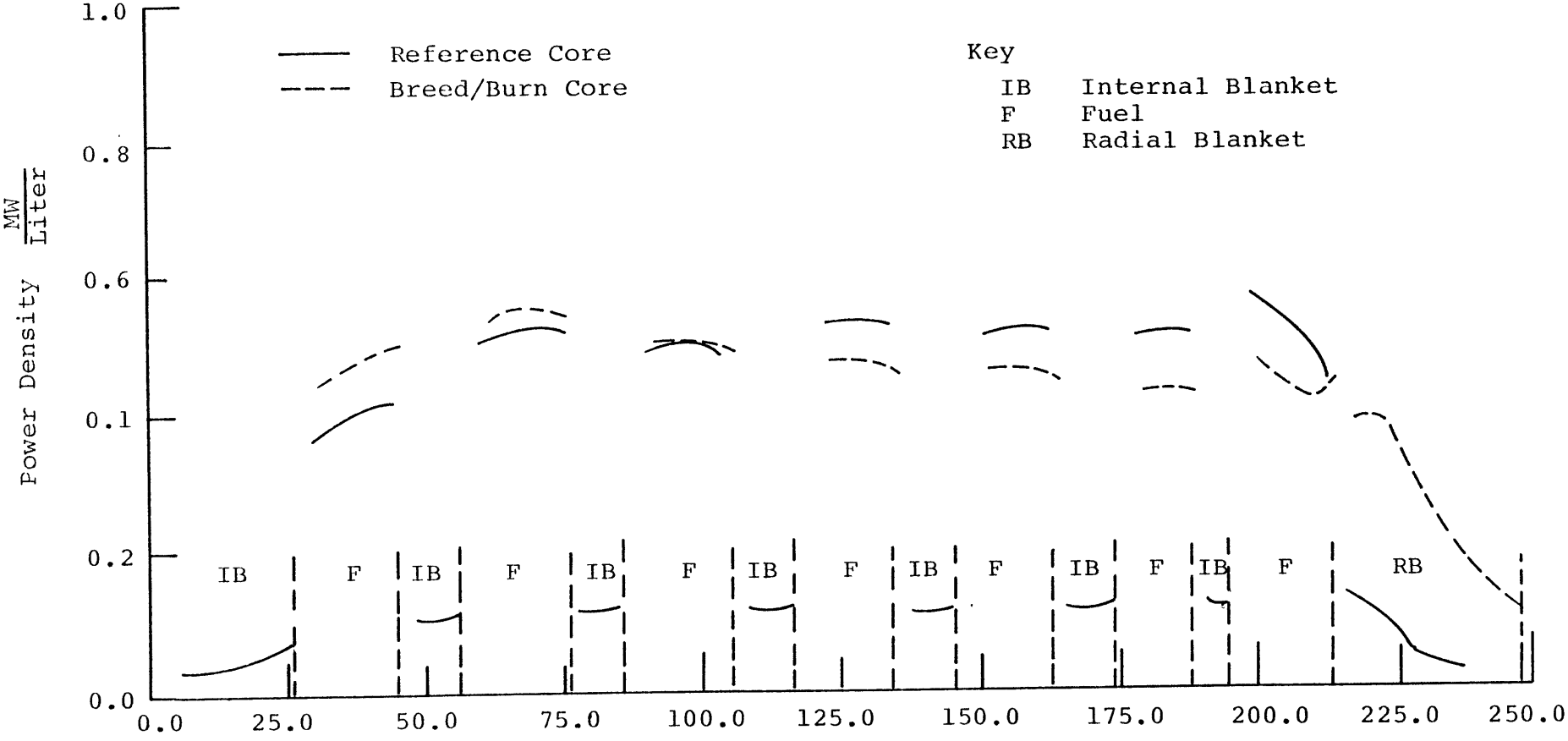

Fig. 6.3 Beginning of Equilibrium Cycle Midplane Power Distribution in the Reference Core and the Breed/Burn Core

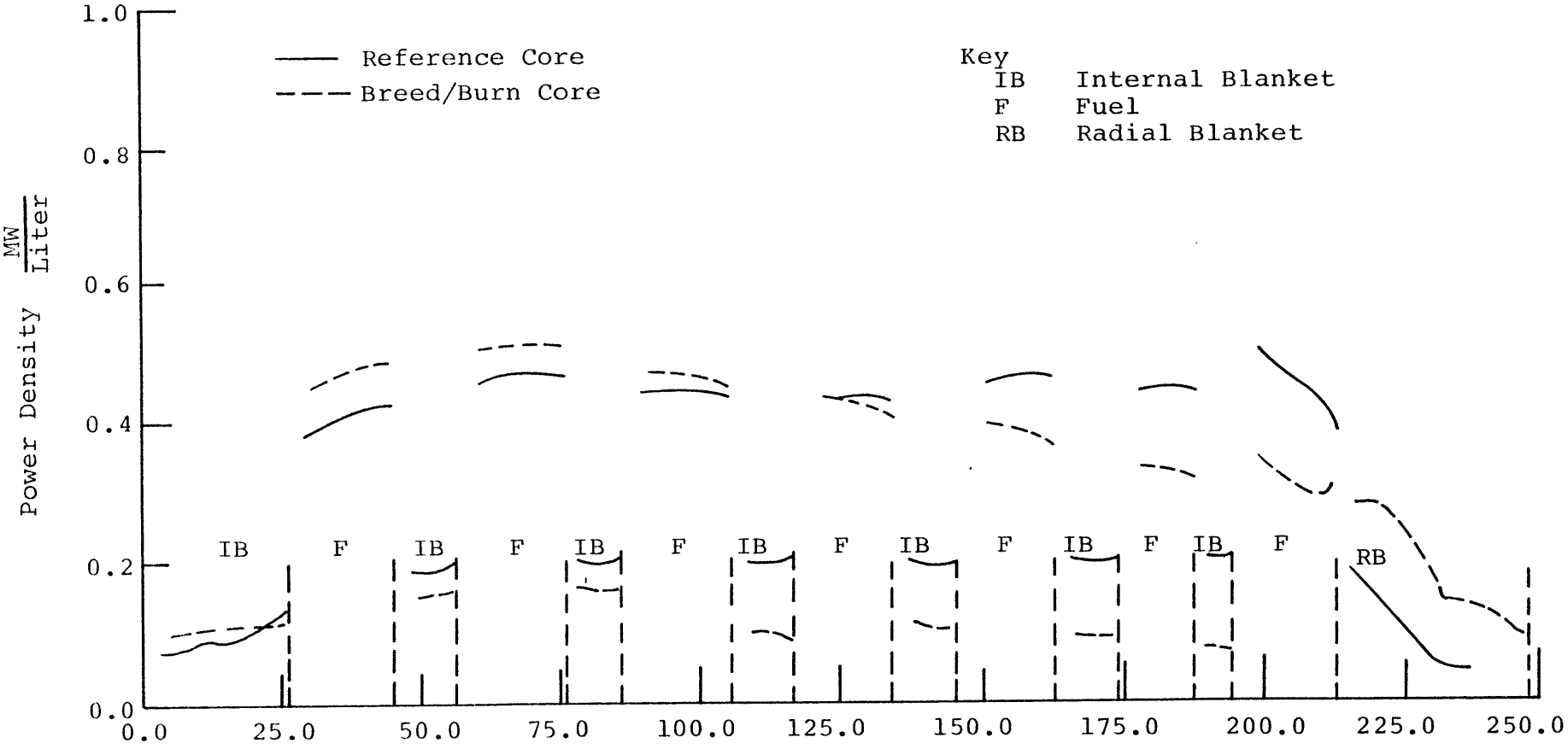

Fig. 6.4 End of Equilibrium Cycle Midplane Power Distribution in the Reference Core and the Breed/Burn Core

Table 6.2

Beginning of the Equilibrium Cycle Power Contribution and Peak Linear Heat Generation Rates in the Reference Core and the (U-Pu)O_2 Core With a Two-Cycle-Burned, In/Out, Moderated Radial Blanket

Reactor Region	Power Contribution (%)		Peak Linear Heat Generation Rate (KW/ft)	
	Reference Core	Breed/Burn Core	Reference Core	Breed/Burn Core
Fuel	84.57	78.12	11.23	10.13
Internal Blanket	9.43	0.51	4.56	2.68
Axial Blanket	2.42	2.32	--	--
Radial Blanket	3.58	19.05	5.42	17.67
	100.00	100.00		

Table 6.3

Average Discharged Burnups of the Reference Core and the Two-Cycle-Burned, In/Out Shuffled Breed/Burn Core

Reactor Region	Average Burnup (MWD/MTHM)	
	Reference Core	Breed/Burn Core
Core	68,040	62,450
Internal Blanket*	11,856	10,575
Axial Blanket	1,692	2,221
Radial Blanket*	10,852	31,941
Blanket Discharge Burnup		42,516

*Same assembly successively occupies both positions in the breed/burn core.

is three times higher than the reference core. Also note that once the internal blankets are fabricated for the breed/burn core, they remain in the internal and radial blanket positions for four years with an average cumulative burnup of 42516 $\frac{MWD}{MT}$.

With respect to reprocessing requirements, in the reference core half of the fuel and internal blanks and 1/6 of the radial blankets are replaced annually. In the breed/burn core, the fuel and internal blanket assemblies are replaced every two years, which is the same as 1/2 of the fuel and internal blanket assemblies being replaced every year. But there are no separate radial blanket assemblies, so in the reference core there are 252 blanket assemblies replaced annually compared to 207 assemblies in the reference core. This is a net reduction of 18% in the blanket assembly fabrication and reprocessing requirements. As far as the plutonium bearing assemblies are concerned, in the reference core there are 642 fuel and blanket plutonium-bearing assemblies being transported and reprocessed annually against 390 plutonium bearing assemblies per year for the breed-burn core: a reduction of almost 40%. Note that the U233-bearing internal blanket assemblies in the breed/burn core can be made substantially more proliferation resistant--if a few percent U238 is added to the original thorium fuel. This can be effected without any appreciable change in the neutronic performance of the core and blankets.

Finally, as far as the effect of irradiation on the moderator pins in the radial blanket is concerned, the peak fast flux above 0.04 Mev in the radial blanket of the breed/burn core is 0.65×10^{15} n/cm^2-sec. In a two-year period of residence of zirconium hydride moderator pins in the radial blanket the peak fluence is equal to 2.56×10^{22} n/cm^2. As was mentioned earlier, in one series of tests, zirconium hydride samples were irradiated in EBR II at a temperature of 400°C and fluences of 5 to 7×10^{22} n/cm^2 with no irradiation damage. Thus it can be seen that the zirconium hydride pins can stay in the radial blanket for several cycles without any anticipated problems.

To see if the power production from the radial blanket can be increased any further, several other (U-Pu)O_2 cores having thorium blankets and employing the in/out, moderated fuel management strategy were studied--here only brief mention will be made of these case studies. To see if higher enrichment in the radial blanket would result in higher power production, a four-cycle-burned internal blanket system was moved to the 40% moderated radial blanket. The average U233 enrichment in this case was 6.1% U233. The 40% moderated radial blanket exhibited power peaking problems, so the moderation level was reduced to 30%. The percentage of the total power produced by the radial blanket increased from 19.05% for the two-cycle-burned, 40% moderated blanket system to 26.04% for the four-cycle-burned,

30% moderated case, with an additional 5% reduction in the peak LHGR. The next core studied consisted of 6 rows of radial blanket assemblies. In this case the number of internal blanket assemblies is equal to half the number of radial blanket assemblies and thus the internal blankets after two cycles of residence in the core are moved to the radial blanket where they stay for four years. The BOEC power contribution of the radial blanket in this case is 24.04%, compared to 19.05 for the two cycle burned, 40% moderated radial blanket system. This modest increase does not appear to justify the use of three additional rows of radial blanket assemblies. Looking at Fig. 6.3, it can be seen that the power distribution in the radial blanket of the breed/burn core decreases monotonically as one moves away from the core-blanket interface. In an attempt to increase the power production of the radial blanket, in the core with six rows of radial blanket assemblies discussed above, the first three rows were left unmoderated and the last three were moderated with 40% zirconium hydride. This was done so that the flux attenuation by the first few rows would be reduced. The power contribution from the radial blanket in this case dropped to 23.74%. The next core studied included a variably-moderated radial blanket. In this case the first two rows of the radial blanket were 40% moderated, the next two rows were 50% moderated and the last two rows were 60% moderated. The power contribution from the radial blanket was calculated

to be 23.64% of the total core power, which is fairly similar to the two previous cases studied. The reason for the small change in power contribution is the fact that almost 80% of the total power produced by the radial blanket is produced in the first two rows of the radial blanket. Thus the ability to increase power by modifying outer row design is very restricted: leakage to the shield is just too debilitating. Finally, a core with half the number of internal blanket assemblies as the cores studied previously was considered. By cutting the number of internal blanket assemblies to half the original value, the average enrichment of the core dropped from 23% fissile plutonium to an average of 18% fissile plutonium; on the other hand the sodium void coefficient in this core is higher than for the cores analyzed before. The power contribution from the radial blanket in this case was 20%.

Based on the above results it can be concluded that the basic advantage of the in/out, moderated shuffling strategy lies in the production of 20-30% of the total power from the radial blanket, which in turn leads to a 10-15% reduction in the peak linear heat generation rate (LHGR) in the core. This 10-15% reduction in the peak LHGR can be translated into a 10-15% increase in power production from the breed/burn core without exceeding the allowable peak core power density for the reference core, or it can be translated into a 15-20% reduction in the number of core

fuel assemblies required for a core with the same power production as the reference core.

6.3.2 Blanket Criticality Calculations

The second objective in moving the enriched internal blankets to the radial blanket was to create a very reactive i.e., critical or near critical radial blanket so that the leakage of the core neutrons to the blanket can be reduced, resulting in a reduction of the core average enrichment. With respect to this idea a blanket criticality calculation as a function of moderation was performed for both the U-Pu and Th-U233 blanket systems. To do this a two dimensional model of the upper half of the blanket assemblies including their axial blanket extensions was used in 2DB by assuming a reflective boundary condition on the left, right and bottom boundaries and a vacuum boundary condition on the top boundary. These conditions, in an approximate manner, simulate a critical internal blanket system located inside a critical environment. For radial blankets the leakage of neutrons to the radial shield is very significant and hence the right reflective boundary condition would not hold.

For both the U-Pu and Th-U233 systems the beginning of cycle clean critical enrichment and breeding ratio as a function of moderation was calculated. The results are shown in Table 6.4. There are several points worth noting: first, the epithermal Th-U233 systems have considerably

Table 6.4

Beginning of Cycle Clean Critical Enrichments and Breeding Ratios for the U-Pu and Th-U233 Blanket Systems as a Function of Moderation

Moderation (Volume Percent Zr $H_{1.6}$)*	Enrichment ($N_{fissile}/N_{HM}$)		Breeding Ratio $C_{fertile}/A_{fissile}$	
	U-Pu	Th-U233	U-Pu	Th-U233
0	9.30	10.34	1.2851	1.1821
30	10.67	5.82	0.8269	0.9737
40	6.98	4.66	0.7307	0.8749
50	5.08	4.17	0.6796	0.7559
70	--	4.71	--	0.4915

*As noted in the text: percent refers to the number of fuel pins replaced by moderator pins.

lower clean critical enrichments than the U-Pu systems; second, the only two systems with breeding ratios greater than one are the unmoderated Th-U233 and U-Pu systems, with the latter having the highest BOC breeding ratio. This implies, although not conclusively, that a moderated once through breeder similar to the Fast Mixed Spectrum Reactor (FMSR) (F1) cannot be built due to the low breeding ratio of these epithermal systems. Also note that the critical enrichment of an unmoderated U-Pu system is about 10%. The plutonium buildup rate in a fast reactor blanket is about 2%/yr initially, and progressively slower as the enrichment increases. Thus to build plutonium up to critical enrichment levels takes a long time--this is the reason for the long time (17 years) to reach the equilibrium cycle in the FMSR.

To get a critical radial blanket enough U233 must be bred into the internal blanket assemblies so that once they are moved to the moderated radial blanket the epithermal system thereby created can be critical. Figure 6.5 shows the U233 buildup in the internal blanket assemblies as a function of blanket residence in the core. From this figure, the U233 buildup after four years is 6.1%, which is higher than the critical enrichment of the 40% moderated blanket system shown in Table 6.4

To see the effect of the radial blanket enrichment on the k_{eff} of the system, k_{eff} at the BOEC of a core with a 40% moderated radial blanket shuffled from the core after

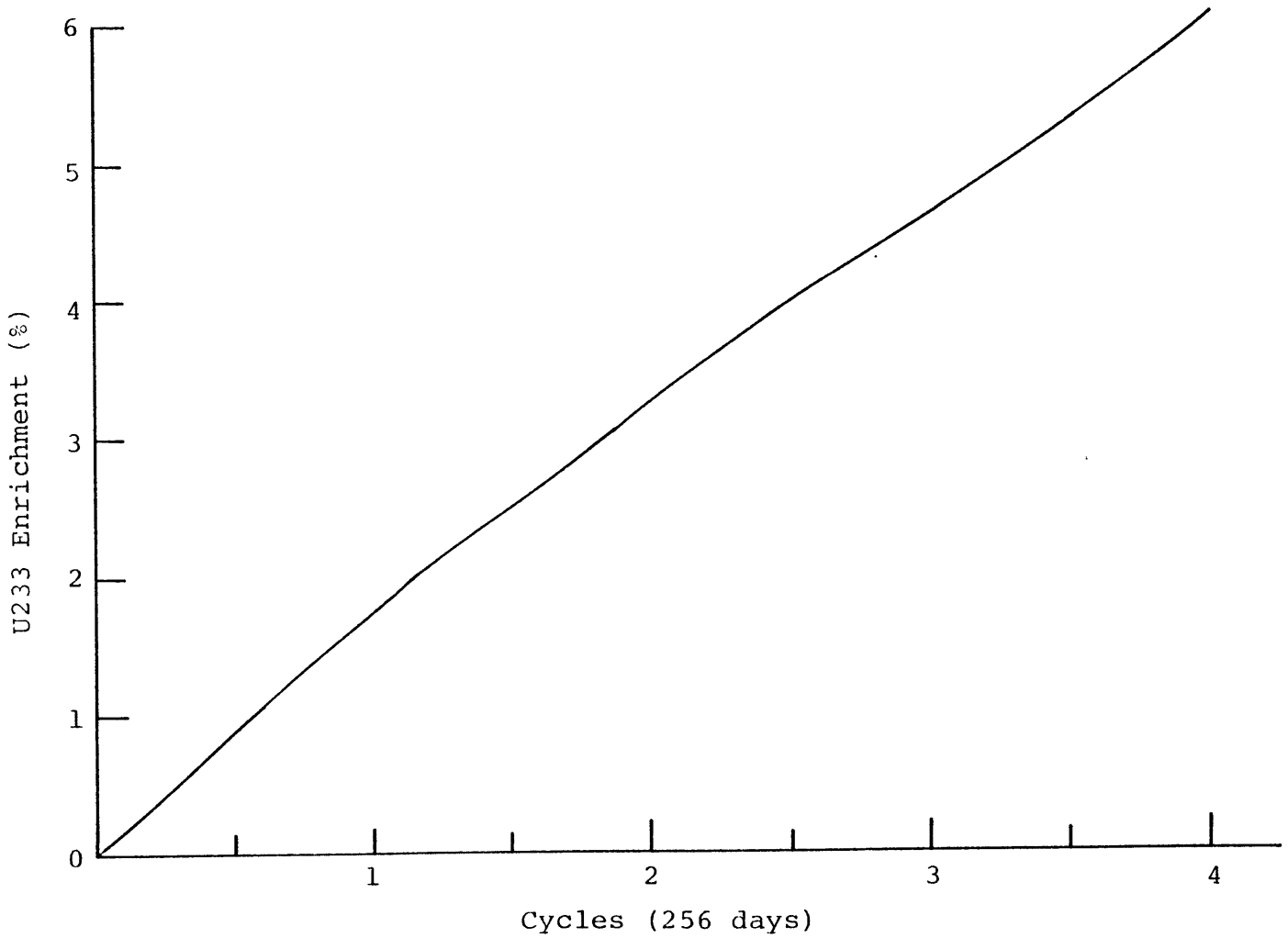

Fig. 6.5 U233 Buildup in the Internal Blanket

two, three and four-cycles of residence was studied. Table 6.5 shows the increase in BOEC k_{eff} of the cores mentioned above over a $(U\text{-}Pu)O_2$ core with thorium internal and radial blankets and with no moderation or enrichment in the radial blanket.

It can be seen that the shuffling of the enriched internal blankets to the radial blanket has resulted in a substantial gain in reactivity, which results in a sizable reduction of the average fissile core enrichment. This can be seen by noting that the fissile enrichment of $(U\text{-}Pu)O_2$ cores with thorium blankets is approximately 15 to 20% higher than $(U\text{-}Pu)O_2$ cores with depleted uranium blankets (H1). In the case of the breed/burn cores with thorium blankets the BOEC average enrichment is 23% fissile plutonium compared to an average enrichment of 22% fissile plutonium for the reference core. Hence the creation of the reactive radial blanket using an epithermal Th-U233 system has resulted in a net reduction of 2 to 3% in the average-fissile plutonium requirement. Unfortunately this gain only helps to lower the penalty associated with utilization of thorium internal blankets in fast reactors, and bring the $(U\text{-}Pu)O_2$ core with thorium blankets to a competitive level with uranium-blanketed fast breeder reactors.

Another point worth noting is that the 6.1% U233 enrichment of a four-cycle-burned internal blanket assembly, which is moved into a 40% moderated radial blanket, is higher

Table 6.5

Increase in the BOEC k_{eff} of a $(U\text{-}Pu)O_2$ Core with an In/Out, 40% Moderated Radial Blanket as a Function of Blanket Enrichment

Internal Blanket Residence* in the Core (Years)	Average U233 Enrichment in the Radial Blanket	Δk** (%)	$ (β=0.004)
2	3.66	7.66	19.15
3	4.62	8.69	21.72
4	6.10	10.88	27.2

*This is the number of years the internal blanket assemblies have resided in the core before being moved to the radial blanket.

**Basis of comparison: a $(U\text{-}Pu)O_2$ core with thorium blankets without blanket moderation or enrichment

than the clean critical enrichment of 4.66% for this level of moderation. Despite this, no substantial reactivity gain is observed. The reason for the lack of a much larger increase in k_{eff} is that there is a considerable leakage of neutrons to the radial shield. To see if this situation can be corrected by using a better reflector, a $(U\text{-}Pu)O_2$ core with the four-cycle-burned, 40% moderated blanket having a zirconium hydride reflector instead of the conventional steel reflector was studied. The gains in k_{eff} and power production from the radial blanket over the case with the steel reflector were quite modest, indicating that the rate of leakage of neutrons to the radial shield is very high.

Since the leakage of neutrons from the radial blanket to the radial shield prohibits the creation of a critical blanket system, it was concluded that rather than moving the enriched internal blankets outward to the radial blanket it would be more advantageous to move the blankets inward and create a critical or near-critical central island.

To do this the core configuration was rearranged by replacing the six innermost blanket and fuel assembly rings with a central island consisting of several-cycle-burned, 40% moderated internal blanket assemblies that are moved from the remaining four rows of the internal blankets to this position. Figure 6.5 shows the arrangement of the core and blankets. The six innermost rings consist of 312 assemblies. The remaining four rings of internal blanket consist of 318

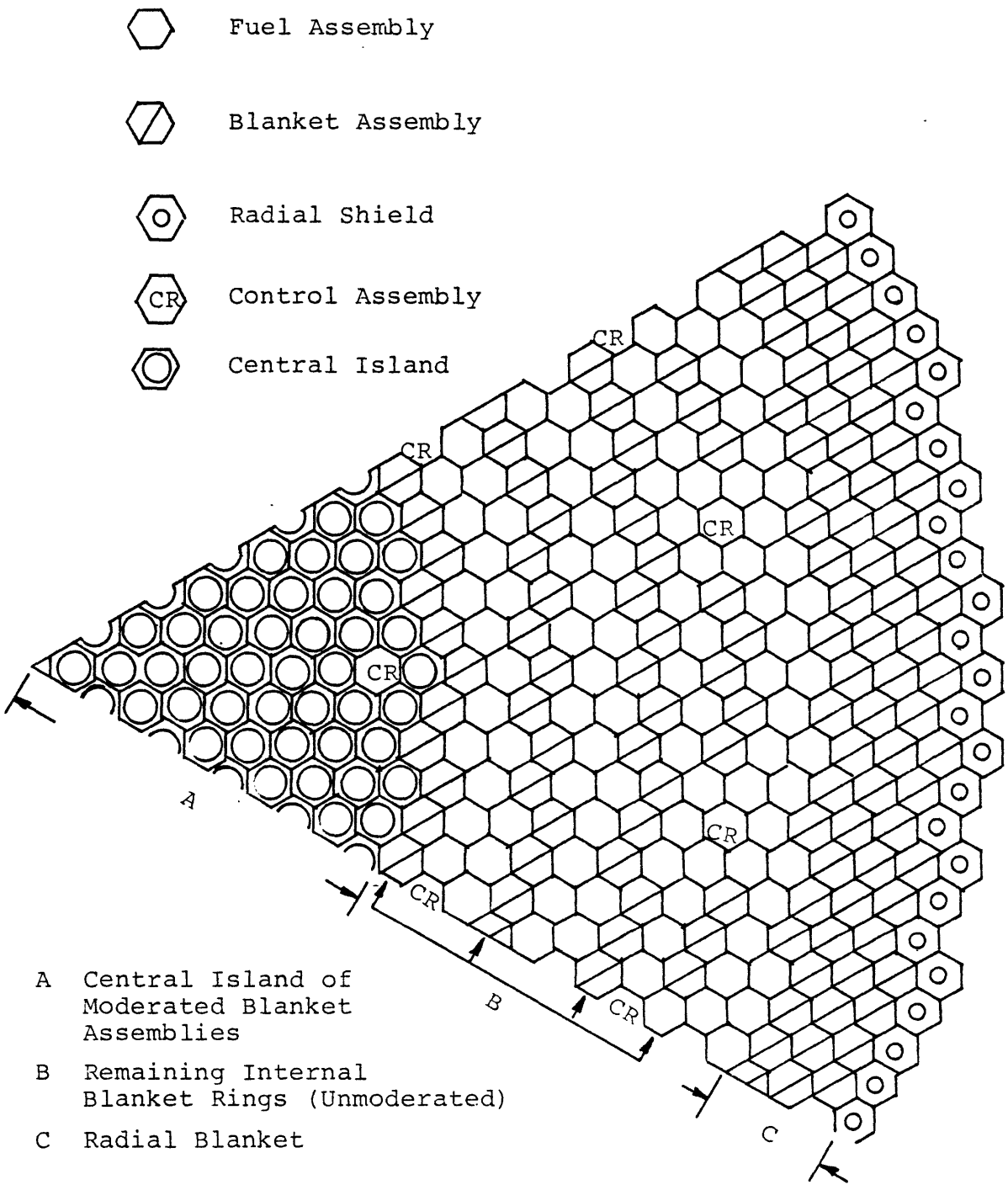

Fig. 6.6 New Core Arrangement Including a Central Island

assemblies which are surrounded by 564 fissile-fueled assemblies. The basic fuel management strategy is to breed in U233 in the four rings of internal blanket assemblies and then move these assemblies to the central island. Preliminary studies showed that to avoid power peaking in the core it is also necessary to have a reactive radial blanket that produces a reasonable amount of power. This suggested that the internal blanket shuffling should be alternated between the central island and the radial blanket.

With respect to the shuffling of internal blankets to the central island, three cases moving either two-, three- or four-cycle-burned internal blankets to the central island were studied. With the four-cycle-burned internal blankets the combination of high enrichment in the blanket assemblies and the moderation resulted in a very large power peak in the central island.

Moving three-cycle-burned internal blankets into the central island provided the best power distribution. Thus the basic fuel management strategy evolved for this core is as follows: the fuel assemblies have an annual refueling schedule, where half of the total fuel assemblies are replaced every year. The internal blanket assemblies are replenished every five years. The path that the internal blankets take over each five year period alternates between a) three cycles of internal blanket residence (and fissile buildup) followed by shuffling of the blanket assemblies to the moderated

central island where they burn for two years; b) two cycles of internal blanket residence followed by a shuffling of the blanket assemblies to the moderated radial blanket where they burn for three years. In both cases the blanket assemblies remain in the core for five years. Figure 6.7 shows the beginning-of-cycle midplane power distribution in the core described above. The major advantage of this core is its lower fissile requirement. For example, in the above core, 216 fuel assemblies with an average of 22% fissile plutonium enrichment have been replaced with a moderated Th-U233 blanket system that has an average enrichment of only 4.84% U233, all of which is produced in the core. Also, 96 internal blanket assemblies in the central island have been replaced by 4.84% U233 enriched assemblies. If the fissile plutonium in the 216 fuel assemblies is smeared over the 312 fuel and blanket assemblies (considering the difference in the fuel volume fraction) the overall fissile enrichment is 10.36% fissile plutonium. Thus, by creating a near critical central island it has been possible to replace an average enrichment of 10.36% fissile plutonium in 312 assemblies (or an average of 22% fissile plutonium in 216 assemblies) with a moderated Th-U233 system having a U233 enrichment of only 4.84% U233. Again note that the U233 is produced in the core. The beginning of cycle k_{eff} of the core is 1.043, which is high enough to insure a critical core after one cycle (256 days) of depletion.

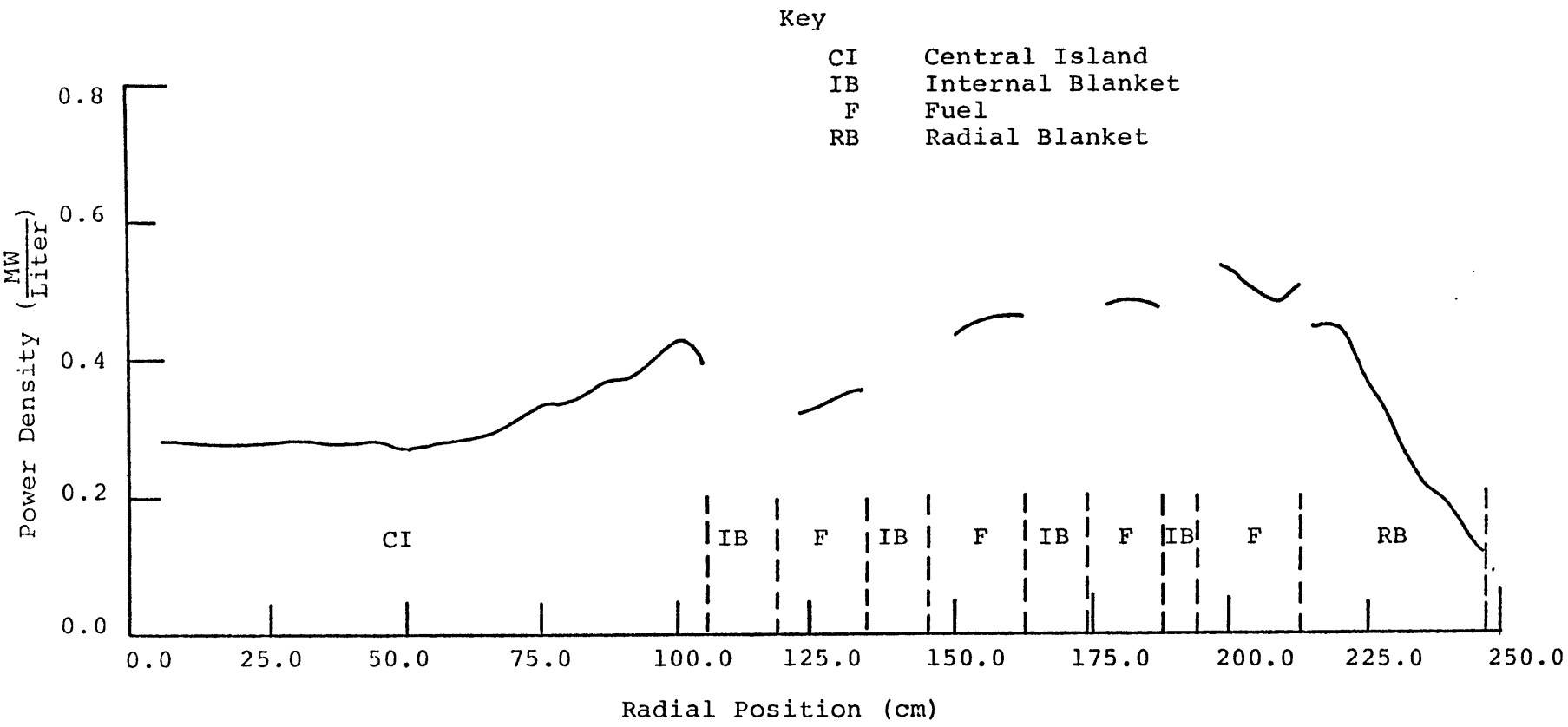

Fig. 6.7 Beginning-of-Cycle Midplane Power Distribution in the $(U\text{-}Pu)O_2$ Core with a 40% Moderated, Three-Cycle-Burned Central Island

Compared to the reference core the breed/burn core with the central island discussed above has 27% fewer fissile fueled assemblies, roughly half as many total assemblies to be reprocessed, and only about 40% as many plutonium-bearing assemblies to be shipped and reprocessed. Also note that no detailed analysis was done to optimize the configuration or arrangement of the core and blanket assemblies or to optimize the core for this particular fuel management strategy. Further advantages might be forthcoming following a more detailed analysis of the properties of this core.

6.3.3 Use of Moderator in the Internal Blanket Assemblies to Control Excess Reactivity

As was shown earlier, inclusion of moderator in the internal blanket assemblies of a heterogeneous core results in a large decrease in the reactivity of the system. This result prompted reconsideration of the old idea of using the moderator as a means to control the excess reactivity of the core. This concept is particularly suitable for the breed/burn cores studied in this work since the internal blankets already have empty tubes that can be used for the moderator insertion.

To examine this possibility, the beginning of equilibrium cycle k_{eff} of the $(U\text{-}Pu)O_2$ core with a two-cycle-burned, in/out, 40% moderated radial blanket was calculated for two cases: complete moderator insertion in first 163 and then 247 out of 415 internal blanket assemblies. Table 6.6 shows the resulting BOEC k_{eff}s. Based on linear interpolation

Table 6.6

k_{eff} at the Beginning of Equilibrium Cycle as a Function of the Number of Moderated Internal Blanket Assemblies

Number of Moderated Internal Blanket Assemblies*	Inner Rows of Internal Blanket*	k_{eff}
0	0	1.0428
163	4	1.0025
247	5	0.9835

*of a total of 415 assemblies in 7 rows

in the results of Table 6.6, by complete insertion of moderator in approximately 190 internal blanket assemblies the beginning of cycle excess reactivity (which corresponds to a $k_{eff} = 1$ at the end of cycle) can be controlled.

It should be noted the above calculation was done only to prove that moderation can control the excess reactivity of the core. Complete insertion of moderator in only the inner rows of the internal blanket will result in power peaking in the other regions of the core: in actual use, the moderated assemblies would have to be dispersed throughout the entire active core and the insertion pattern programmed to shape the radial power profile.

6.3.4 Depletion Analysis of the (U-Pu)O_2 Core with Depleted Uranium Blankets Employing the In/Out Shuffling Strategy

All the breed/burn cores analyzed so far have included thorium internal and radial blankets. This is due to the superior neutronic performance of the epithermal Th-U233 system. To see the effect of the in/out fuel management strategy on (U-Pu)O_2 cores with depleted uranium blankets two cases were studied. In the first case internal blankets, after two years of fissile buildup, were moved into the radial blanket. No moderation was included in the radial blanket. In the second case the 40% voided internal blanket assemblies, again after two cycles of fissile buildup, were moved into a 40% moderated radial blanket. The beginning of the equilibrium cycle k_{eff} was found to increase from 1.0079 for the original

reference core to 1.0223 for the unmoderated but shuffled core; this value rose to 1.0547 for the moderated blanket case. The fraction of total core power produced by the radial blanket in the unmoderated case was slightly higher than the power produced by the radial blanket of the reference core. In the moderated system, the total power production from the radial blanket nearly doubled. Hence this core may be of interest since it reduces the amount of ex-core plutonium handling. In addition the blanket assemblies are less suitable as a source of clean weapons grade plutonium than from a conventional FBR.

6.4 Economic Analysis

An economic analysis was performed using levelized fuel cycle cost calculations derived from Abbaspour's (A4) simple model which, in turn, is based on earlier work by Brewer (B6). The only noteworthy change here was to replace one-step revenue and depreciation cash flows by continuous cash flows. Using the simple model, the levelized fuel cycle cost e (mills/KWhe) can be written as

$$e = \frac{1}{E} \Sigma_i \, M_i \, C_i \, F_i \, G_i \qquad (6.1)$$

where

E is the total electricity generated by a batch of fuel (or blanket) during its residence in the reactor, (MWhe)

M_i is the mass flow in step i, (Kg)

C_i is the unit cost of the material in step i, ($/Kg)

F_i is a financial weighting factor

G_i is the escalation factor

For the case where all fuel cycle expenses and credits are capitalized and depreciated, F_i is given by:

$$F_i = \left[\frac{1}{1-\tau} \frac{t_r \, (P/F, x, t_i)}{(P/A, x, t_r)} - \frac{\tau}{1-\tau} \right] \qquad (6.2)$$

where

τ is the tax rate

x is the discount rate, and is given by

$$x = (1 - \tau) r_b f_b + r_s f_s \qquad (6.3)$$

r_b is the rate of return to bond holders

f_b is the fraction of the total investment from bonds

r_s is the rate of return to the stockholders

f_s is the fraction of the total investment from stock; $f_s + f_b = 1.0$

t_i is the lag or lead time for transaction i, measured from the beginning of the batch's irradiation (yr)

t_r is the total residence time for a batch of fuel (or blanket) assemblies in the reactor (yr)

(P/F, x, t) is the present worth factor for transactions which occur t years from the reference time (beginning of batch irradiation in the present calculations)

$(P/\bar{A},x,t)$ is the present worth factor for a continuous cash flow $\bar{A}$. When the escalation of the price of electricity is equal to the escalation rate for other transactions, the escalation factor is given by:

$$G_i = \frac{(P/\bar{A},\ y,\ t_r)}{t_r(P/F,\ y,\ t_i)} \qquad (6.4)$$

One key assumption involved in the use of this model is that all fuel or blanket batches are steady-state batches, i.e. there is no separate account made of startup batches. Over the 30 year or longer life of a unit this is not a significant distinction; moreover in fast reactors the startup batches differ less from steady state batches than in LWRs. Abbaspour (A4) compared the results of the simple model with the more sophisticated code MITCOST II (C7) and found good agreement (the average error over a wide range of parameters was about 2%).

To calculate the levelized fuel cycle cost an economic environment consisting of unit costs for the various transactions and the other financial parameters involved was defined. It was observed that there is a large degree of uncertainty associated with many of these parameters, the most important of which is the unit price of plutonium.

Different studies have adopted different methods for setting a price for plutonium. In the cycle cost calculations, in one method the cost of plutonium is set equal to the cost of its recovery from light water reactor spent fuel, with no additional value due to scarcity or demand added to it (T3, N4). For typical PWR discharged fuel having a concentration of 0.66% plutonium (N3), the unit cost of plutonium following this convention would be equal to 23.11 $/gr, 38.51 $/gr and 57 $/gr based on a unit reprocessing cost of 150 $/Kg (S8), 250 $/Kg (N3) or 370 $/Kg (N3), respectively. Note that once the fraction of breeder reactors in a mixed LWR-FBR economy increases, the cost of recovery would presumably be based on plutonium recovery from fast breeder reactor spent fuel. In this case, since the FBR spent fuel has a much higher concentration of plutonium (on the order of 7-10% including the

axial blanket), the unit price of plutonium based on recovery from FBR fuel would be in the range of 6.5 to 10 $/gr.

In another method the unit cost of plutonium is calculated based on the indifference value of plutonium in light water reactors. The indifference value of plutonium is that value of plutonium which would make the fuel cycle cost of a LWR plutonium burner equal to that of a low-enrichment-uranium fueled light water reactor producing plutonium for sale. The logic behind this pricing method for plutonium is that if reprocessing and recycle of plutonium is allowed in LWRs, then in a nuclear economy consisting of a mixture of light water and breeder reactors the operator of a LWR would be willing to pay this price to run the reactor on a plutonium cycle, and for a breeder operator to compete for this plutonium in an open market, he should be able to pay at least this price for the plutonium.

Using the relationship for the indifference value of plutonium as a function of the price of ore and separative work units (SWU) found by Abbaspour (A4) and unit prices of $40/lb for U_3O_8 and 100 $/Kg for SWU, a value of 27 $/gr was found for fissile plutonium. Abbaspour (A4) also found

a relationship for the indifference value of U233 in LWRs. Based on the above unit prices the indifference value of U233 was found to be equal to 45.2 $/gr.

Finally, it has been suggested by some people that since breeder reactors will be owned and operated by the same utilities that operate LWRs, assigning any price to plutonium and including any carrying charges in fuel cycle cost calculations would not be correct (B8, R2). In this case it is suggested that any comparison between the performance of breeder reactors and other reactors should be done based on the economic and neutronic performance of the reactors excluding plutonium charges. This argument seems plausible if one assumes that all the utilities owning a mixture of light water and breeder reactors are large enough that no transactions will take place between utilities or other outside entities. Also, if due to safeguards or resource requirement considerations the government decides not to permit the recycle of plutonium in light water reactors then the above argument supporting a low price for plutonium would be strengthened.

In our calculations it is assumed that plutonium could be recycled back to either light water or breeder reactors. Based on this, the 27 $/gr indifference value of plutonium in LWRs was used in the fuel cycle cost

calculations. Table 6.7 gives the rest of the unit prices and parameters used in the present calculations (N3).

Using the relationship for the levelized fuel cycle cost and the values given in Table 6.6, the levelized fuel cycle costs for the reference core, the breed/burn core consisting of a (U-Pu)O_2 core with a two-cycle-burned, in/out, 40% moderated blanket, and the core with the central island analyzed in Chapter 3 were calculated. The results are given in Table 6.8. The fuel cycle cost calculations shown in Table 6.8 were performed for two plutonium prices: the indifference value of plutonium in LWRs (27 $/gr) and a zero value for plutonium, representing a case where there is no commercial value attached to plutonium.

As can be seen, based on a plutonium price of 27 $/gr, the breed/burn core with in/out fuel management has a slightly lower fuel cycle cost, and the core with the central island has an approximately 20% lower fuel cycle cost than the reference heterogeneous core. Based on a zero value for plutonium, the fuel cycle cost of the breed/burn core with in/out fuel arrangement is 25% lower than the reference core and the breed/burn core with a central island has a 40% lower fuel cycle cost that the reference core. These results indicate the importance of the price of plutonium and its dominant effect on the levelized fuel cycle cost.

Table 6.7

Unit Cost and Financial Parameters Used

in the Fuel Cycle Cost Calculations

Fabrication		
$(U\text{-}Pu)O_2$ Fuel Assembly	650 $/Kg	
UO_2 Blanket Assembly	140 $/Kg	
ThO_2 Blanket Assembly	150 $/Kg	
Zirconium Hydride Rods	65 $/Kg	$Zr\ H_{1.6}$
Spent Fuel Shipping		
$(U\text{-}Pu)O_2$	90 $/Kg	
$(U\text{-}Th)O_2$	100 $/Kg	
Reprocessing		
$(U\text{-}Pu)O_2$ Fuel Assembly	450 $/Kg	
UO_2 Blanket Assembly	390 $/Kg	
ThO_2 Blanket Assembly	430 $/Kg	
Waste Shipping and Storage		
$(U\text{-}Pu)O_2$	125 $/Kg	
$(U\text{-}Th)O_2$	125 $/Kg	
Financial Parameters	uninflated	actual*
Bond rate of return	2.5 %/yr	8.1 %/yr
Bond fraction	0.55	
Stock rate of return	7.0 %/yr	12.9 %/yr
Stock fraction	0.45	
Income tax fraction,	0.5	
Discount rate, x**	3.83 %/yr	8.03 %/yr

* Based on an inflation rate of 5.5% per year

** $x = (1-\tau) f_b\ r_b + f_s\ r_s$

Table 6.8

Levelized Fuel Cycle Cost of the Reference Core and the Two Breed/Burn Cores Studied in this Work

Reactor	Fuel Cycle Cost, e (mills/KWhe) C_{Pu} = 27$/gr	C_{Pu} = 0$/gr
Reference	7.94	5.01
Breed/Burn (Two-cycle-burned, in/out, 40%-moderated, radial blanket)	7.79	3.74
Breed/Burn (Core with a central island)	6.15	3.00

6.5 Gamma and Neutron Heating Analyses

The importance of gamma and neutron heating in fast breeder reactors is that a large part of the energy produced in a blanket assembly at the beginning of cycle is due to gamma and neutron heating. Thus, to determine the extent of overcooling at BOL and establish coolant orifice settings for EOL it is necessary to calculate these non-fission heating sources. Gamma heating is more important than neutron heating in a conventional blanket assembly. However, in the moderated blanket assemblies studied in the present work neutron heating is the major source of energy production in the moderator pins. Thus, to assure that the moderator pins can operate in the blanket environment, neutron heating calculations are necessary.

The gamma heating calculations were performed using a 40 group coupled neutron-gamma set (01) and the one dimensional transport code ANISN (E2). Figure 6.8 shows the volumetric heat generation rates due to gamma heating in the reference core and the (U-Pu)O_2 core with the two-cycle-burned, in/out, 40% moderated thorium radial blanket. To appreciate the importance of gamma heating as far as the peak linear heat generation rate (LHGR) is concerned, note that at a linear power of 20 KW/ft, the contribution of gamma heating to the LHGR is 0.56 KW/ft.

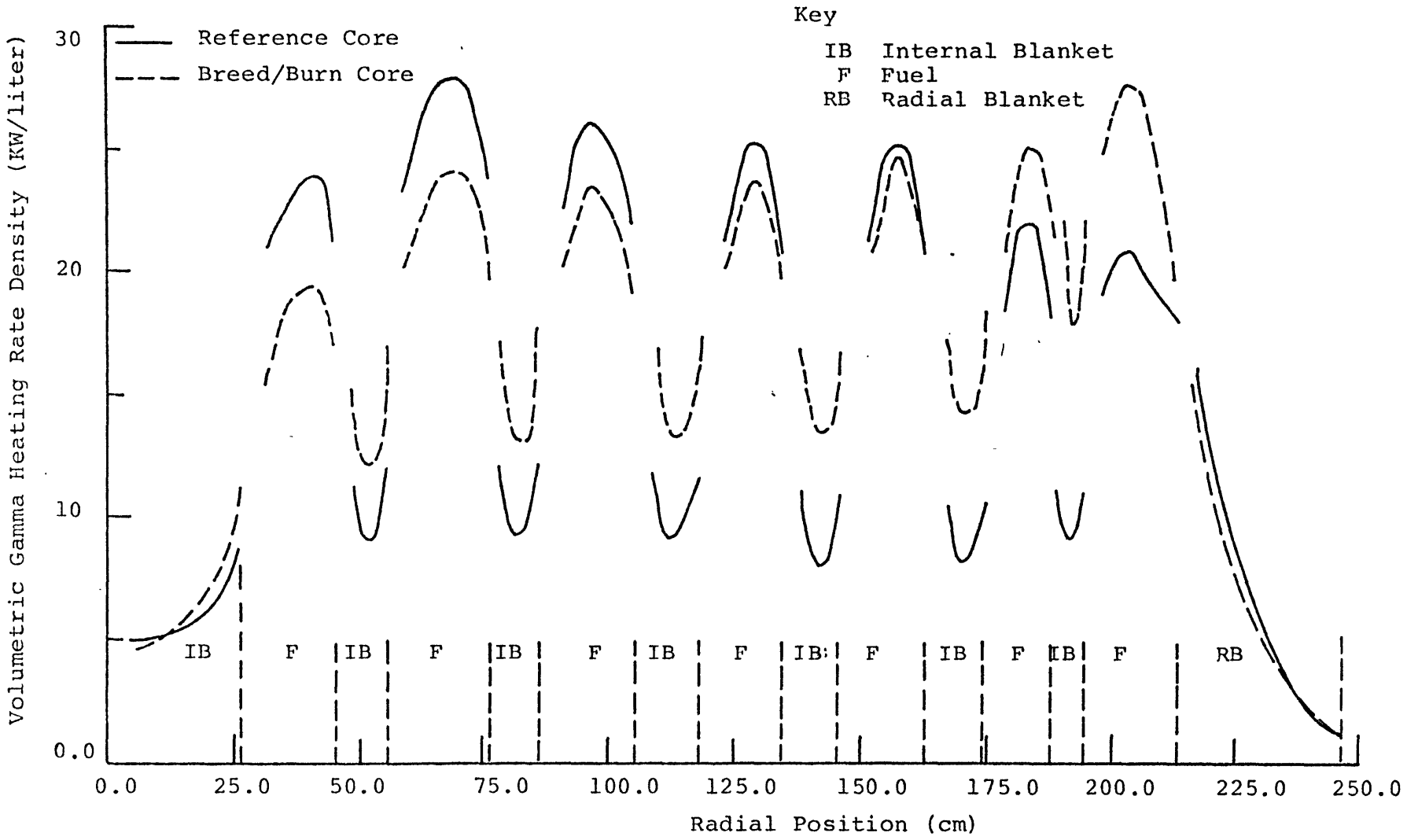

Fig. 6.8 Volumetric Gamma Heating in the Reference Core and the (U-Pu)O_2 Core having a Two-Cycle-Burned, In/Out-40%, Moderated Radial Blanket

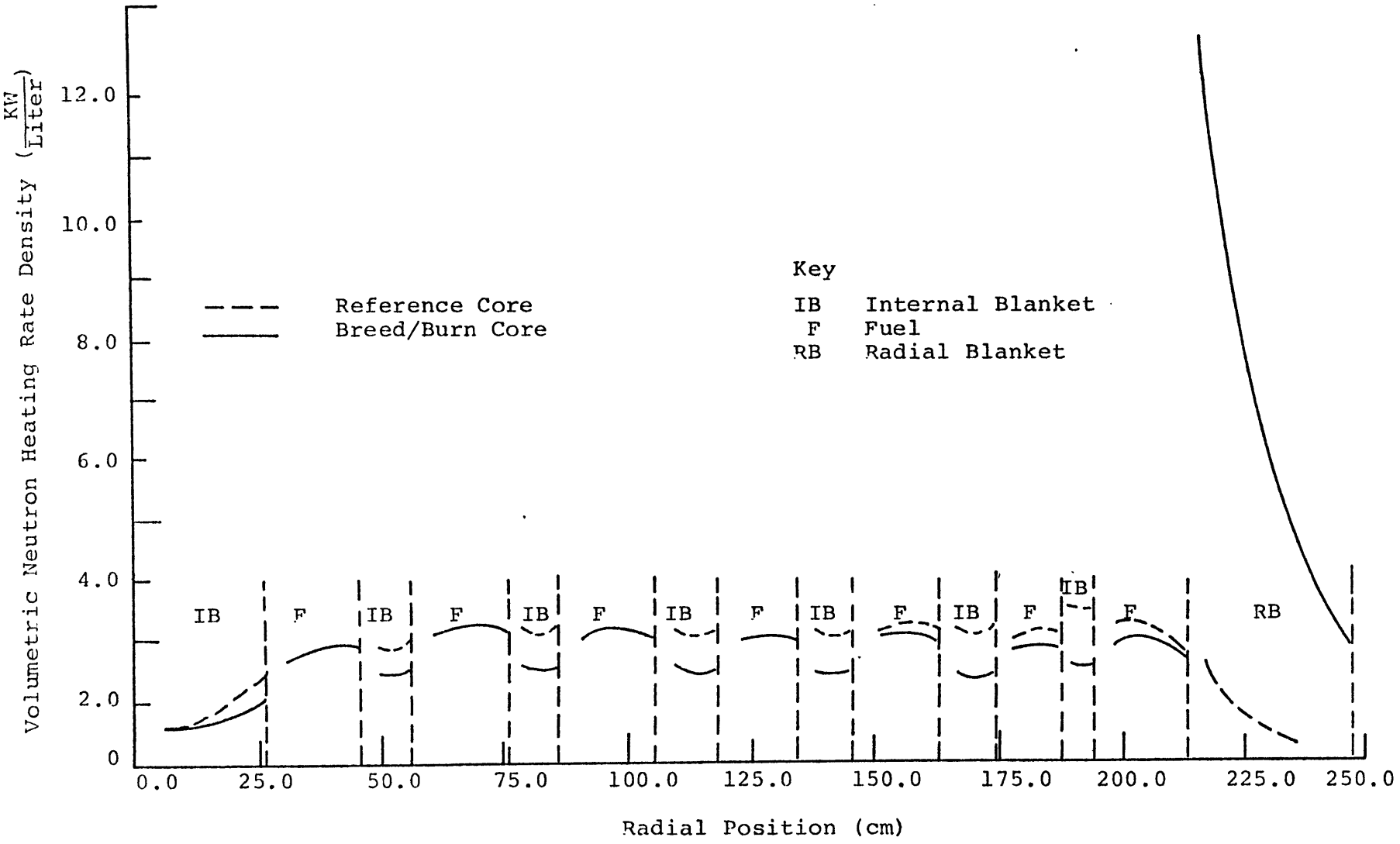

Fig. 6.9 Volumetric Neutron Heating Rates in the Reference Core and the $(U\text{-}Pu)O_2$ Core with a Two-Cycle-Burned, In/Out-40% Moderated, Radial Blanket

The neutron heating calculations were done using the 20G group Bondarenko format cross section set ABN-FTR-200 (B7, N2) and the one-dimensional diffusion code 1DX (H4). Figure 6.9 shows the volumetric neutron heating rate in the reference core and the breed/burn core with a two-cycle-burned, in/out, 40% moderated radial blanket. Compared to the gamma heating, it can be seen that neutron heating's contribution to the total energy generation is much smaller. Using the results of the gamma and neutron heating, zirconium hydride's centerline temperature as a function of the moderator pin diameter was calculated. The results are given in Table 6.9. The calculations were based on the peak centerline power density of 11.53 KW/liter and an outlet sodium temperature of 895^{o}F, to get a conservative estimate. Previous experience with SNAP reactors (L3), and other sources (S7), have indicated that zirconium hydride can be operated at temperatures up to 750^{o}C (1382^{o}F) without any problems. Thus, it was concluded that large zirconium hydride pins can be used without exceeding the allowable operating temperature.

6.6 Recommendations for Further Work

The reference core used in this study represents a rather conservative design, and is larger than typical heterogeneous cores. This is due in part to the low

Table 6.9

Peak Zirconium Hydride Moderator Rod Centerline Temperature as a Function of Pin Diameter*

Moderator Pin Diameter (cm)	Maximum Centerline Temperature (°F)	(°C)
1.0	908.78	487.10
2.0	916.42	491.34
4.0	933.14	500.63

*Calculations based on a peak power density of 11.53 KW/liter and maximum coolant bulk temperature of 895°F.

thermal efficiency of the overall system and the large number of internal blanket assemblies, used to achieve a particularly low sodium void coefficient. Using a smaller core and blanket system, representative of more efficient heterogeneous designs, which would have stronger coupling between the core and radial blanket, is recommended to determine if any additional advantage can be obtained using the in/out, moderate fuel management strategy proposed here.

In studies done on the breed/burn cores in the present work, most of the effort was put into examining different core and fuel management ideas, and no significant attempt was made toward optimization of the core configuration itself. In future work it is recommended that the core configuration, and especially the internal blanket arrangement, and enrichment zoning, be optimized for the particular in/out shuffling scheme under consideration.

Among the many cores studied, the breed/burn core concept with a central island has shown very interesting features, such as considerably lower fissile plutonium requirements. Most of the work related to this core was very preliminary and more detailed work on this core is strongly recommended. In this and other cores, some attention should be given to the initial startup cycles enroute

to the steady state--particularly since U233 is not readily available with which to simulate a steady-state-like initial loading.

Since the use of blanket assemblies containing zirconium hydride was found to offer potential advantages in FBR core design and fuel management, a more detailed neutronic/thermal/hydraulic/mechanical design of a representative assembly should be carried out with particular attention paid to local power peaking. Although intra-assembly calculations were done in the present study for a FBR lattice containing zirconium hydride pins, and no excessive peaking was found, the calculations employed diffusion theory and infinite-medium cross sections, each of which may detract from the overall precision of the results. It should be noted that the German hydride-moderated, sodium-cooled, $(Pu\text{-}U)O_2$-fueled reactor used a heterogeneous arrangement of fuel and moderator pins, hence there is ample precedent for coping with such problems.

Finally, related to the economic analyses and fuel cycle cost calculations, the unit price of plutonium is one important area that has a large uncertainty associated with it. It is recommended that a study be done on the many issues related to plutonium pricing so that a logical and

acceptable method can be found to calculate this parameter for use in the economic analysis of breeder reactor fuel cycles and fuel management strategies.

In conclusion, the breed/burn fuel management strategy offers potentially interesting improvements in fast reactor performance, as summarized in Table 6.10, at an only modest increase in complexity. It also testifies to the inherent flexibility in the core design of fast reactors, adding one more option to an already wide range of practical variations which could be employed starting with the same basic core frame.

Table 6.10

Summary of Breed/Burn FBR Fuel Cycle Characteristics

Advantages:

* Retains essentially all of the advantages of other heterogeneous core designs: lower sodium void reactivity, higher breeding ratio, lower fluence
* Reduces the number of plutonium-bearing assemblies transported and reprocessed by as much as 60%
* Reduces the number of blanket assemblies transported and reprocessed by as much as 75%
* Permits denaturing of blanket assemblies
* Reduces fuel cycle fabrication and reprocessing costs substantially, which leads to a noticeable reduction in overall fuel cycle costs (~20%), based on a plutonium price of 27$/gr and 40% based on a zero value for plutonium
* Compatible with the use of variable moderation control
* Produces a premium fuel (U-233) for use in LWRs
* Avoid the reactivity/enrichment penalty otherwise caused by the internal blankets

Disadvantages:

* Retains most of the disadvantages of other heterogeneous core designs: higher fissile inventory, internal blanket cooling
* Requires fuel shuffling and moderator addition
* Complicates the approach to a steady state fuel cycle
* Requires full deployment of the thorium fuel cycle for best performance.

APPENDIX A

REFERENCES

A1 "Alternative Fuel-Cycle Deployment Strategies: Their Influence on Long-Term Energy Supply and Resource Usage," INFCE/5-TM-2 (July, 1978).

A2 Avery, A., "Coupled Fast-Thermal Power Breeder," Nuclear Science and Engineering, Vol. 3, p. 129 (1958).

A3 Andriyevskii, R. A., et al., "Properties and Behavior of Moderator Materials under Irradiation," 4th International Conference on Peaceful Uses of Atomic Energy, Vol. 10, p. 383, Geneva (1971).

A4 Abbaspour, A. T. and M. J. Driscoll, "The Fuel Cycle Economics of Improved Uranium Utilization in Light Water Reactors," COO-4570-9, MITNE-224, MIT-EL-79-001, Massachusetts Institute of Technology (January, 1979).

A5 Asmussen, K. E. and R. K. Lane, "U233 Indifference Value for Use in HTGRS," GA-A12204 (August, 1972).

B1 Bethe, H. A., "Primary and Alternative Sources of Energy," American Energy Choices Before the Year 2000, p. 3, Lexington Books, Mass (1978).

B2 Barthold, W. P. and J. C. Beitel, "Performance Characteristics of Homogeneous Versus Heterogeneous Liquid-Metal Fast Breeder Reactors," Nuclear Technology, Vol. 44, p. 44 (June, 1979).

B3 Bailey, H. S. and Y. S. Lu, "Nuclear Performance of Liquid-Metal Fast Breeder Reactors Designed to Preclude Energetic Hypothetical Core Disruptive Accident," Nuclear Technology, Vol. 44, p. 76 (June, 1979).

B4 Barthold, W. P. and Y. J. Chang, "Breeding Ratio and Doubling Time Definitions Used for Advanced Fuels Performance Characterization," Trans. Am. Nucl. Soc., Vol. 26, p. 588 (June, 1977).

B5 Barthold, W. P. and C. P. Tzanos, "Performance Potential of Reference Fuel in 1200 MWe LMFBRs," Argonne National Laboratory, FRA-TM-104 (November, 1977).

B6 Brewer, S. T., E. A. Mason and M. J. Driscoll, "The Economics of Fuel Depletion in Fast Breeder Reactor Blankets," COO-3060-4, MITNE-123 (November, 1972).

B7 Bondarenko, I. I., "Group Constants for Nuclear Reactor Calculations," Consultants Bureau, New York (1964).

B8 Brewer, S. T., Department of Energy, Private Communication (December, 1979).

C1 Chang, Y. I., "Review of the French Concept of Heterogeneous Core to Improve Doubling Time," Argonne National Laboratory, FRA-TM-77 (August, 1975).

C2 Chang, Y. I., Barthold, W. P. and C. E. Till, "An Evaluation of the Cylindrical Parfait Core Concept," Argonne National Laboratory, FRA-TM-88 (April, 1976).

C3 Calamai, G. J., S. K. Varner and R. A. Doncals, "Optimization of Fuel Resources in Commercial Oxide LMFBRs," Trans. Am. Nucl. Soc., Vol. 23, p. 434 (June, 1976).

C4 Chang, Y. I., et al., "Alternative Fuel Cycle Options: Performance Characteristics and Impact on Nuclear Power Growth Potential," ANL-77-70 and RSS-TM-4 (1977).

C5 Cappiello, M. W. and D. R. Marr, "LMFBR Design with the Composite Fuel Assembly," Trans. Am. Nucl. Soc., Vol. 28, p. 608 (June, 1978).

C6 Cook, J. L., "Fission Product Cross Sections," AAEC/TM-549 (1970).

C7 Croff, A. G., "MITCOST-II - A Computer Code for Nuclear Fuel Cycle Costs," N. E. Thesis, Massachusetts Institute of Technology, Department of Nuclear Engineering (1974).

D1 Davis, W. J., et al., "SPHINX, A One Dimensional Diffusion and Transport Nuclear Cross Section Processing Code," WARD-XS-3045-17 (August, 1977).

E1 Elias, D. and E. J. Munno, "Reactor Fuel Management Optimization in a Dynamic Environment," Nuclear Technology, Vol. 12, p. 46 (1971).

E2 Engle, W. W., Jr., "A User's Manual for ANISN, a One Dimensional Discrete Ordinates Transport Code with Anisotropic Scattering," K-1693, Union Carbide Corporation, Nuclear Division (March, 1967).

F1 Fischer, G. J., et al., "The Fast-Mixed Spectrum Reactor Interim Report," Draft, Brookhaven National Laboratory (December, 1978).

G1 Gyle, J. D., et al., "Evaluation of Zirconium Hydride as Moderator in Integral Boiling Water - Super Heat Reactors," USAEC Report NAA-SR-5943, North American Aviation (1962).

H1 Hafner, D. R. and R. W. Hardie, "Reactor Physics Parameters of Alternative Fueled Fast Breeder Reactor Core Designs," Nuclear Technology, Vol. 42, p. 123 (February, 1979).

H2 Hasnain, S. D. and D. Okrent, "On the Design and Management of Fast Reactor Blankets," Nuclear Science and Engineering, Vol. 9, p. 314 (1961).

H3 Harde, R. and K. W. Stohr, "A Sodium Cooled Power Reactor Experiment Employing Zirconium Hydride Moderator," 3rd International Conference on Peaceful Uses of Atomic Energy, Vol. 6, p. 537, Geneva (1965).

H4 Hardie, R. W. and W. W. Little, Jr., "1DX, a One-Dimensional Diffusion Code for Generating Effective Nuclear Cross Sections," BNWL-954 (March, 1969).

K1 King, H. M., "World Oil and Natural Gas Reserves and Resources," Project Independence: U.S. and World Energy Outlook through 1990, Congressional Research Service, Library of Congress, U.S. Government Printing Office, Washington (1977).

K2 Kidman, R. B., et al., "LIB-IV, a Library of Group Constants for Nuclear Reactor Calculations," Los Alamos Scientific Laboratory, LA-6260-Ms (1976).

K3 Kikuchi, Y., et al., "Fission Product Fast Reactor Constants System of JNDC," JAERI (November, 1976).

K4 Kalra, M. S. and M. J. Driscoll, "Gamma Heating in LMFBR Media," MITNE-179, COO-2250-18 (February, 1976).

K5 Keepin, G. R., "Physics of Nuclear Kinetics," Addison-Wesley, Reading, Mass. (1965).

L1 Ligon, D. M. and R. H. Brogli, "International Symbiosis: The Role of Thorium and the Breeders," GA-A15272 (February, 1979).

L2 Ligon, D. M. and R. H. Brogli, "Analysis of Reactor Strategies to Meet World Nuclear Energy Demands," GA-A15538 (July, 1979).

L3 Little, A. F., et al., "Zirconium Hydride Fuel Element Performance Characteristics," USAEC Report AI-AEC 13084, Atomics International (June, 1973).

L4 Lancaster, D. B., "An Assessment of the Use of Internal Blankets in Gas Cooled Fast Breeder Reactors," Ph.D. Thesis, Massachusetts Institute of Technology, Nuclear Engineering Department (March, 1980 estimated).

L5 Loh, W. T., "Evaluation of the Fast-Mixed Spectrum Reactor," S. M. Thesis, Massachusetts Institute of Technology, Nuclear Engineering Department (January, 1980 estimated).

L6 Little, W. W., et al., "2DB, User's Manual, Revision 1," Battelle Memorial Institute, BNWL-954 (1969).

L7 Lam, P. S. K., "Potential and Limitations of Heterogeneous LMFBR Reactor Concepts, Part IV: Neutron and Gamma Transport Effects," FRA-TM-106, Argonne National Laboratory (July, 1977).

L8 Lamarsh, J. R., "Introduction to Nuclear Reactor Theory," Addison Wesley (1966).

M1 Mougniot, J. C., et al., "Breeding Gains of Sodium-Cooled Oxide-Fueled Fast Reactors," Trans. Am. Nucl. Soc., Vol. 20, p. 348 (1975); Full Text Translated as ORNL-TR-2994.

M2 Marr, D. R., et al., "Performance of Thorium-Fueled Fast Breeders," Nuclear Technology, Vol. 42, p. 133 (February, 1979).

M3 Mayer, L., "Studies on the Optimum Design of the Radial Blanket on the Basis of a Steam-Cooled Fast Breeder," EUR-FNR-377, PSB No. 263/67 (May, 1967).

N1 Nethaway, D. R. and G. W. Barton, "Compilation of Fission Product Yields in Use at the Lawrence Livermore Laboratory, UCRL-51458 (October, 1973).

N2 Nelson, J. V., "Cross Sections for Preliminary Design of FTR, FTR Set No. 200," HEDL-TME-71-65 (1971).

N3 Nonproliferation Alternative System Assessment Program (NASAP), Preliminary Results (Fall, 1979).

N4 Newman, B., Westinghouse Advanced Reactor Division, Private Communication (December, 1979).

O1 Oak Ridge National Laboratory, "40 Group Coupled Neutron and Gamma-Ray Cross Section Data," DLC-23 (April, 1974).

P1 "PLBR Core Selection for Low CDA Energetics," AI-FBR-77 (February, 1977).

P2 Perks, M. A. and R. M. Lord, "Effect of Axial and Radial Blanket Design on Breeding and Economics," Proceeding of the Conference on Breeding, Economics and Safety in Large Fast Power Reactors, Argonne, Ill., ANL-6792 (December, 1963).

P3 Pai, H. L. and D. G. Andrews, "The Slope Constant of the Exponential Prompt - Neutron Yield Formula," Trans. Am. Nucl. Soc., Vol. 32, p. 477 (June, 1979).

P4 Pai, H. L. and D. J. Andrews, "A Simple Estimation of the Spontaneous and Delayed - Neutron Yield for Transuranics," Trans. Am. Nucl. Soc., Vol. 24, p. 464 (November, 1976).

P5 Pai, H. L. and D. J. Andrews, "The (3Z-A) Dependence of Prompt - Neutron Yield (ν) from Spontaneous Fission of Transuranics," Trans. Am. Nucl. Soc., Vol. 28, p. 752 (June, 1978).

P6 Project Management Corporation, "CRBR Preliminary Safety Analysis Report," Vol. 4 (December, 1975).

R1 "Radial Parfait Core Design Study," Westinghouse Advanced Reactor Division, WARD-353 (June, 1977).

R2 Rudolph, R., Argonne National Laboratory, Private Communication (December, 1979).

R3 Rothstein, M. P., et al., "The Neutronic Value of U233 and U236 in the HTGR," GA-A13728 (November, 1975).

S1 Sege, C. A., et al., "The Denatured Thorium Cycle - An Overview," Nuclear Technology, Vol. 42, p. 144 (February, 1979).

S2 Shin, J. I. and M. J. Driscoll, "Evaluation of Advanced Fast Reactor Blanket Designs," COO-2250-25, MITNE-199 (March, 1977).

S3 Simnad, M. T., "Shielding and Control Materials for the Gas-Cooled Fast Breeder Reactor," GA-A14478 (December, 1977).

S4 Simnad, M. T., et al., "Fuel Elements for the TRIGA Mark III Reactor," Trans. Am. Nucl. Soc., Vol. 7, p. 110 (1964).

S5 Simnad, M. T., F. C. Foushee and G. B. West, "Fuel Elements for Pulsed TRIGA Reactors," Nuclear Technology, Vol. 28, p. 31 (October, 1975).

S6 Shaeffer, M. K., M. J. Driscoll and I. Kaplan, "A One-Group Method for Fast Reactor Calculations," MIT-4105-1, MITNE-108 (September, 1970).

S7 Simnad, M. T., General Atomics Company, Personal Communication (December, 1979).

S8 Matzie, R. A., et al., "Assessment of Thorium Fuel Cycles in Pressurized Water Reactors," TIS-5114 (November, 1976).

S9 Stauffer, T. R., R. S. Palmer and H. L. Wyckoff, "Breeder Reactor Economics," Prepared for Breeder Reactor Corporation (July, 1975).

T1 Turski, R. B. and W. P. Barthold, "Optimum Pin Diameters for 1200 MW(e) Oxide LMFBRs Using CW316SS as Structural Material," Trans. Am. Nucl. Soc., Vol. 23, p. 434 (June, 1976).

T2 Tomlinson, E. T., "Neutronic Analysis of LMFBRs during Severe Core Disruptive Accidents," Oak Ridge National Laboratory, ORNL/CSD-35 (January, 1979).

T3 Thomson, B., General Atomic Company, Private Communication (December, 1979).

V1 Vasiler, G. A., et al., "Space-Energy Distribution of Reactor Neutrons in Metal Hydrides," Vapr. Fiz. Zashch. Reacktorov, Vol. 15, p. 91 (1972).

W1 Wood, P. J. and M. J. Driscoll, "Assessment of Thorium Blankets for Fast Breeder Reactors," C00-2250-2, MITNE-148 (July, 1973).